TABLE OF CONTENTS

Page

LIST OF TABLES

Page

LIST OF FIGURES

LIST OF ABREVIATIONS

AVR	Automatic Voltage Regulator
CA	Control Agent
CSVC	Coordinated Secondary Voltage Control
DCSVC	Decentralized Coordinated Secondary Voltage Control
DG	,Distributed Generations
DMPC	Decentralised Model Predictive Control
DNP	Distributed Network Protocol
EDF	Electricite De France
EMTP-RV	Electro-Magnetic Transient Program - Restructured Version
EXST	IEEE Type ST1 Excitation System
FACTS	Flexible Alternating Current Transmission System
FCM	Fuzzy C-Means
GA	Genetic Algorithm
GENROU	Round Rotor Generator Model (Quadratic Saturation)
HCSD	Hierarchical Clustering with Single electrical Distance
HCVS	Hierarchical Clustering in Var control Space
HQ	Hydro-Quebec
HV	High Voltage
IP	Integer Programming

IREQ	Institute de Recherché d'Hydro-Quebéc
LTC	Load Tap-Changers
LTI	Linear Time Invariant
MIMO	Multi-Input Multi-Output
MPC	Model Predictive Control
MPCSVC	Model Predictive Coordinated Secondary Voltage Controller
NLMPC	Non-Linear Model Predictive Control
NN	Neural Network
OEL	Over Excitation Limiter
OLTC	On Load Tap Changers
OPNET	OPtimized Network Engineering Tools
PI	Proportional-Integral
PMF	Probability Mass Function
PMU	Phasor Measurement Unit
PQ	Load bus
PVC	Primary Voltage Controller
QP	Quadratic Programming
QR	Reactive power Regulator
QSS	Quasi Steady State
RVR	Regional Voltage Regulator

SA	Simulated Annealing
SKC	Spectral K-way Clustering
SM	Synchronous Machine
SNR	Signal to Noise Ratio
SPP	Steam Power Plant
STAB	Speed Sensitive Stabilizing Model
STATCOM	STATic synchronous COMpensator
SVC	Secondary Voltage Control
TGOV	Steam Turbine-Governor
TSO	Transmission System Operator
TVR	Tertiary Voltage Controller
VAR	Volt Ampere Reactive

INTRODUCTION

In nowadays power systems, higher utilization of transmission assets, increased distance between production sites and the load centers, delays in building new transmission projects, larger interconnections and increased meshing, connection of large capacity units to higher voltage levels have led the grid to work closer to its operational limits. In this situation, the automatic control of grid's voltage and reactive power becomes more critical and any inappropriate strategy toward control of the grid may cause instabilities which could consequently lead to cascading black-outs such as the one occurred in 2003 in North America.

On the other hand, in HQ transmission network, despite the existence of AVR on individual generators or using FACTS devices, suitable voltage and VAR control solutions, capable of maintaining reactive power supply and demand in presence of network contingencies while considering higher loads and associated transmission losses, does not exist and the lack of real-time and closed-loop automatic coordination of reactive power resources to improve voltage profile in the grid is unjustifiably continuing.

To resolve these issues, hierarchical voltage control approach can be used in which voltage control problem is broken into three levels hierarchically, with different considerations at each level. In this hierarchy, the primary controllers are taking care of local voltage stability, while the secondary level controller tries to control voltage of sensitive buses of the network, called pilot nodes, by balancing of reactive power supply and demand over a control region. This reactive power can be injected to the power system through generation level by means of generators or through transmission level by means of VAR compensation devices such as capacitor banks, tap-changers & static var compensators. In the highest level of this hierarchy, there is tertiary level controller which deals with the economic and security concerns of the overall power system. These levels operate also in different timescales so that their actions do not affect each other. While the primary controllers take action in few milliseconds, the secondary

level controllers update their control each few seconds and for the tertiary level it is in the order of minutes.

This work is a part of research project with HQ. The thesis focuses on the secondary level voltage control problem considering coordination between continuous and discrete type compensators in one control area while taking into account the effect of the neighbor areas. In this chapter, first, the problem statement and motivations of the research work are presented. The objectives and the methodology of the thesis are discussed afterwards. It is then followed by a section discussing the contributions of the thesis. Finally the organization of the thesis is discussed.

0.1 Motivation and problem statement

In HQ's transmission network, manual voltage control is still in use and it typically involves: dispatching the generating units' forecast reactive powers, scheduling the power plants' high side voltages, switching shunt capacitor or inductor banks for power factor correction and voltage regulation, and setting the voltage set-points of LTC and FACTS controllers. This conventional approach to solving the network voltage control problem is nowadays unsatisfactory because dispatching units' reactive power and scheduling plants' high side voltages are based on off-line forecasting and actual network operating conditions may be often quite different from their forecast values. Moreover, voltage set-points coordination is often operated according to written operator instructions or requested by the system operator when strongly needed: untimely or inadequate control actions may occur during slow dynamic phenomena following unexpected events.

To resolve these problems, HQ have planned to change the structure of its network from manually regulated to an hierarchical automated controlled structure so that the network can maintain reactive power supply and demand automatically over the network. Such a control could be

done in generation level (by means of generators) and also in transmission level (static var compensator, Capacitor/Inductor banks). Important issues that should be considered for such a control strategy are as follows:

1. Optimal compensation of reactive power and voltage control considering compensators' MVAR limits : one of the issues in CSVC is to compensate voltage deviation with minimum reactive power injection/absorption by the compensators so that extra MVAR can be used as a reserve for extreme system conditions. In addition, the control strategy should consider the MVAR limits of each compensator and try to manage these reactive power resources based on their limits;
2. For large disturbances, the operating point of the system on the $p-v$ curve moves closer to the critical point in which the behavior of the system is nonlinear. Therefore the method should consider these nonlinearities;
3. Coordination of continuous type compensators (generators, static var compensators) and discrete type compensators (capacitor banks, LTC) in an optimal way. For HQ network with tens of compensators installed on transmission lines, considering both discrete and continuous nature of these compensators along with nonlinear behavior of the system transforms the control problem into an NP-hard problem which is challenging to be implemented in real-time in one time step of the secondary voltage controller, i.e. few seconds. The strategy toward CSVC should be so that it can be finally applicable in real-time for large scale power grids;
4. Voltage control is naturally done using local controllers in an area where the distrubance has occurred. In this regard using a centralized control strategy for a problem which is by nature decentralized is not reasonable. Moreover a centralized approach is not computationally beneficial since it has to solve a far more larger optimization problem. In this way, the proposed method should have a decentralized architecture;

5. Despite decentralized architecture of the control approach, a secondary voltage controller in one region should coordinate itself with the actions of the secondary voltage controller in a neighbor area. An uncoordinated action between regional SVCs might lead to oscillatory behavior in the two and finally lead to voltage collapse.

0.2 Objectives

0.2.1 General Objectives

The general objective of this research is to propose both centralized and decentralized coordinated secondary voltage control strategy for a large scale transmission network which could be implemented in real-time. The following issues should be considered:

1. Use the maximum capability of currently installed compensators without installing new ones;
2. Apply secondary voltage control in an optimal way so that minimum reactive power is injected into the power network and the remaining reactive power capacity can be preserved for emergency conditions. Physical limits such as compensators' MVAR limits should also be considered in control approach;
3. Ensure coordination of continuous compensators (generators, static var compensators) and discrete compensators (capacitor banks, LTC) in an optimal way;
4. Propose a decentralized strategy which fits well with nowadays multi-area power network structure;
5. Consider interactions between areas and coordination between regional controllers.

0.2.2 Specific Objectives

1. Model identification of each area of multi area power system considering the nonlinearities within the model;
2. Development of a real-time centralized optimization based control strategy to regulate voltage at pilot buses using only continuous type compensators;
3. Development of a real-time decentralized optimization based control strategy which considers only continuous type compensators and takes into account the effect of the neighbor areas in the control design;
4. Development of a real-time centralized optimization based control strategy to regulate voltage at pilot buses using both discrete and continuous type compensators;
5. Development of a real-time decentralized optimization based control strategy which takes into account both continuous and discrete type compensators. It should also take into account the effect of the neighbor areas in control design;
6. Validation of the proposed control strategies on realistic power grids in real-time.

0.3 Methodology

Different methods are used and proposed throughout this thesis. In the following, the main methodologies are categorized:

1. To address the specific objective 1, two different approaches are used to identify a model which relates the inputs, i.e. action of the compensator devices, to the outputs, such as voltage magnitude on pilot buses, voltage on compensator buses and reactive power injection by machines. In both methods, first a series of input-output data is generated. Then a model is fitted to the data. The two approaches are as follows:
   (a) Use sub-space method to identify a linear dynamical state-space model;
   (b) Use neural network approach to fit a nonlinear static model to the input-output data.

2. To address specific objectives 2, centralized MPC method is used. This approach is based on the linear dynamical state space model of the whole network obtained using methodology 1a. This model is then used to formulate a predictor function based on which an optimization problem is established to minimize voltage error on pilot nodes using reactive power injection by continuous type compensators;
3. To address specific objectives 3, decentralized MPC method is used. The difference between this method and methodology 2 is that for decentralized MPC a separate controller is designed for each region of the grid. Also the interaction between neighbor areas are taken into account by considering measured reactive power flowing through inter area tie-lines in the identified model and defining it as measured disturbance;
4. To address specific objective 4, SA based optimization is used. This method is proposed to solve mixed continuous-discrete type optimization problem. It can handle both discrete and continuous type compensators considering nonlinear static model of the network mentioned in methodology 1b;
5. To address specific objective 5, SA based optimization is used. The difference between this method and methodology 4 is that for decentralized control strategy the coordination between two neighbor regional controllers is done by a multi-agent solution in which the secondary level controllers as well as the primary level controllers of some specific compensators which have a considerable impact on the two regions come up with a consensus;
6. To address specific objective 6, the proposed methods are tested on different power system test-cases such as IEEE 39 bus and 118 bus standard systems. These test cases include the dynamics of the generators, excitation systems, turbine governors, power system stabilizer's as well as the effect of the over and under excitation limiters. To validate methodologies on more realistic and larger scale power grid, a 5000-bus power system is also been used.

Moreover, to investigate the real-time performance of the proposed methodologies, the model of the power systems are built inside ePHASORsim software which is a phasor domain solver from Opal-RT Technology. These models are run on a real-time simulators which is also provided by Opal-RT Technologies. These real-time simulation models also take into account the effect of the communication channel to investigate the impact of the communication noise and delay on the controller performance.

0.4 Contributions

Guided by the objectives presented in Section 0.2 and using the methodology proposed in Section 0.3, this thesis presents the following important and novel contributions:

1. Proposing a novel nonlinear sensitivity model based on NN which maps reactive power injection by compensators to the corresponding voltage variation on pilot nodes considering different demand levels of the network;
2. Proposing a novel closed loop suboptimal secondary voltage controller which uses SA to solve a mixed discrete-continuous type optimization problem with NN based sensitivity model as nonlinear constraint and quadratic objective function at each time step of the controller;
3. Proposing a novel technique to generate rich data for training Neural Network as the nonlinear sensitivity model;
4. Proposing a novel consensus strategy which does not require communication between regional controllers;
5. Defining PVC of the shared compensators as an agent which communicates with neighbor SVCs. This agent can then make a decision on its degree of participation on SVC control of each neighbor area;

6. Proposing a modified version of sensitivity analysis presented in Corsi (2015) in which control regions can overlap. Some compensators might be selected for SVC which belong to the shared area;
7. Proposing a decentralized MPC approach in which the two neighboring MPCs does not require any communication links between to coordinate their actions. Moreover, each regional controller does not need to consider any model of its neighbors. The supplementary information about neighboring areas are gathered from measuring tie-line reactive power deviations using installed PMUs. In this way each regional controller considers the effect of the other regions indirectly from this measurement;
8. Presenting a real-time simulation test-bed to validate the proposed methodologies in which detailed dynamics of the network as well as standard communication protocols used to send and receive the data in power systems are employed. The test-bench also benefits from the multi-core simulation technologies on which the proposed decentralized controller is tested and validated;
9. Using realistic test-cases with detailed dynamics to validate the controller. Such a validation has been missing in the literature where usually simplified academic test-cases such as IEEE39 bus or IEEE118 bus networks are used for validation of the control algorithms. Although using a smaller test-case can be considered at early stages of validation for controller techniques, the final validation should be done on a more realistic data set to show that the proposed methodologies are capable of handling complexity of large scale power grids.

0.5 Publications

The contributions listed in Section 0.4 have been presented in three journals and two conference publications. The complete list of publications associated with this research work is presented below.

0.5.1 Journals

Published

[J1]: Morattab A., Akhrif O., Saad M., *Decentralized Coordinated Secondary Voltage Control of Multi-Area Power Grids using Model Predictive Control,* Accepted for publication in IET Generation, Transmission & Distribution; May 2017;

Submitted

[J2]: Morattab A., Saad M., Akhrif O., Lefebvre S., Dalal A., *Nonlinear Sensitivity-based Coordinated Control of Reactive Resources in Power Grids Under Large Disturbances,* submitted to International Journal of Electrical Power and Energy Systems; May 2018;

[J3]: Morattab A., Akhrif O., Saad M., *Secondary Voltage Control with Consensus Between Regional Controllers,* submitted to IEEE Transactions on Power Systems. February 2018;

0.5.2 Conferences

Published

[C1]: Morattab A., Dalal A., Akhrif O., Saad M., Lefebvre S., *Model Predictive Coordinated Secondary Voltage Control of Power Grids*, 2012 International Conference on Renewable Energies for Developing Countries (REDEC), Pages: 1-6, November 2012, Beirut, Lebanon;

[C2]: Morattab A., Saad M., Akhrif O., Dalal A., Lefebvre S., *Decentralized coordinated secondary voltage control of multi-area highly interconnected power grids*, 2013 IEEE PowerTech Conference, Pages: 1-5, June 2013, Grenoble, France.

0.6 Thesis Outline

The thesis is organized as follows: The next chapter reviews the fundamental concepts regarding to voltage stability and control as well as secondary voltage control method. This chapter is then followed by Chapter 2 which includes literature review related to our addressed problems. Chapters 3-5 show the contribution of this research work.

Chapter 3 presents the first accepted journal paper (J1) corresponding to decentralized MPC approach. This work is related to the first phase of this research work in which only the continuous type compensators are considered. Chapter 4 and chapter 5 present the second and third papers (J2 and J3) respectively and they are related to the second phase of the research work in which both continuous and discrete type compensators are considered. In chapter 4 the mixed discrete-continuous type optimization methodology based on NN model and SA optimizer is presented. However the control architecture is centralized. In chapter 5 the same idea is adapted on a decentralized architecture in which a consensus strategy is also presented to coordinated the decentralized controllers.

The thesis ends by conclusions that provide a summary of the addressed problems, the proposed solutions and the future research works.

This thesis also includes two Appendices. In appendix I, the conference paper (C1) is presented in which our early achievements on using centralized MPC is discussed. The idea presented in this appendix was further extended in chapter 3. Moreover in appendix II, the second published conference paper (C2) is presented which is an early evaluation of decentralized control architecture and comparison to the centralized case.

CHAPTER 1

FUNDAMENTAL CONCEPTS

In this chapter, basic concepts regarding to voltage stability and control are first discussed. Afterwards, classical secondary voltage control which was first presented in Arcidiacono *et al.* (1977); Arcidiacono (1983) is reviewed. Finally the coordinated secondary voltage control, presented first in Paul *et al.* (1987), is discussed.

1.1 Fundamentals of Voltage Stability and Voltage Control

1.1.1 Power flow, active and reactive power transfer limits

Consider the simple two bus network in Figure 1.1. An ideal voltage source with voltage $E\angle 0$ supplies a remote load through a transmission line modeled as a series reactance. The receiving end voltage V and angle θ depend on the active and reactive power transmitted through the line. The power flow equation on the load bus can be written as follows:

$$S = P + jQ = -(V\angle\theta)I^* = -V\angle\theta\left(\frac{V\angle\theta - E}{jX}\right)^* \tag{1.1}$$

Expanding the right hand side of Equation 1.1 and finding its real and imaginary parts, active and reactive power equations can then be written as Equations 1.2 and 1.3.

$$P = -\frac{EV}{X}\sin(\theta) \tag{1.2}$$

$$Q = \frac{EV}{X}\cos(\theta) - \frac{V^2}{X} \tag{1.3}$$

After eliminating θ using the trigonometric identity we get:

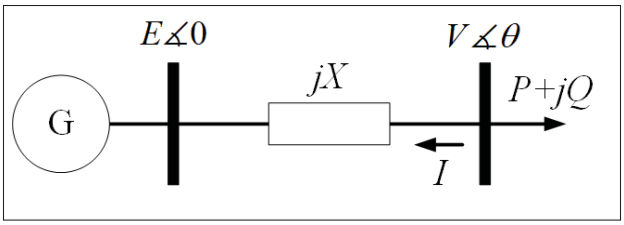

Figure 1.1 Two bus system with generator at one side and a load on the other side

$$\left(Q+\frac{V^2}{X}\right)^2+P^2=\left(-\frac{EV}{X}\right)^2 \tag{1.4}$$

Solving for V^2 yields:

$$V^2=\frac{E^2}{2}-QX\pm X\sqrt{\frac{E^4}{4X^2}-P^2-Q\frac{E^2}{X}} \tag{1.5}$$

Thus, the problem has real positive solutions if:

$$P^2+Q\frac{E^2}{X}\leq\frac{E^4}{4X^2} \tag{1.6}$$

This inequality shows which combinations of active and reactive power line can supply to the load. Substituting the short-circuit power at the receiving end, $S_{sc}=\frac{E^2}{X}$, we get:

$$P^2+QS_{sc}-(\frac{S_{sc}}{2})^2\leq 0 \tag{1.7}$$

The locus of all (P,Q) pairs satisfying Equation 1.7 is shown in Figure 1.2, underneath the parabola curve representing the case where the left side of 1.7 is equal to zero. As can be seen the parabola is symmetric with respect to the Q axis. Moreover, the active power transfer limits when $Q=0$ are defined as $-\frac{S_{sc}}{2}$ as lower and $\frac{S_{sc}}{2}$ as higher limit. On the other hand, the reactive power has only a maximum transfer limit when $P=0$ and it is equal to $\frac{S_{sc}}{4}$.

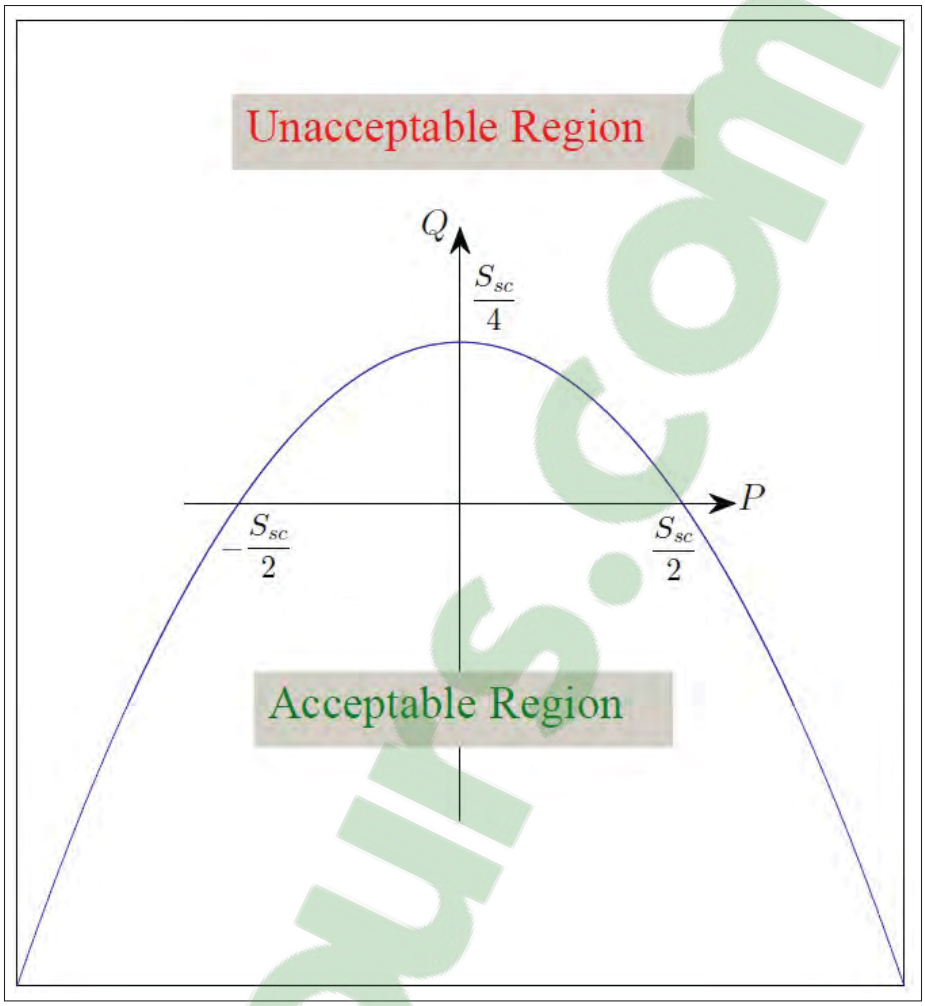

Figure 1.2 Acceptable region satisfying Equation 1.7

Observing Figure 1.2, the following could be deduced:

1. An injection of reactive power at the load end, i.e. reducing Q, increases the transfer limit for active power;
2. Both active and reactive power transfer limits are proportional to the short circuit power, S_{sc}. Based on the definition of S_{sc}, one can also say that increasing the line admittance, X, reduces the transfer limits while increasing the voltage on the generation bus, E, increases these limits;
3. The transfer of positive reactive power through the inductive line is limited to $\frac{S_{sc}}{4}$. However, any amount of active power can be transferred through the line by injecting enough

inductive load on the load side. This fact confirms that transfer of reactive power is more difficult than active power over the inductive lines.

1.1.2 PV curve, voltage stability and voltage control

For simplicity, we assume that the load shown earlier in Figure 1.1 is a constant impedance type. Mathematically:

$$P + jQ = V^2 G(1 + j\tan(\phi)) \tag{1.8}$$

With this assumption, one can say that the load produces reactive power for leading power ($\tan(\phi) < 0$) and absorbs reactive power for lagging power ($\tan(\phi) > 0$). Now we convert the variables to their per unit (p.u.) equivalent, assuming S_{sc} as the base power and E as the base voltage:

$$p = \frac{P}{S_{sc}} \tag{1.9a}$$

$$q = \frac{Q}{S_{sc}} \tag{1.9b}$$

$$v = \frac{V}{E} \tag{1.9c}$$

$$g = \frac{G}{\frac{1}{X}} \tag{1.9d}$$

Using per unit quantities, the positive solution to Equation 1.5 can be written as:

$$v = \frac{1}{\sqrt{g^2 + (1 + g\tan(\phi))^2}} \tag{1.10}$$

We also have the following equations for p and q:

$$p = v^2 g \tag{1.11a}$$

$$q = v^2 g \tan\phi \tag{1.11b}$$

For a constant $\tan(\phi)$, one can plot a parametric curve of per unit voltage versus per unit active power, called $p - v$ curve, based on Equation 1.10 and Equation 1.11a for different values of parameter g changing from 0 to infinity, Figure 1.3 shows the p-v curves for different values of $\tan(\phi)$.

The green area shown in Figure 1.3 is defined as voltage controlled region in which the voltage magnitude is within $5\% p.u.$ of tolerance from the $1 p.u.$. Moreover, for a constant $\tan(\phi)$, the nose of each curve, marked using star, defines the maximum active power transfer. The corresponding voltage is often referred to as the critical voltage. Connecting the nose of the curves together forms a new curve, called critical curve, which divides the $p - v$ plane into stable and unstable regions in which the unstable region is shown as shaded area.

To clarify the concept of voltage stability, Figure 1.4 illustrates the $p - v$ curve, shown in blue, considering $\tan(\phi) = 0$. As can be seen in this figure, for a specific load value two different operating points, shown as A and B, exist. The load characteristic curve, defined in Equation 1.11a, is also shown in green for each operating point. As can be seen in this figure, at point A, by increasing the load by ΔP, the operating point changes to a new one A' which has a lower voltage magnitude. However, the load has a tendency to decrease p when voltage decreases. This represents a stable fixed-point at operating point A which leads the system to return back to its original equilibrium point, A. On the other hand, at point B which is located underneath of the nose of the curve, the load characteristic curve along with the $p - v$ curve forms an unstable fixed-point which causes a divergent pattern of perturbed point B' from the original point B.

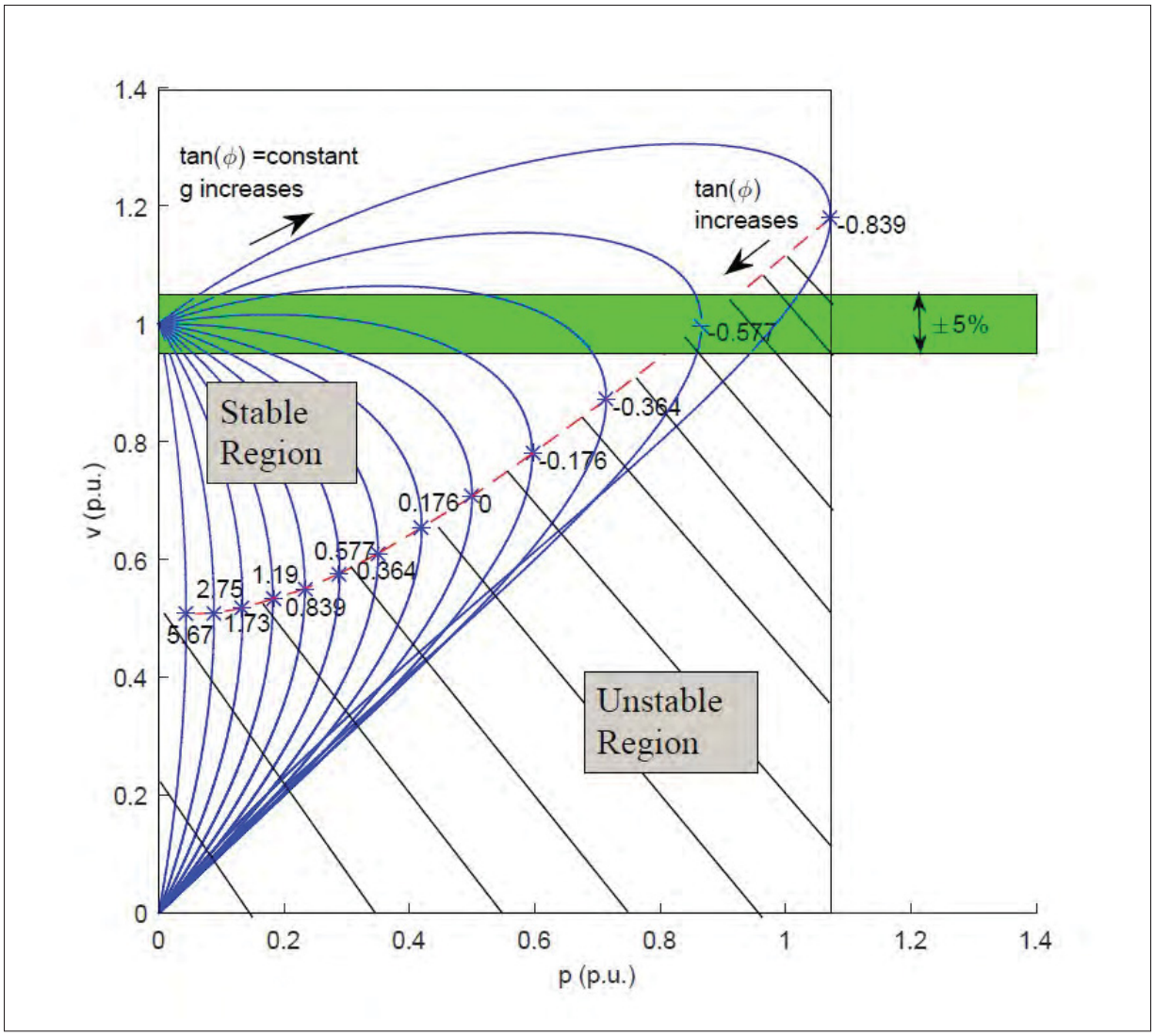

Figure 1.3 $p-v$ curves for different values of tan(ϕ)

The same conclusion can be made for other operating points on the $p-v$ curve, hence it could be divided into stable and unstable regions as depicted in Figure 1.3.

1.1.3 Effect of different compensation devices

In normal conditions of a power system, voltage magnitude is mostly affected by reactive power injection. For the simple two bus network of Figure 1.1, this could be seen by calculating the derivatives, $\frac{\partial P}{\partial V}$ and $\frac{\partial Q}{\partial V}$, based on Equations 1.2 and 1.3. These derivatives are shown below:

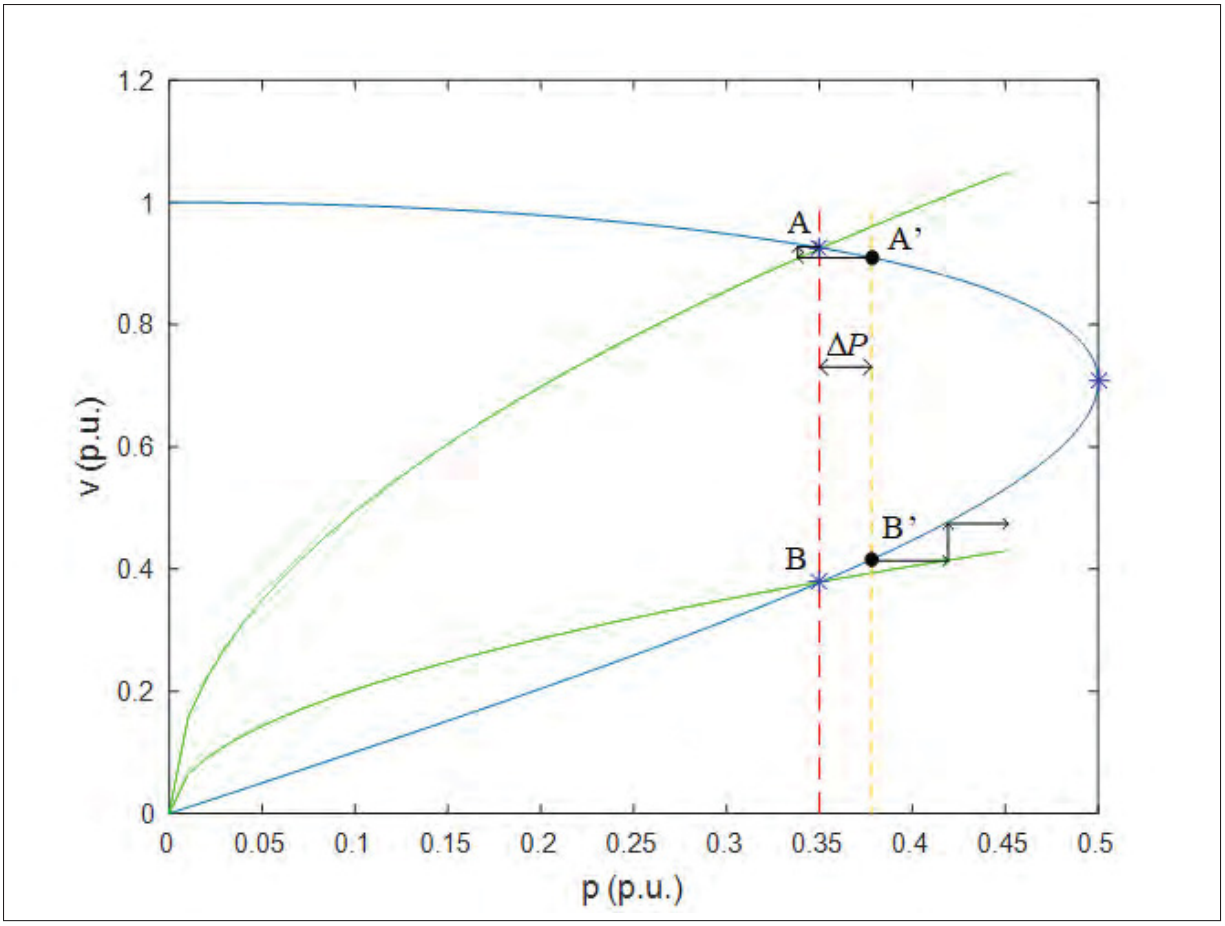

Figure 1.4 $p-v$ curve with load characteristic curves at two operating points A & B

$$\frac{\partial P}{\partial V} = -\frac{E}{X}\sin(\theta) \tag{1.12}$$

$$\frac{\partial Q}{\partial V} = \frac{E}{X}\cos(\theta) - \frac{2V}{X} \tag{1.13}$$

Since in normal conditions $\theta \approx 0$, then $\sin(\theta) \approx 0$ and $\cos(\theta) \approx 1$. In this way, $\frac{\partial P}{\partial V} \approx 0$ and $\frac{\partial Q}{\partial V} \approx \frac{E}{X} - \frac{2V}{X}$. This result confirms the decoupling of voltage magnitude and active power in normal conditions. The same conclusion could be made about decoupling of voltage angle and reactive power. These two facts are the basic assumptions which are considered in decoupled

power flow algorithm and shows that in practice, it is reasonable to control voltage magnitude by reactive power and voltage angle by active power injection/absorption.

Various reactive power compensation devices are used throughout a power grid to control voltage locally. However, they can be categorized into two main groups which are continuous type and discrete type compensators. Continuous type compensators are devices which are able to deliver any continuous value of reactive power within their operational limits. Synchronous generators, synchronous condensers and FACTS devices are examples of this type of compensators. On the other hand, discrete type compensators are switch base devices which can only deliver discrete amounts of reactive power to the grid. Capacitor banks, inductor banks and tap changers are considered as discrete type compensators.

To show the effect of different compensation devices, Figure 1.5 illustrates a three-bus power system with one generator bus connected to the neighbor bus through an inductive transmission line with a capacitor in series. This bus is then connected to the load bus with a tap changer. A shunt capacitor and a shunt inductor are also connected to the load bus. Moreover, Figure 1.6 shows the $p-v$ curve for the load bus and the effect of these reactive power compensation devices as well as the terminal voltage of the generator on this curve. As can be seen in this figure, these elements can be considered as control actuators to change the system stiffness, critical voltage and the theoretical and practical transfer limits so that the voltage remains in the acceptable bound considering any disturbances on the network.

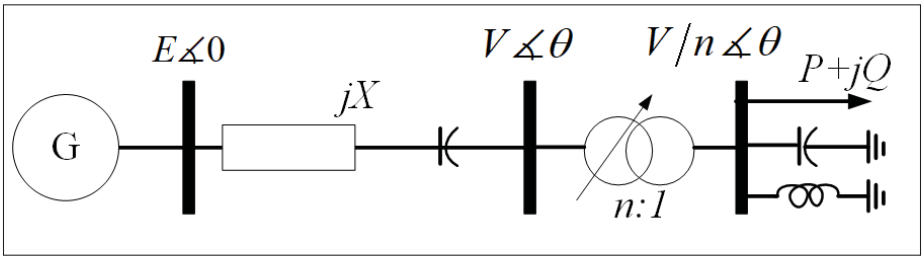

Figure 1.5 Three bus system with transformer

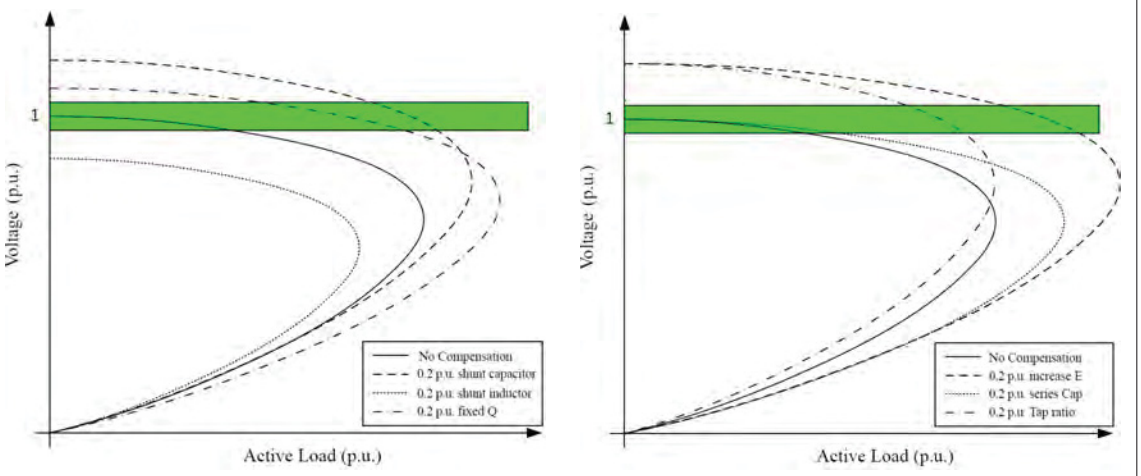

a) Shunt capacitor, shunt inductor, fixed reactive power injection

b) Increase reference voltage of generator, series capacitor, tap ratio

Figure 1.6 The effect of different compensation devices on the PV curve

1.2 Secondary Voltage Control

Secondary voltage control consists of two main steps. The first step is to partition the transmission system into several voltage coherent regions and finding a representative bus, called pilot bus, for each area. The participant reactive power compensators for each region which control the voltage of the pilot node in that region are also allocated in this step. The second step is then to design the secondary level control loop which calculates the control signals based on the measurements from the pilot nodes and sends them to the primary level controllers, which control the compensation devices. These two steps are discussed in this section.

1.2.1 Network partitioning and pilot node selection in SVC

In this section, the method presented in Corsi (2015) to find pilot nodes and partitioning the network is presented. This method is based on sensitivity analysis and the criterion to choose is based on the weakest buses to the reactive power disturbances.

Suppose a power system with n buses, N of which are PQ buses and g are generator buses (PV and slack buses). We assume that pilot buses are always a subset of PQ buses. Sensitivity

matrix, S_{vq}, as defined in Equation 1.14 relates reactive power injection on each PQ bus to the voltage variation of all PQ buses.

$$S_{vq} = \begin{bmatrix} \frac{\partial V_1}{\partial Q_1} & \frac{\partial V_1}{\partial Q_2} & \cdots & \frac{\partial V_1}{\partial Q_N} \\ \frac{\partial V_2}{\partial Q_1} & \frac{\partial V_2}{\partial Q_2} & \cdots & \frac{\partial V_2}{\partial Q_N} \\ \vdots & \vdots & \ddots & \vdots \\ \frac{\partial V_N}{\partial Q_1} & \frac{\partial V_N}{\partial Q_2} & \cdots & \frac{\partial V_N}{\partial Q_N} \end{bmatrix} \tag{1.14}$$

The procedure toward finding pilot buses is as follows:

1. Matrix S_{vq} rows and columns are reordered to satisfy the condition:

$$\begin{cases} \left(S_{vq}\right)_{11}^{(1)} < \left(S_{vq}\right)_{rr}^{(1)} \\ \left(S_{vq}\right)_{11}^{(1)} > \left(S_{vq}\right)_{21}^{(1)} > \left(S_{vq}\right)_{31}^{(1)} > \cdots > \left(S_{vq}\right)_{N1}^{(1)} \end{cases}$$

   with $r = 2, \cdots, N$.

2. The "electrical distance" ratios are computed as follows:

$$\beta_{ij} = \frac{\left(S_{vq}\right)_{ij}^{(1)}}{\left(S_{vq}\right)_{jj}^{(1)}}$$

   with $i = 1, 2, \cdots, N$ and $j = 1, 2, \cdots, Z$. It should be noted that $0 \leq \beta_{ij} < 1$ and Z is the number of pilot nodes, to be defined at the end.

3. After the lower limit of the electrical distance among the pilot nodes is established, we exclude from subsequent selections those buses related to the first N_1 rows of the $S_{vq}^{(1)}$ reordered matrix having coupling coefficient β_{i1} with bus “1” greater than ϵ_p, i.e.:

$$\epsilon_p < \frac{\left(S_{vq}\right)_{\mu 1}^{(1)}}{\left(S_{vq}\right)_{11}^{(1)}} \leq 1; \mu = 1, \cdots, N_1.$$

4. The remaining $(N - N_1) = n_1$ columns of the $S_{vq}^{(1)}$ matrix are reordered in such a way that the new matrix $S_{vq}^{(2)}$ satisfies the following inequalities:

$$\begin{cases} \left(S_{vq}\right)_{11}^{(2)} < \left(S_{vq}\right)_{rr}^{(2)} \\ \left(S_{vq}\right)_{11}^{(2)} > \left(S_{vq}\right)_{21}^{(2)} > \left(S_{vq}\right)_{31}^{(2)} > \cdots > \left(S_{vq}\right)_{N1}^{(2)} \end{cases}$$

where $S_{vq}^{(2)} \in R^{n_1 \times n_1}$ and $r = 2, \cdots, n_1$. This corresponds to arranging the $(n - N_1)$ remaining buses in order of electrical vicinity, with bus 1, among them, having the highest power.

5. Similar to step 3, in the steps that follow we no longer consider the first N_2 of the n_1 nodes (that is, the first N_2 rows of the reordered matrix $S_{vq}^{(2)}$ having coupling coefficient with bus "1":

$$\epsilon_p < \frac{\left(S_{vq}\right)_{\mu 1}^{(2)}}{\left(S_{vq}\right)_{11}^{(2)}} \leq 1; \mu = 1, \cdots, N_2.$$

6. The reordering procedure of the matrices is repeated, starting from the $(n_1 - N_2) = n_2$ remaining nodes, in accordance with the indicated procedure up to the $(Z+1)^{th}$ reordering, which is when among the $(n_{Z-1} - N_Z) = n_Z$ remaining buses, the coefficient $S_{vq}^{(Z+1)}$ of the reordered matrix $S_{vq}^{(Z+1)}$ is greater than a predefined value $\frac{1}{\gamma}$, which represents the minimum admissible value of the short circuit power for a pilot node:

$$\left(S_{vq}\right)_{11}^{(Z+1)} > \frac{1}{\gamma}.$$

7. The Z pilot nodes are those corresponding to the first row of the matrices: $S_{vq}^{(1)}, S_{vq}^{(2)}, S_{vq}^{(3)}, \cdots, S_{vq}^{(Z)}$.

8. After having defined the pilot nodes, the buses belonging to each region are classified using the electrical distance values calculated at step 2. In this way, the i^{th} bus is linked to area j if it has the highest coupling coefficient with the j^{th} pilot node. That is, the i^{th} bus is associated to area j if:

$$\beta_{ij} > \beta_{ik}. \forall k \neq j.$$

1.2.2 SVC Control structure

Although the voltage of local buses to which reactive power compensator devices are connected are regulated, voltages of other buses might deviate from their desired values due to load variations or contingencies. In this way, besides their local control responsibilities, these compensators should also contribute to the long term voltage/reactive power stability and control. Such a regional control should be done in a way that takes into account the limitation of each compensator and its droop characteristics. For this reason SVC has been introduced by Arcidiacono *et al.* (1977); Arcidiacono (1983) and Paul *et al.* (1987). Based on this method the network is first partitioned into theoretically non-interacting zones, within which, voltage is controlled independently. SVC adjusts automatically the reactive power of certain generating units to control the voltage at a specific point, known as the pilot nodes, considered as the representative bus of the zone.

The structure of SVC is shown in Figure 1.7. The SVC system measures the instantaneous voltage of the pilot bus of the zone V_p, compares it with the voltage set-point V_p^{ref}, generated by TVR level, and applies a PI law using RVR to determine a signal representing the reactive power required for this zone, q. The RVR control law is defined as Equation 1.15.

$$\begin{aligned} & q = K_{PV}\left(V_p^{ref} - V_p\right) + K_{VI}\int_0^t \left(V_p^{ref} - V_p\right) dt \\ & with: \\ & q_{max} \leq q \leq q_{min} \end{aligned} \tag{1.15}$$

q_{max} and q_{min} are normalized upper and lower limits of the RVR which are equal to -1 and +1. The normalized power is then converted to its actual level using $Q_{ref} = qQ_{lim}$.

Q_{ref} is then used by local QRs at reactive power sources, to control their reactive power output with respect to their own reserves by modulating the input of the corresponding AVR.

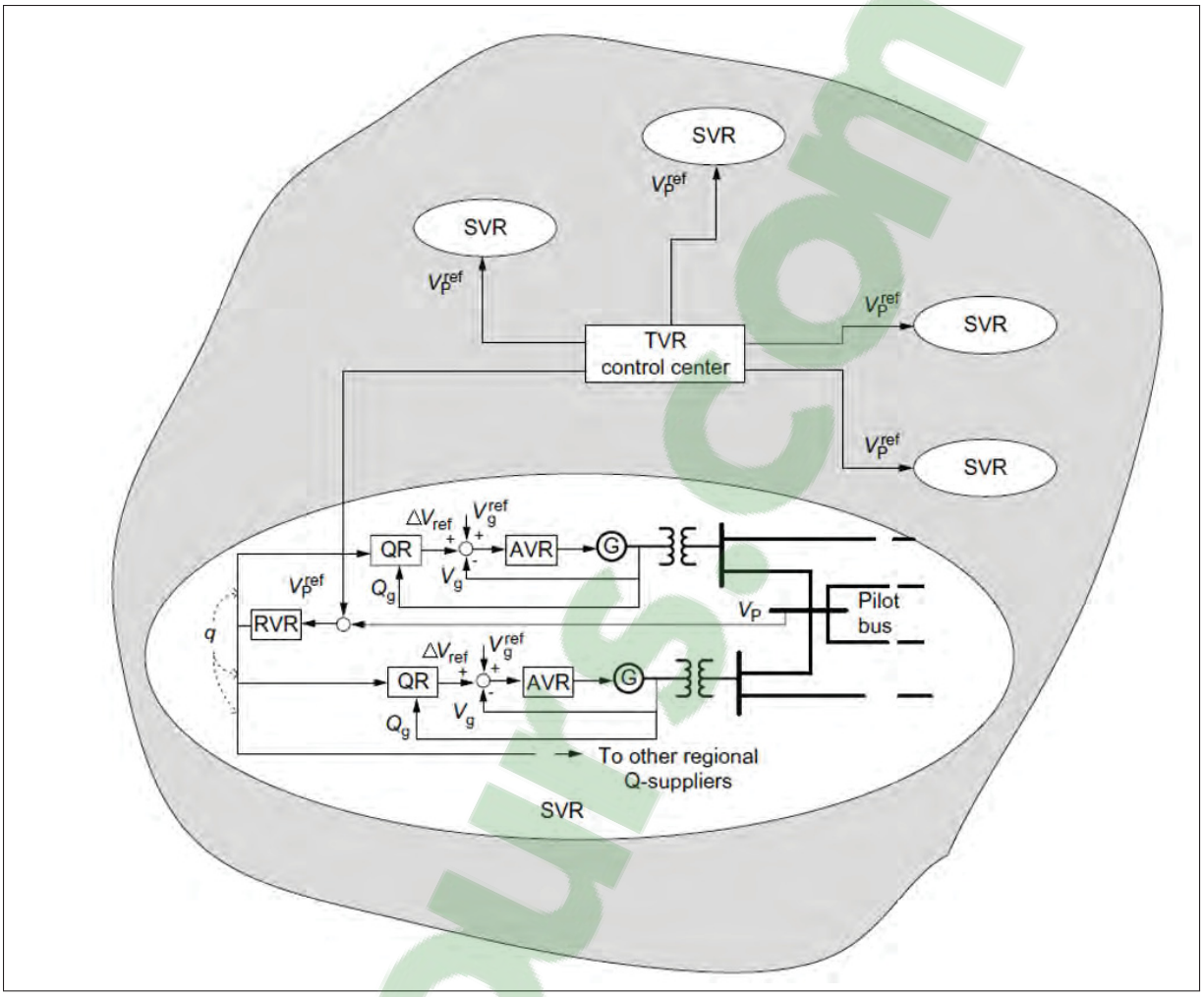

Figure 1.7 Structure of secondary voltage controller, Corsi (2015)

$$\Delta V_{ref} = K_{IQ} \int_0^t (Q_{ref} - Q_g)\, dt$$
$$with: \qquad (1.16)$$
$$V_{max} \le V \le V_{min}$$

Despite the advantages of SVC, the following limitations are pointed out in Lefebvre *et al.* (2000):

1. In some regions, coupling between theoretically independent zones has increased as a result of grid development subsequent to implementation of SVC. To avoid instability, we must therefore correct the number of zones or accept degradation in control dynamics;
2. SVC requires reactive-power alignment of the generating units involved, but makes no allowance for excessive demand that might be made on certain units as a result of differences in physical proximity;
3. The internal reactive-power control loop at generating-unit level is a destabilizing factor that can actually amplify the initial disturbance in the first few instants following certain incidents (generator dropout, for example);
4. The system makes only partial allowance for operating constraints. For example, it does not fully integrate monitoring of permissible voltage limits or generating set operating limits;
5. Control loop parameters are fixed, which precludes optimum allowance for operating conditions;
6. The signal representing the required reactive power level varies at a rate that makes no allowance for generating unit response capabilities.

Due to the limitations above, Paul *et al.* (1987); Lefebvre *et al.* (2000) presented Coordinated SVC which is discussed in the following.

1.3 Coordinated Secondary Voltage Control

The original method for CSVC is based on optimization which has been first introduced by EDF Paul *et al.* (1987) for French integrated power network. The cost function to be minimized is defined as follows:

$$\begin{aligned}\min_{\Delta U} \Big[& \lambda_V \left\| \alpha \left(V_C - V_P \right) - C_V \Delta U \right\|^2 \\ & + \lambda_q \left\| \alpha \left(Q_{ref} - Q \right) - C_q \Delta U \right\|^2 \\ & + \lambda_u \left\| \alpha \left(U_{ref} - U \right) - \Delta U \right\|^2 \Big]\end{aligned} \tag{1.17}$$

and it is subject to the following constraints:

$$
\begin{aligned}
&|\Delta U| \leq \Delta U_{max} \\
&V_{THT}^{min} \leq V_{THT} + C_V \Delta U \leq V_{THT}^{max} \\
&\alpha \left(Q + C_q \Delta U\right) + b\Delta U \leq c
\end{aligned}
\tag{1.18}
$$

where α is the control gain, U & ΔU are respectively terminal voltage reference of generators and its deviation, V_p and V_{THT} are voltage at pilot buses and voltage at high voltage side of the generators respectively, V_C is set-point values at pilot points and Q_{ref} and U_{ref} are set-point values for reactive power generation and for terminal voltage. Moreover, C_V and C_q are sensitivity matrices linking terminal voltage variation to pilot node voltage variation and generators' reactive power variation respectively. Mathematically:

$$
\begin{aligned}
\Delta V_p &= C_V \Delta U \\
\Delta Q &= C_q \Delta U
\end{aligned}
\tag{1.19}
$$

Unlike classical SVC which is based on PI control law, the optimization problem formulated in Equations 1.17 to 1.19 is a MIMO control problem which considers a linearized model of the system and takes into account all of the constraints when solving for the terminal voltage of the generators within one region. In this way, many pilot nodes could be controlled simultaneously by coordinating many generators in a region considering physical limitations.

CHAPTER 2

LITERATURE REVIEW

2.1 Introduction

In this chapter, a thorough review of the literature regarding to secondary voltage control is presented. In this regard, a brief history of different implementations of this method around the world is discussed. Afterwards a systematic approach is used to classify all related works in this domain. The classification is based on different considerations regarding to SVC problem which have been taken into account in the research work. The works are finally presented in tables.

2.2 Literature Review

The origins of wide area voltage and reactive power control could be traced back to reactive power dispatch problem in which the reactive power resources are allocated throughout the network to minimize power loss while maintaining voltage of the buses within desired limits. However this approach is based on the study of off-line forecasting while actual network operating conditions are often different from forecasted values and therefore unpredictable. In this way, some works at early 70s have considered real-time voltage/reactive power control, namely Hano *et al.* (1969); Nakamura & Okada (1969); Narita & Hammam (1971a,b) have proposed a centralized and decentralized real-time two stage optimization method which first minimizes voltage deviation using conjugate gradient method and second minimizes reactive power loss over transmission lines using direct search technique. In this work both continuous and discrete value compensators are considered, however discrete values are calculated by round off. The method was successfully implemented by Kyushu Electric Power Company in Japan.

Although the works presented earlier propose the partitioning of the transmission system for regional voltage control, the concept of hierarchical voltage control as well as classical secondary voltage control methodology are explicitly proposed in Arcidiacono *et al.* (1977);

Happ & Wirgau (1978); Arcidiacono (1983); Paul *et al.* (1987). In this method, the power network is divided into many theoretically non-interacting zones and at each zone, the most sensitive bus to reactive power disturbances is selected as pilot node. Voltage at this bus is then measured and compared with a desired voltage dictated by tertiary level controller. Regional controller, which is basically a PI controller calculates the total amount of reactive power that is needed to compensate the voltage deviation and sends this signal to the regional participant generators. At generation level, a reactive power control loop, which is also a PI controller, calculates the new voltage set-point for the AVR, considering the generator's participation factor as well as its reactive power limits. The proposed method was successfully implemented in Italian and French Power grids.

As has been discussed further in Lefebvre *et al.* (2000); Vu *et al.* (1996), the assumption of one sensitive bus per control zone may not be realistic for a densely meshed network, such as French transmission grid. For these networks, they have proposed CSVC algorithm, which is basically an optimal, model based, multi-input/multi-output, regional controller. CSVC uses voltage measurements from many sensitive buses in a control zone and calculates new set-points for generators that take part in secondary voltage control loop considering their reactive power and voltage limits. CSVC utilizes a linear sensitivity model which relates voltage magnitude to reactive power injection for all PQ buses in the grid. It also uses another sensitivity matrix which relates voltage at PV buses to voltage at PQ buses of the grid. Recalculation of these sensitivity matrices are triggered by an event or an incident (change of topology, unit tripping, major load change). Further details on the advantages of model based CSVC compared to the method presented in Arcidiacono *et al.* (1977); Arcidiacono (1983), can be found in Lefebvre *et al.* (2000); Vu *et al.* (1996).

Another approach regarding to the SVC is proposed by Ilic-Spong *et al.* (1988) which combines pilot bus selection and voltage control together to find minimal number of pilot nodes which are able to maintain voltage at the desired reference as well as the control gain. This method solves a mixed integer nonlinear program using SA.

The works presented so far have paved the way for hierarchical voltage control to be implemented in different countries around the world. A comprehensive review of different implementations of SVC in different countries can be found in Martins & Corsi (2007) and Corsi (2015).

Triggered by the above major works, a lot of effort has been made in academic domain also to improve these methods or to present alternative approaches. Each of these manuscripts investigate different aspects of SVC problem and take into account different considerations. However, by investigating these works, some common features are extracted and are used to classify the literature regarding to the SVC control design problem.

In the following, relative research works are summarized in two sections. In Section 2.3, research works related to Network partitioning, pilot bus selection and compensator allocation are reviewed. Afterwards, in Section 2.4 a general classification map is extracted based on the different aspects of secondary voltage control problem. An analysis of the current literature is presented and based on the drawbacks of the recent works the objectives of the proposed research are justified.

2.3 Network partitioning and pilot node selection

One of the earliest methods for pilot bus selection and network partitioning is presented in Corsi (2015) and applied in Italian network. The method is based on short-circuit capacities and sensitivity analysis of the network. In this approach, the buses are sorted from the most to the least sensitive one. Afterwards the least sensitive buses are selected as pilot nodes based on an iterative process. The number of pilot buses are dependent on two predefined parameters. The first parameter, $\frac{1}{\gamma}$, defines the minimum admissible threshold value of the short circuit power for a pilot node. Any bus with short circuit power smaller than this threshold will not be considered as a pilot bus. The second parameter is called coupling coefficient threshold, ϵ_p, which defines the minimum admissible limit for coupling of remote buses to a pilot bus. Any

remote bus with coupling value smaller than ϵ_p will not be considered in the same control area as the pilot bus.

Another major work regarding to pilot bus selection is presented in Ilic-Spong *et al.* (1988), in which a minimal number of pilot nodes are allocated using SA method to control the voltage in the network. In this approach pilot node selection and feedback gain design are mixed together and are done simultaneously. Conejo *et al.* (1994) compares different optimization algorithms to solve the same problem stated in Ilic-Spong *et al.* (1988). Also Sancha *et al.* (1995, 1996) and Amraee *et al.* (2012, 2010) have proposed different versions of the same method as Ilic-Spong *et al.* (1988).

Another category of network partitioning and pilot node selection is based on clustering methods. La Gatta *et al.* (2014) & Alimisis & Taylor (2015) have surveyed these methods thoroughly. In general, network partitioning based on clustering includes two steps: 1) A zoning algorithm which breaks the network into areas appropriate for SVC control and 2) A pilot node selection algorithm that identifies a representative bus of the zone for voltage control.

Clustering techniques to partition power grid are usually composed of three parts as below:

1. A proximity measure: An “electrical distance” that represents the degree of similarity for any two nodes;
2. A clustering criterion: A cost function or some other type of rule to form a number of zones utilizing the proximity measure;
3. Optimal number of clusters: A way to assess the appropriate number of clusters.

Table 2.1 summarizes the methods presented in the literature for network partitioning and pilot node selection.

Table 2.1 Summary of clustering techniques for network partitioning and pilot node allocation

Method	**Paper**	**Proximity measure**	**Clustering criterion**	**Optimal No. of cluster**
HCSD	Lagonotte *et al.* (1989)	Logarithm of the product of ratios of elements in vq sensitivity matrix	Agglomerative clustering (bottom to top) using complete linkage criterion	Where relative diameter for two consecutive no. of clusters are maximum
HCVS	Sun *et al.* (2013)	Euclidean norm of difference between vq sensitivity elements of two node	Agglomerative clustering (bottom to top) using average linkage criterion	Where average inter-cluster distance is maximum
SKC	Mehrjerdi *et al.* (2013b)	Normalized laplacian. Weights of adjacency matrix are the same as electrical distance defined in HCSD	Change of centroid points are below threshold	Given
FCM	Mehrjerdi *et al.* (2013a)	Same as HCSD	Weighted distance from centroid is smaller than a threshold. Weights are defined as fuzzy membership functions.	Given

2.4 Classification of SVC control design literature based on different aspects

Figure 2.1 shows a general scheme of different aspects of any SVC problem. Moreover Figures 2.2 to 2.6 illustrate each of these aspects in detail and classify the literature for each one which is sorted in a chronological order.

Figure 2.1 Classification of SVC Control desing aspects

2.4.1 Analysis of the literature

The analysis of the literature in this section follows the following assumptions:

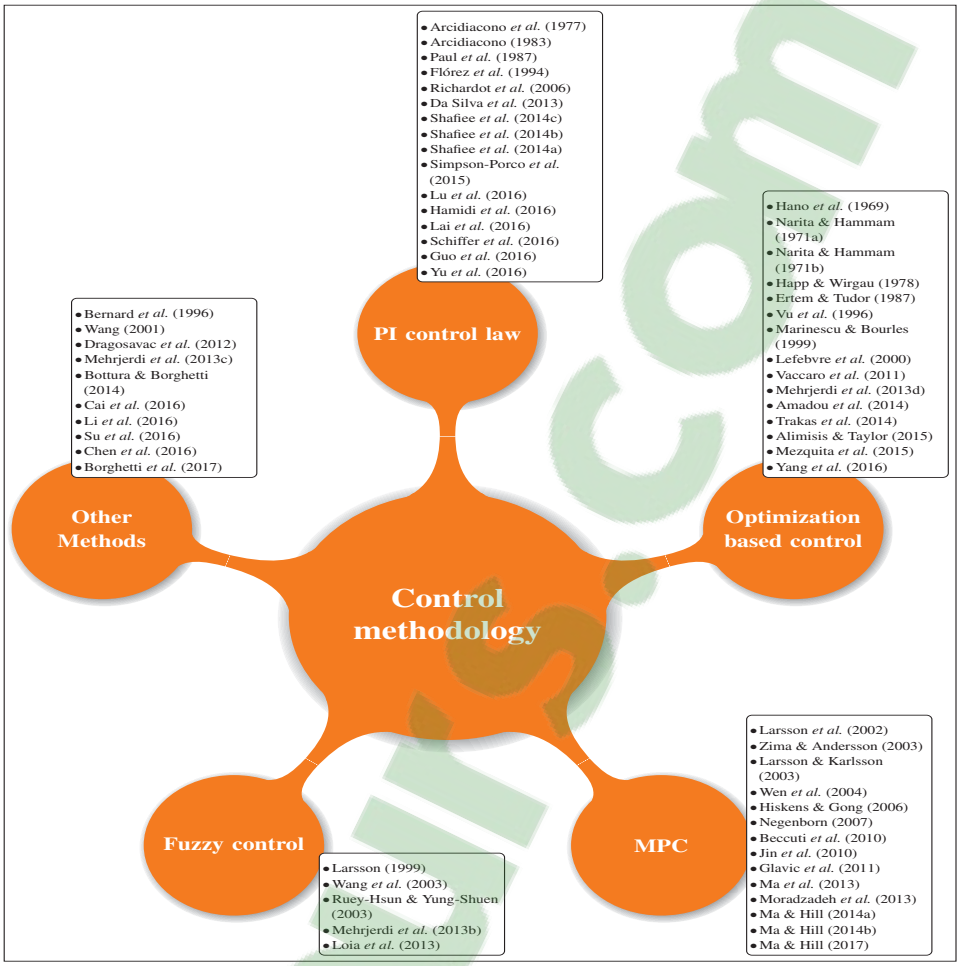

Figure 2.2 Classification based on control methodologies

- Due to the focus of this research work on the SVC in transmission system, only literatures implementing SVC in transmission grid are considered;
- To limit the scope of the analysis to recent literature, only works published from 2010 are considered.

Considering the above assumptions, the literature is narrowed down to Table 2.2.

In Beccuti *et al.* (2010) the SVC problem is formulated in a centralized way. However the optimization problem is decomposed using Lagrangian decomposition. In this way only local measurements are employed to achieve global optima.

Table 2.2 Summary of recent research works for SVC in transmission grid

Reference	**Control Method**	**Type of Model**	**Control Architecture**	**Type of compensator**
Beccuti *et al.* (2010)	MPC	Linear, Dynamic	Centralized	Continuous
Jin *et al.* (2010)	MPC	Linear, Dynamic	Centralized	Continuous & Discrete
Glavic *et al.* (2011)	MPC	Nonlinear, Static	Centralized	Continuous & Discrete
Dragosavac *et al.* (2012)	Feedback gain	Linear, Static	Centralized	Continuous
Mehrjerdi *et al.* (2013b)	Fuzzy control	Nonlinear, Static	Decentralized, considers the effect of neighbor areas, no consensus	Continuous
Ma *et al.* (2013)	MPC, multi-objective	Nonlinear, Dynamic, adaptive	Centralized	Continuous & Discrete
Moradzadeh *et al.* (2013)	MPC	Nonlinear, Dynamic	Decentralized, considers the effect of neighbor areas, no consensus	Continuous & Discrete
Da Silva *et al.* (2013)	PID control	Linear, Static	Decentralized, no consideration neighbor areas, no consensus	Continuous
Mehrjerdi *et al.* (2013d)	Optimization	Nonlinear, Static	Decentralized, considers the effect of neighbor areas, no consensus	Continuous
Mehrjerdi *et al.* (2013c)	Neural Network	Nonlinear, Static	Decentralized, considers the effect of neighbor areas, no consensus	Continuous
Ma & Hill (2014a)	MPC, multi-objective	Nonlinear, Dynamic	Centralized	Discrete
Ma & Hill (2014b)	MPC, multi-objective	Nonlinear, Dynamic	Centralized	Discrete
Amadou *et al.* (2014)	Optimization	Linear, Static	Decentralized, no consideration neighbor areas, no consensus	Continuous
Trakas *et al.* (2014)	Optimization	Nonlinear, Static, Probabilistic	Decentralized, considers the effect of neighbor areas, no consensus	Continuous
Mezquita *et al.* (2015)	Optimization	Nonlinear, Static	Centralized	Continuous
Su *et al.* (2016)	Successive Minimization	Nonlinear, Static	Centralized	Continuous

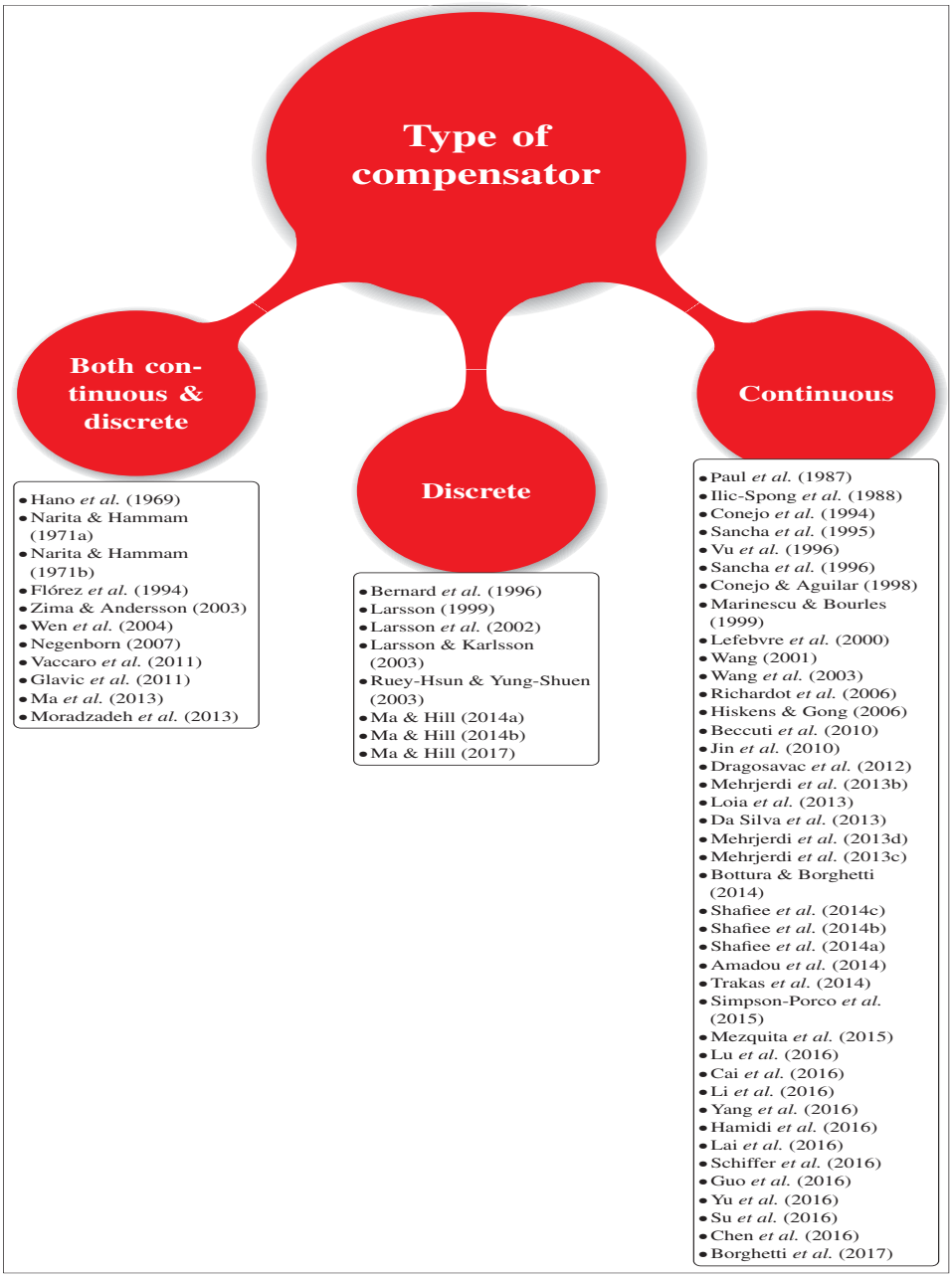

Figure 2.3 Classification based on type of compensator

In Jin *et al.* (2010) a real-time protection and security scheme is presented with centralized MPC in its core. Voltage stability margins are also considered as constraints inside optimization problem. The optimization problem is formulated as QP and then the calculated continuous values are discretized.

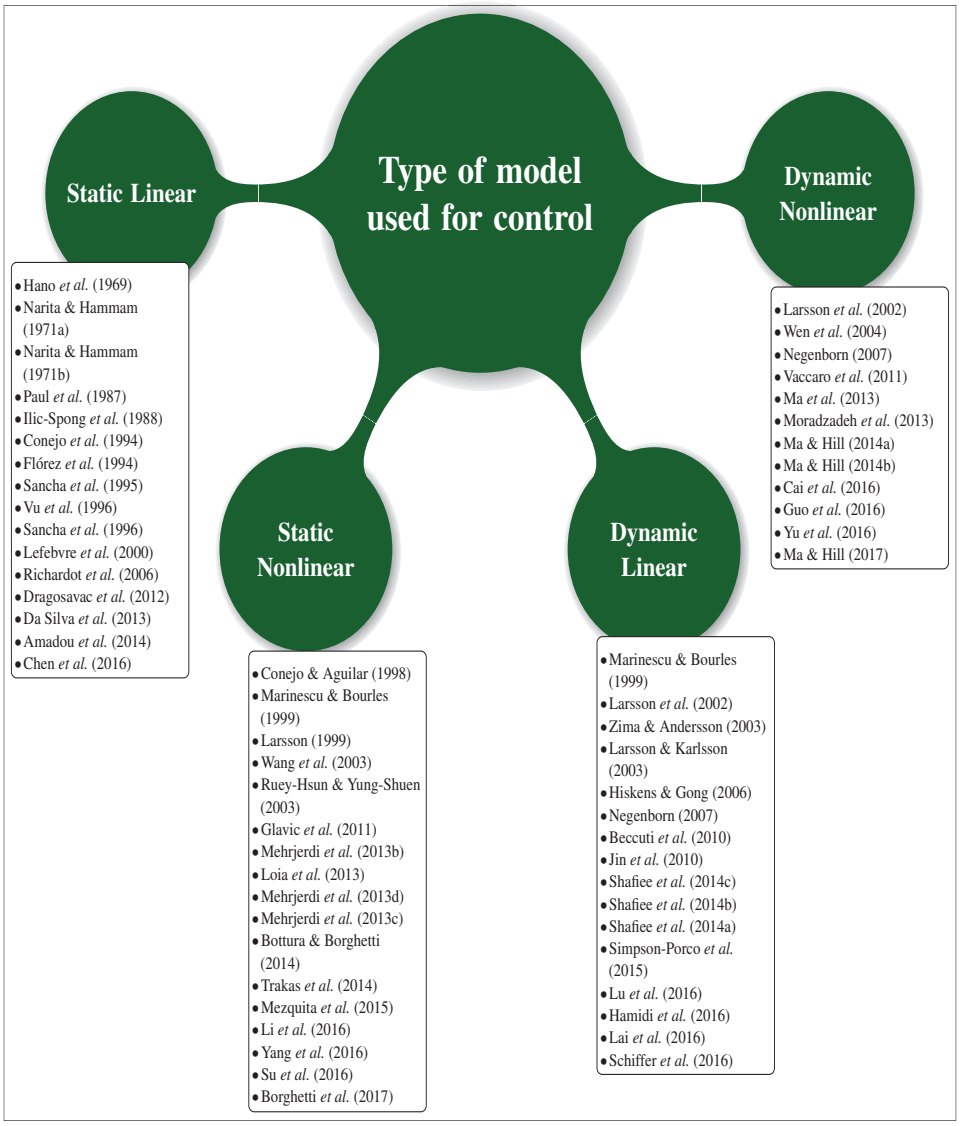

Figure 2.4 Classification based on type of model used for control

Also in Glavic *et al.* (2011) unlike MPC which uses dynamic model of the system, a static power flow model is used for few consecutive time steps considering a time varying model of the load. Discrete variables are assumed to be continuous and then rounded off to the closest discrete value. The effect of Over excitation limiter is also modeled as constrains which are only forced at the end of control horizon .

On the other hand, Dragosavac *et al.* (2012) coordinates all generators in one power plant based on the QV sensitivities while maintaining the voltage of the connected bus during con-

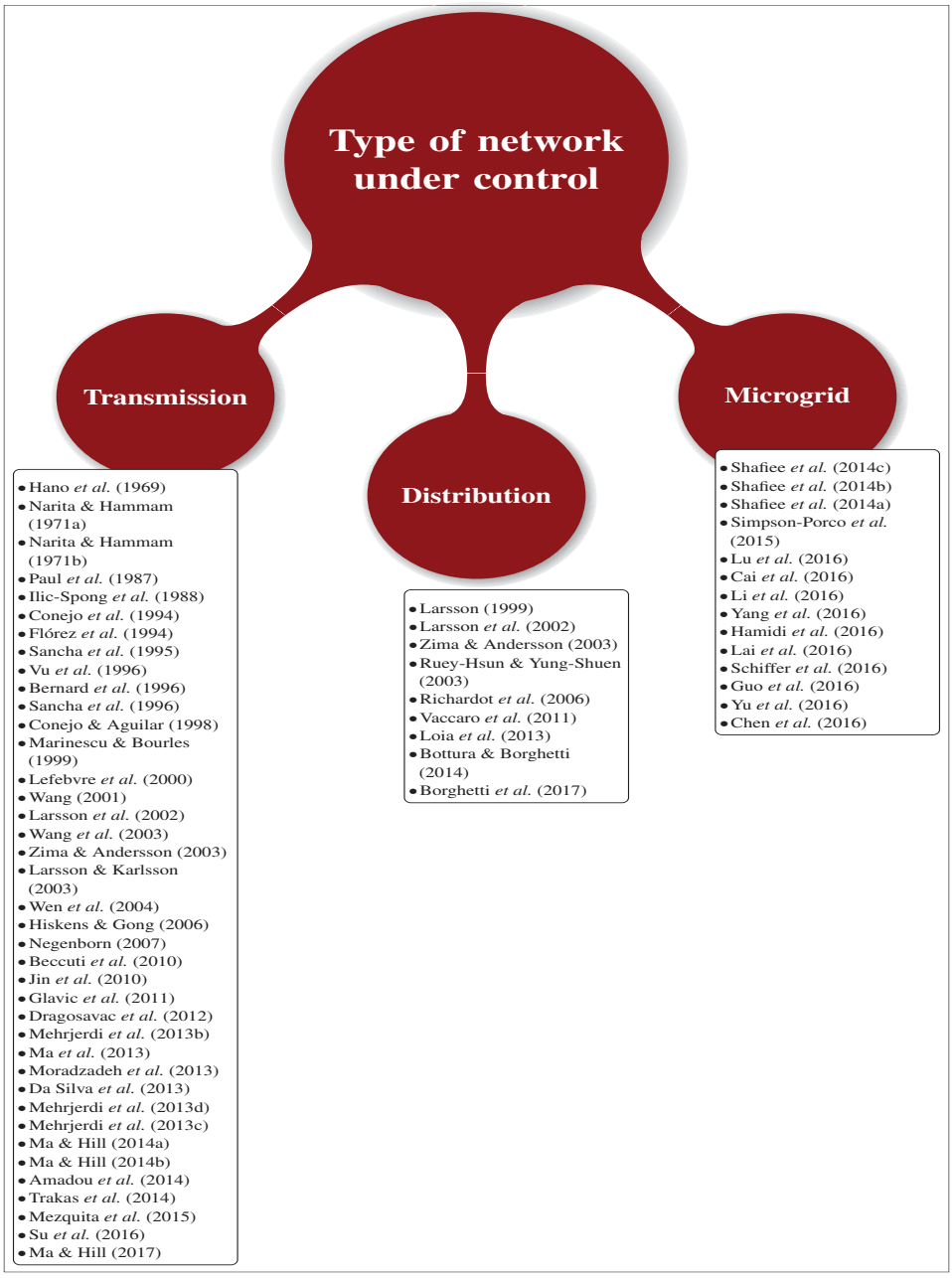

Figure 2.5 Classification based on type of network under control

tingencies. The control is done in two steps: 1-Voltage controller which relates the voltage of power plant bus bar (high side) to the total required reactive power. 2-Reactive power controller which defines the share of each generator for the compensation. Outputs are defined as reference voltage variations.

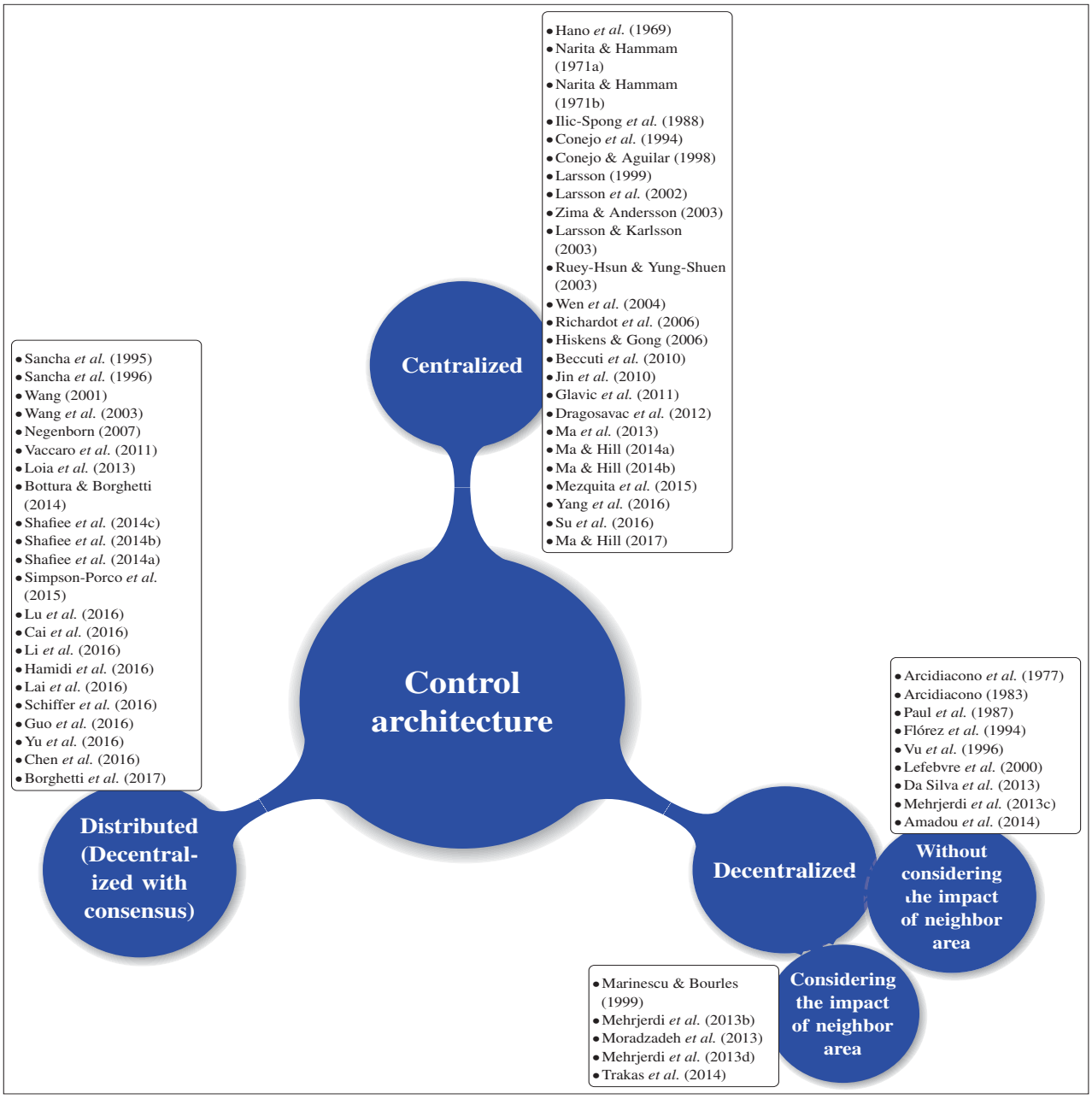

Figure 2.6 Classification of SVC literature based on controller design architecture

Mehrjerdi *et al.* (2013b) present a K-way partitioning method to divide the Laplacian graph of the network. Then pilots are selected as most sensitive buses through applying different levels of disturbance to each region. Finally, a fuzzy controller is designed for each region which considered the effect of the neighbors by measuring tie-line reactive power.

Also in Ma *et al.* (2013) a multi-objective optimization method is formulated and solved using GA. First objective is to maintain voltage at reference while the second one is to minimize the switching steps of the compensators. At each run, the solution is saved in a knowledge based memory which will be used later in the initial population of the GA when similar situation occurs.

Moreover, Moradzadeh *et al.* (2013) propose a nonlinear hybrid model as a model of the system which includes the model of OLTC and OEL. Greedy method is used to solve combinatorial optimization problem for each area. The planned local value is communicated to the neighbor areas for their next time step.

In Da Silva *et al.* (2013), a classical SVR using PI control law is presented. The novelty is to add joint line droop compensation to the control loop.

In Mehrjerdi *et al.* (2013d), coordination between regional controllers is studied. A connection matrix is defined which represent the connection between regional controllers and also between the controllers of the neighbor areas. Based on this matrix, the regions which have connection between their controllers are aggregated and the optimization is solved for the aggregated network.

Also in Mehrjerdi *et al.* (2013c) the model of each region is identified using Neural Network. From this model then a reverse model is identified as the controller who is also a neural network.

In addition, in Ma & Hill (2014a) same approach as Ma *et al.* (2013) with more details and discussion on how to create an off-line data base of knowledge. How the controller works. And how the knowledge is integrated to the controller. Then Ma & Hill (2014b) discuss the adaptive feature of the controller in details.

In Amadou *et al.* (2014), first the compensators clusters are identified using agglomerative hierarchical algorithm. The proximity of the nodes which is based on the normalized susceptance matrix is used as the criterion. Second the load buses are classified and the pilot nodes are

selected using method presented in Arcidiacono *et al.* (1977). For control, method presented in Paul *et al.* (1987) is used.

Also in Trakas *et al.* (2014) particle swarm optimization is used to solve probabilistic optimization problem to find optimal voltage reference of generators as well as reactive power injection by capacitors. Voltage of the boundary buses are also kept constant to avoid the interference of the areas on each other.

Moreover Mezquita *et al.* (2015) propose a self organizing map to partition the network based on the electrical distance metric. For pilot bus selection, method presented in Ilic-Spong *et al.* (1988) is used. For control, optimal power flow is used. Calculated continuous shunt values are finally discretized to the closest discrete value.

Finally in Su *et al.* (2016), a successive linearization of nonlinear function is used to solve nonlinear optimization problem in which the objective function is defined as the infinity norm of voltage error.

Analysing the methods above, the following drawbacks are observed:

1. In Jin *et al.* (2010); Glavic *et al.* (2011); Mezquita *et al.* (2015) the optimization problem is originally solved as a continuous type problem and the value for discrete type compensators are then approximated by rounding off continuous values. Although this assumption is computationally beneficial, neglecting the round-off error especially when the discrete steps are large, may lead to oscillatory behavior when the problem is solved for consecutive time steps;
2. The method presented in Ma *et al.* (2013); Ma & Hill (2014a,b) is a centralized approach which has only considered discrete type compensator. The algorithm lacks considering the continuous type compensators. Moreover due to the local nature of the voltage control problem there is no need to apply a centralized approach which is computationally inefficient;

3. Decentralized methods presented in Mehrjerdi *et al.* (2013b); Moradzadeh *et al.* (2013); Da Silva *et al.* (2013); Mehrjerdi *et al.* (2013d,c); Amadou *et al.* (2014); Trakas *et al.* (2014) have not considered any consensus between regional controllers. In this regard, action of some compensators in one region might have impacts on the voltage of the pilot bus for a neighbor region which is not seen by the SVC of the neighbor region. In some cases, such an uncoordinated strategy between regional controllers may lead to oscillatory behaviors and voltage collapse;
4. Validation of the methods is limited to off-line simulations while only small test-cases such as IEEE 39 and 118 bus system are considered. Although the methods are proved to be operational for such test-cases, their operation might face challenges which comes to a large scale power system, hence they should be evaluated for such realistic test-cases.

2.5 Conclusion

Based on the analysis of the literature review done in Section 2.4.1, the need for a decentralized SVC method which considers the nonlinearities of the system and takes into account both continuous and discrete type compensator in the optimization problem while considering consensus between regional controllers is felt. This is inline with the objectives and methodologies of this research work which are presented in sections 0.2 and 0.3 respectively.

CHAPTER 3

DECENTRALIZED COORDINATED SECONDARY VOLTAGE CONTROL OF MULTI-AREA POWER GRIDS USING MODEL PREDICTIVE CONTROL

Arvin Morattab[1], Ouassima Akhrif[1], Maarouf Saad[1]

[1] Department of Electrical Engineering, École de Technologie Supérieure,
1100 Notre-Dame Ouest, Montréal, Québec, Canada, H3C 1K3

Paper published in *IET Generation, Transmission & Distribution*, May 2017

Abstract

This manuscript presents a decentralized control scheme for CSVC of large-scale power networks. In this way, for each area of the power grid, an MPC which modifies the set-points of reactive power compensators participating in CSVC algorithm is designed. The proposed controller takes into account reactive power limits of these compensation devices. The novelty of the method lies in the consideration of measured reactive power deviation on tie-lines between neighboring areas as measured disturbance and compensation of the disturbance by regional MPC controllers. As another contribution of this work, the validation of the proposed algorithm is done in real-time simulation environment in which the decentralized MPC controllers are run in parallel on separate computational cores. The stability and robustness of the presented algorithm is validated for a large scale realistic transmission network with 5000 buses considering standard communication protocols to send and receive the data. Simulation results show that the proposed method can regulate the voltages on the pilot buses at the desired values in presence of load variations and communication delays. Finally, the computational burden of the proposed method is evaluated in real-time.

Introduction

One of the well-known strategies toward voltage control in large-scale multi-area power networks is to use a hierarchical control structure. In this method, the controller consists of three

levels in which the lowest level, i.e. primary controller, tries to maintain transient voltage stability at local buses, while the secondary level controller works regionally to maintain long-term voltage stability by balancing reactive power supply and demand through injection/absorption of reactive power into/from the network. The latter is done by controlling the voltage of some sensitive load buses (PQ buses) of each area, called pilot nodes. The reactive power needed for such control can be either injected/absorbed by generators or using VAR compensation devices such as capacitor/inductor banks, static var compensator and FACTS. Finally, at the highest level of the hierarchical controller, i.e. tertiary level, economic and security concerns of the overall power system are maintained. The operation of different levels of this hierarchical controller is divided geographically and temporally so that they have minimum interference between each other. In this way, the primary, secondary and tertiary level controllers react in few seconds, few minutes and up to 15 minutes while they operate locally, regionally and nationally.

A lot of research has been done regarding hierarchical secondary voltage control since its introduction by EDF in 1985 Paul *et al.* (1987). This research covers many aspects of such strategy including division of the large-scale power network into electrically distant areas (Mehrjerdi *et al.* (2013b); Kamwa *et al.* (2009); Tuglie *et al.* (2008)), selection of the pilot buses (Mehrjerdi *et al.* (2013b); Conejo & Aguilar (1998); Lerm (2006); Amraee *et al.* (2012)), locating the reactive power compensators over the network (Ghahremani & Kamwa (2013); Pretelt (1971); Mendoza *et al.* (2007); Happ & Wirgau (1978); Ertem & Tudor (1987)) as well as controller design techniques (Vu *et al.* (1996); Lefebvre *et al.* (2000); Richardot *et al.* (2006); Sancha *et al.* (1995); Wang (2001); Wang *et al.* (2003); Larsson (1999); Larsson *et al.* (2002); Fenichel (1979); Juang & Pappa (1985); Moore (1981); Marinescu & Bourles (1999); Zima & Andersson (2003); Larsson & Karlsson (2003); Wen *et al.* (2004); Hiskens & Gong (2006); Beccuti *et al.* (2010)). Since the contributions of this manuscript are mostly related to control design technique and its validation, the following literature review is mainly focused on this aspect of the works.

Regarding controller design techniques, these researches mostly consider CSVC of reactive compensators in transmission and distribution networks, as well as the interaction between neighbor areas and the impact of DG. In this way, Vu *et al.* (1996); Lefebvre *et al.* (2000) have applied a centralized multivariable optimal control strategy for meshed power grids to minimize voltage deviations at pilot buses considering generators reactive power limits, generator buses and pilot buses voltage limits. Moreover, sensitivity matrices have been used to describe input-output relations of the network. The static optimization approach discussed in Paul *et al.* (1987) has been used in Richardot *et al.* (2006) considering DGs effect in CSVC algorithm. Also Sancha *et al.* (1995) has proposed a decentralization of the same approach for CSVC of multi area power systems. In Larsson *et al.* (2002), a predictive control with tree search optimization method is applied to coordinate capacitor banks and tap-changers. Moreover Wang (2001); Wang *et al.* (2003); Larsson (1999); Fenichel (1979) apply different fuzzy control techniques for CSVC problem. In this regard, Wang (2001) and Wang *et al.* (2003) have proposed a multi-agent, fuzzy based control method for coordination of AVRs, SVCs and STATCOM in the case of power system contingencies. Moreover Larsson (1999) has used a fuzzy rule based controller to coordinate cascade tap-changers in radial distribution feeders. In addition, Fenichel (1979) utilizes a set of information collected by modal analysis to formulate a two stage fuzzy logic-based model, considering voltage variation on load buses and reactive power reserve of compensators as input, and also generator's reference voltage as output.

The control methods discussed so far have designed secondary voltage controllers assuming post-contingency stability of the network, i.e the transient response of the system is assumed to vanish after few seconds and the network reaches its new steady state due to the operation of the primary level controllers. In this way, a static model of the system can be used for secondary level controllers. Although this assumption is computationally beneficial, there are certain slow dynamics in the network which might result in voltage instability and eventually voltage collapse when the system is working close to its limits or faces harsh disturbances such as change of topology, unit tripping and major load changes. A solution to this problem is to

use MPC method in which a real-time optimization problem is solved at each time step of the controller based on a pre-identified dynamic model of the power network.

Considering MPC applications in secondary voltage control, Marinescu & Bourles (1999) has proposed an MPC based algorithm using both static and dynamic optimization methods. In Zima & Andersson (2003), MPC has been used for emergency voltage control and the model is defined based on sensitivity analysis of network's dynamic model. Larsson & Karlsson (2003) has applied tree search optimization techniques inside MPC algorithm to coordinate generators, tap changers as well as load shedding in extreme conditions. In Wen *et al.* (2004), the nonlinear model of the grid has been used as the model for MPC and Euler state prediction and pseudo gradient evolutionary programming is used to develop the coordinated controller. In Hiskens & Gong (2006), MPC method is used to determine minimum amount of load shedding to restore system voltages. Beccuti *et al.* (2010) has considered both coordination of generators and load shedding using MPC and the optimization is formulated as a centralized quadratic programming via Lagrangian decomposition. In Jin *et al.* (2010), shunt capacitors are switched based on control commands generated by MPC to prevent voltage collapse and to maintain a desired stability margin after a contingency. Also Glavic *et al.* (2011) has used a multi-step optimization method for MPC controller to improve voltage profile in transmission network and to prevent long-term voltage instability. Finally, Moradzadeh *et al.* (2013) has applied MPC algorithm in a distributed way for CSVC of multi-area power systems. In this method, a communication line is established between CAs designed for each area so that regional controllers take into account decisions made by their neighboring areas' optimization algorithm.

In recent years, the growing trend toward smart grids with integration of DERs has led to a major shift in researches regarding to voltage control. These works have mostly focused on the application of adaptive cooperative multi-agent control techniques in transmission & distribution Vaccaro *et al.* (2011); Loia *et al.* (2013); Ma *et al.* (2013); Ma & Hill (2014a,b); Bottura & Borghetti (2014); Su *et al.* (2016); Borghetti *et al.* (2017) as well as micro-grids Shafiee *et al.* (2014c,b,a); Simpson-Porco *et al.* (2015); Lu *et al.* (2016); Cai *et al.* (2016); Li *et al.*

(2016); Yang *et al.* (2016); Hamidi *et al.* (2016); Lai *et al.* (2016); Schiffer *et al.* (2016); Guo *et al.* (2016); Yu *et al.* (2016); Ma & Hill (2017).

Focusing on the works on transmission & distribution, Vaccaro *et al.* (2011) proposes a decentralized non-hierarchical voltage regulation architecture in which the states regarding to the dynamics of the neighbor areas are synchronized to the weighted average of the variables sensed by all the controllers in the smart grid. Moreover, Loia *et al.* (2013) proposes decentralized and non-hierarchal voltage control architecture based on cooperative fuzzy agents to achieve consensus. Also Ma *et al.* (2013); Ma & Hill (2014a,b) propose an adaptive centralized CSVC method in which a multi-objective optimization problem is solved using GA to find pareto-optimal solution, i.e. switching of OLTC & capacitor banks. In addition Bottura & Borghetti (2014); Borghetti *et al.* (2017) discusses an asynchronous leaderless multi agent approach that coordinates the reactive power compensators. This paper also presents a simulation test-bench in which an electro-mechanical transient program, EMTP-rv, is interfaced with a communication network simulator, OPNET, to validate the performance of the proposed algorithm as well as the effects of communication network latency and packet loss. Finally, Su *et al.* (2016) formulates CSVC as a nonlinear successive ∞-norm minimization problem in which the load disturbances are estimated on-line.

This study proposes a DCSVC approach using MPC method for Multiple TSO power grids. It is assumed that control areas are selected in a way that there are minimum interferences between regional MPCs. Hence, unlike Vaccaro *et al.* (2011), no communication links are established between regional controllers and the DCSVC of each area does not need to know any quasi-state space model of the neighbors. However, the supplementary information on inter-area disturbances is obtained by measuring tie-line reactive power deviations using installed PMU. It is also shown that the proposed method can be implemented on large scale transmission systems such as the 5000 bus power network used in this study.

Another contribution of this work is to propose a real-time test bench to test and validate wide area control algorithms such as the proposed DCSVC. Unlike Bottura & Borghetti (2014);

Borghetti *et al.* (2017), the proposed test-bench operates in real-time. This test-bench is also flexible to apply any control strategy, either for voltage or frequency, and using centralized, decentralized, or distributed control architectures. In case of decentralized and distributed topologies, a dedicated computational core can be assigned to each regional controller, hence making it suitable for performance evaluation of such control strategies.

The real-time test-bench is implemented using OPAL-RT's Real-time simulator, having ePHASORsim as its main phasor domain solver Jalili-Marandi *et al.* (2013),Opal-RT (2018). ePHASORsim is designed for real-time simulation of transient stability phenomena for large-scale transmission and distribution power systems. In contrast to off-line simulation tools such as PSS/e..., the real-time performance of ePHASORsim makes it a suitable tool to play as a backbone simulation engine to test, validate, and tune local and wide area control and protection schemes. The controller and power system can run on separate platforms and link together through Ethernet based protocols (such as DNP, C37.118 , etc.).

The rest of this paper is organized as follows: Section 3.1 discusses the principle of the proposed decentralized MPC algorithm and its application to CSVC problem. Section 3.2 presents the proposed real-time test-bench for decentralized architecture of DCSVC in which computations regarding to regional controllers are done in parallel cores while the phasor domain dynamic model of the power network is run on a separate one. Section 3.3 presents the DCSVC procedure applied on a large power system with 5000 buses in three steps: First step includes pilot bus selection, controllers' allocation and network partitioning using sensitivity analysis described in Corsi (2015). Following, system identification procedure toward finding linear dynamical equivalent of each area of partitioned network suitable for MPC algorithm is discussed. The model is identified considering voltages at pilot buses as measured outputs and set-points of compensation devices as control inputs. Moreover generated reactive power by these compensators are defined as unmeasured outputs. These estimated outputs are used by MPC to respect the reactive power limits imposed by physical limitations. Real-time evaluation of DCSVC algorithm on this network shows its scalability to be implemented on realistic large-scale power grids. Finally, Section 3.4 concludes the paper and discusses future works.

3.1 Decentralized Model Predictive Coordinated Secondary Voltage Control

3.1.1 Model Predictive Control formulation

Consider that the dynamic behavior of a system is approximated by LTI state space model as follows:

$$\begin{aligned} x(k+1) &= Ax(k) + B_u u(k) + B_v v(k) + d(k) \\ y_m(k) &= C_m x(k) + D_{vm} v(k) \\ y_u(k) &= C_u x(k) + D_{vu} v(k) \end{aligned} \tag{3.1}$$

Where $x(k)$ is the n_x-dimensional state vector of the system, $u(k)$ is the n_u-dimensional vector of control inputs, $v(k)$ is the n_v-dimensional vector of measured disturbances, $d(k)$ is the n_d-dimensional vector of unmeasured disturbances entering the system, $y_m(k)$ is the vector of measured outputs, and $y_u(k)$ is the vector of unmeasured outputs. The overall n_y-dimensional output vector $y(k)$ combines both $y_m(k)$ and $y_u(k)$, i.e. $y(k) = [y_m(k), y_u(k)]^t$.

Figure 3.1 illustrates a general scheme of MPC controller. As can be seen, the controller consists of three main blocks which are Estimation, Prediction and optimization. The LTI model of Equation 3.1 is used by the estimation and prediction blocks to estimate the state vector and then to predict future outputs. By employing these two steps, the dynamics of the system are translated to constraints of an optimization problem in which the only unknown is a vector of successive control variables increments in a finite horizon, called control horizon. At time k the procedure toward finding the optimal control input, $u^*(k)$, is described as follows:

3.1.1.1 State estimation

The estimator is a Kalman filter which estimates the state vector, $\hat{x}(k)$, knowing previous estimated state $\hat{x}(k-1)$, measured output $y_m(k)$, measured disturbance $v(k)$ and also previous value of control input, $u^*(k-1)$ in presence of the unmeasured disturbance, $d(k)$. the unmea-

sured disturbance is generally defined as the output of a linear disturbance model for which the input is considered to be a white noise with a known covariance matrix.

3.1.1.2 Prediction

The estimated state is then used by the predictor to define the p-step ahead outputs of the system, $\hat{y}(k+i|k) \quad i = 1, \cdots, p$, as a linear function of future control input increments. In this formulation, p is called prediction horizon. Reference Camacho & Alba (2013) derives predictor equations as shown in Equation 3.2 & Equation 3.3.

$$\begin{bmatrix} \hat{y}(k+1|k) \\ \hat{y}(k+2|k) \\ \vdots \\ \hat{y}(k+p|k) \end{bmatrix} = S_x \hat{x}(k) + S_{u*} u^*(k-1) + S_u \begin{bmatrix} \Delta u(k) \\ \Delta u(k+1) \\ \vdots \\ \Delta u(k+p) \end{bmatrix} + S_v \begin{bmatrix} v(k) \\ v(k+1) \\ \vdots \\ v(k+p) \end{bmatrix} \tag{3.2}$$

in which:

$$S_x = \begin{bmatrix} CA \\ CA^2 \\ \vdots \\ CA^p \end{bmatrix}, S_{u*} = \begin{bmatrix} CB_u & D_u & 0 & \dots & 0 \\ CAB_u & CB_u & D_u & \dots & 0 \\ \vdots & \vdots & \vdots & \ddots & \vdots \\ CA^{p-1}B_u & CA^{p-2}B_u & CA^{p-3}B_u & \dots & D_u \end{bmatrix}$$

$$S_v = \begin{bmatrix} CB_v & D_v & 0 & \dots & 0 \\ CAB_v & CB_v & D_v & \dots & 0 \\ \vdots & \vdots & \vdots & \ddots & \vdots \\ CA^{p-1}B_v & CA^{p-2}B_v & CA^{p-3}B_v & \dots & D_v \end{bmatrix} \tag{3.3}$$

$$S_u = \begin{bmatrix} D_u + CB_u & D_u & 0 & \dots & 0 \\ D_u + CB_u + CAB_u & D_u + CB_u & D_u & \dots & 0 \\ \vdots & \vdots & \vdots & \dots & \vdots \\ D_u + \sum_{i=1}^{p} CA^{p-i}B_u & D_u + \sum_{i=2}^{p} CA^{p-i}B_u & D_u + \sum_{i=3}^{p} CA^{p-i}B_u & \dots & D_u + CB_u \end{bmatrix}$$

In this formulation, the control input increment is defined as $\Delta u(k+i) = u(k+i) - u(k)$. For simplicity, we also assume that $v(k+i) = v(k)$ for $i = 1, \dots, p$. In this way, the dynamic behavior of the system for duration of $[k, k+p]$ is translated to a set of linear equations in which the only unknowns are control input increments, $\Delta u(k+i)$ for $i = 0, \dots, p$.

3.1.1.3 Optimization

The optimizer then calculates this unknown control sequence by solving an optimization problem which minimizes the quadratic objective function in Equation 3.4 subject to the system constraints. Different QP techniques exist in the literature to solve the optimization problem of Equation 3.4. A comprehensive review of existing QP methods is presented in Camacho & Alba (2013). In this paper, the method presented in Schmid & Biegler (1994) is used.

$$\min_{\Delta u(k),\cdots,u(k+p-1)} \sum_{j=1}^{p} \Delta y(k+j)^t Q \Delta y(k+j) + \Delta u(k+j)^t R \Delta u(k+j)$$

$$\Delta y(k+j) = (y_m(k+j) - r(k))$$

$$s.t:$$

$$1) Equations\ 3.2\ \&\ 3.3$$

$$2) y_{min} < y(k+j) < y_{max}$$

$$3) u_{min} < u(k+j) < u_{max}$$

$$4) \Delta u_{min} < \Delta u(k+j) < \Delta u_{max} \tag{3.4}$$

Beside constraints forced by the predictor, u_{max} and u_{min} define maximum and minimum limits of control inputs and Δu_{max} and Δu_{min} define maximum and minimum limits on control input increments. Moreover, limits on output vectors are defined by y_{max} and y_{min}.

In order to deal with the computational burden of optimal controller, the degrees of freedom of the optimization problem (number of unknown variables) can usually be reduced by considering constant control inputs after several time-steps, i.e. $\Delta u(k+j) = 0$ for $j = m, \cdots, p.$ in which m is defined to be the control horizon. By this assumption, the optimization problem defined by Equation 3.4 can be solved by available methods for quadratic optimization problems. Considering $[\Delta u^*(k), \cdots, \Delta u^*(k+m-1)]$ as the optimal control solution, the first element of this vector, $\Delta u^*(k)$, is finally used to find the control input using $u^*(k) = u^*(k-1) + \Delta u^*(k)$ which will be applied on the real system. The whole procedure will be repeated in the next sampling time with the prediction frame moving one sampling interval forward.

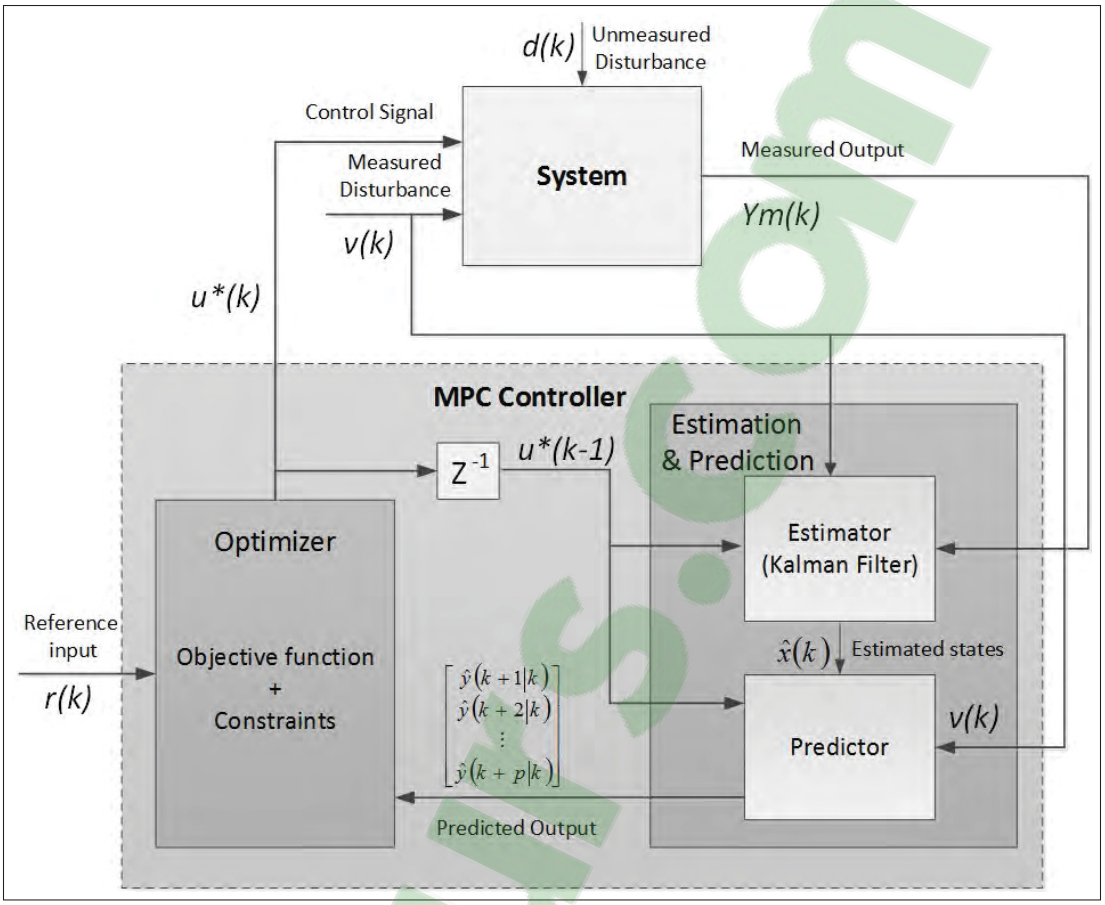

Figure 3.1 General MPC Scheme

In the following, a decentralized version of the MPC method is adopted for large-scale power system's secondary voltage control application.

3.1.2 Proposed DCSVC scheme

Figure 3.2 illustrates a typical three-area power network with their corresponding DCSVC controller. The proposed approach can be generalized to any continuous type reactive power compensator, however in Figure 3.2, we have used exciters connected to synchronous machines, shown as SM in, and SVCs to describe the proposed method. In this figure, V_{PN}^{ij} is the voltage at j^{th} pilot node in Area i which should be maintained close to its desired value, V_{PNd}^{ij}, defined by tertiary level controller. This control is done by voltage for j^{th} exciter or SVC participating in the DCSVC of Area i, V_{ref}^{ij}. Furthermore, the interaction of neighboring

areas is represented by the reactive power transferred through n_{ij} different tie-lines between Area j to Area i defined by Q_{tie}^{ijl} in which $l = 1, \cdots, n_{ij}$. The tie line vector is then defined as $Q_{tie}^{ij} = \left[Q_{tie}^{ij1}, \cdots, Q_{tie}^{ijn_{ij}}\right]$ which is measured on mutual buses of tie-lines. The values of V_{PN}^{ij} and Q_{tie}^{ij} are measured by DCSVCi and then the control input V_{ref}^{ij} is calculated. The objective here is to apply the MPC Algorithm as a DCSVC to each area of multi-area power network in Figure 3.2. The challenges are how to define the model, objective function and constraints in Equation 3.4 for DCSVC problem. For this reason, the inputs and outputs of the system for DCSVC problem based on general MPC scheme in Section 3.1.1, are presented in Table 3.1.

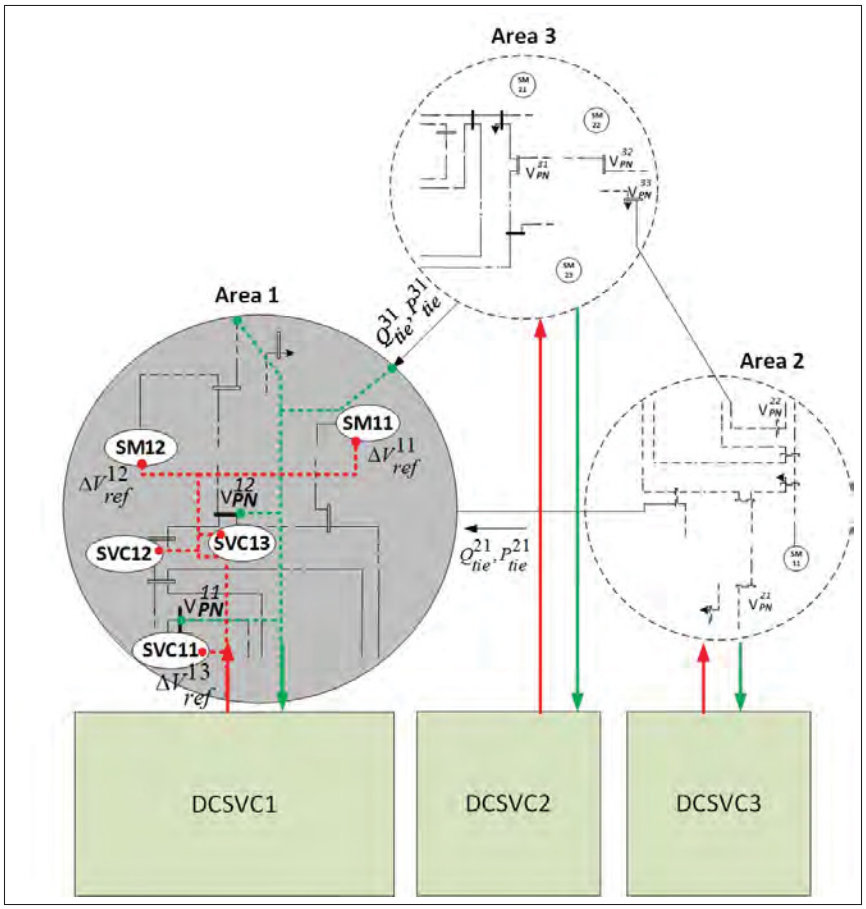

Figure 3.2 DCSVC algorithm for multi-area power grid

According to this table, the state space model for Area i is defined as follows:

Table 3.1 Signal mapping between general MPC scheme and DCSVC scheme

Signal in General MPC Scheme	**Corresponding Signal for DCSVC model**
Reference Input $r(k)$	Desired Voltage at pilot buses $V_{PNd}^{ij}(k)$
Control Input $u(k)$	Changes of reference voltage of compensator devices $V_{ref}^{ij}(k)$
Measured disturbance Input $v(k)$	Tie-line reactive power $Q_{tie}^{ij}(k)$
Unmeasured disturbance Input $d(k)$	Load changes, faults, un-modeled dynamics, ...
Measured Output $y_m(k)$	Pilot bus voltage $V_{PN}^{ij}(k)$
Unmeasured Output $y_u(k)$	Injected reactive power by Compensators (synchronous machines and static var compensators, ...) $Q_{COMP}^{ij}(k)$

$$
\begin{aligned}
x^i(k+1) &= A^i x^i(k) + B_u^i V_{ref}^i(k) + B_v^i Q_{tie}^i(k) + d(k) \\
V_{PN}^i(k) &= C_m^i x^i(k) + D_{vm}^i Q_{tie}^i(k) \\
Q_{COMP}^i(k) &= C_u^i x^i(k) + D_{vu}^i Q_{tie}^i(k)
\end{aligned}
\tag{3.5}
$$

In which x^i is the state vector for Area i, $V_{ref}^i = \left[V_{ref}^{i1}, V_{ref}^{i2}, \cdots, V_{ref}^{in_i}\right]^t$ is the control input vector which includes reference voltages of n_i compensators in Area i, Q_{tie}^i is measured disturbance vector $Q_{tie}^i = \left[Q_{tie}^{i1}, Q_{tie}^{i2}, \cdots, Q_{tie}^{ir_i}\right]^t$ which is reactive power of tie-lines between Area i and all other r_i neighbor areas , $V_{PN}^i = \left[V_{PN}^{i1}, V_{PN}^{i2}, \cdots, V_{PN}^{iN_i}\right]^t$ is measured output vector which includes voltage on N_i pilot buses and finally $Q_{COMP}^i = \left[Q_{COMP}^{i1}, Q_{COMP}^{i2}, \cdots, Q_{COMP}^{ic_i}\right]^t$ is unmeasured output vector representing reactive power injected by synchronous machines and SVCs.

A^i, B_u^i, B_v^i, C_m^i, C_u^i, D_{vm}^i and D_{vu}^i are matrices regarding to the identified state space LTI model for each area.

In this way, the optimization problem for DCSVC can be formulated as Equation 3.6:

$$\min_{\Delta V^i_{ref}} \sum_{j=0}^{p-1} \Big[\Delta V^i_{ref}(k+j)^t \, R \Delta V^i_{ref}(k+j) + \Delta V^i_{PN}(k)^t \, Q \Delta V^i_{PN}(k) \Big]$$

$$in-which : \Delta V^i_{PN}(k) = V^i_{PN}(k) - V^i_{PNd}(k)$$

$$s.t : \tag{3.6}$$

$$1) V^{min}_{ref} < V^i_{ref}(k+j) < V^{max}_{ref}$$

$$2) Q^{min}_{COMP} < Q^i_{COMP}(k+j) < Q^{max}_{COMP}$$

$$3) V^{min}_{PN} < V^i_{PN}(k+j) < V^{max}_{PN}$$

In Equation 3.6, ΔV^i_{ref} is the control input increment. Moreover V^{min}_{ref} and V^{max}_{ref} are lower and upper limits of reference voltage, Q^{min}_{COMP} and Q^{max}_{COMP} are lower and upper limits of reactive power injected by compensators, and V^{min}_{PN} and V^{max}_{PN} are lower and upper limits for voltage on pilot nodes.

3.2 Real-time test-bench

The validation of the proposed control strategy is done on a real-time simulation target, OP4510, from OPAL-RT Technologies. Beside real-time capabilities to validate the performance of complex control strategies, the possibility to implement simulations on multi-cores in parallel and also supports for different industrial communication protocols used in real power systems, makes it easy to validate decentralized control architectures such as the proposed DCSVC. The software used to simulate the dynamics of the power system is ePHASORsim from OPAL-RT which is a phasor-domain solver Jalili-Marandi *et al.* (2013),Opal-RT (2018). It benefits from

state of the art techniques to improve performance and accuracy of simulations for large-scale power grids. It also includes a rich built-in and Modelica based library of different power system components and also supports importing data from various power system stability analysis tools such as PSS/e and CYME.

Figure 3.3 illustrates the configuration of the test-bench to validate the DCSVC in real-time. The software interface to develop the test-bench is Simulink from MathWorks in which OPAL-RT's ePHASORsim block is used to define the power network. The data is also sent through a communication channel with a Gaussian noise model in which the SNR is 100 dB. The communication protocol to send measured data from power gird (i.e. voltage on pilot buses, reactive power injection by machines and SVCs, tie-line reactive powers) to DCSVC controllers is IEEE C37.118 which is used by PMUs in real power grids. OPAL-RT's library supports both slave (sending) and master (receiving) C37.118 protocol. Moreover, the control commands from the DCSVCs are sent to the network using Ethernet protocol. As can be seen from Figure 3.3, a dedicated communication channel is defined to send and receive data from each area of the power grid. Such an architecture is also in-line with the requirements of multi-TSO power grids. To cope with the decentralized architecture of the proposed control strategy, DCSVCs as well as power network model are located in separate subsystems labeled as $Corei, MASTER/SLAVE$. The convention of master and slave subsystems are used by RT-LAB to inform the compiler during code generation process that each subsystem's generated code is transferred and run in a separate physical core on the target computer. In this way, computations on each core are done in parallel with the other cores and the performance of each subsystem can be measured separately without having any overloads caused by other subsystems. Although in this paper MPC algorithm is adopted for DCSVC, the proposed test-bench can be used to run and validate any other decentralized control strategy.

3.3 Simulation results for 5000 bus network

As a realistic test-case, the DCSVC controller is validated on a large-scale power network with 5000 buses. The network and dynamic data is provided by OPAL-RT technologies. Fig-

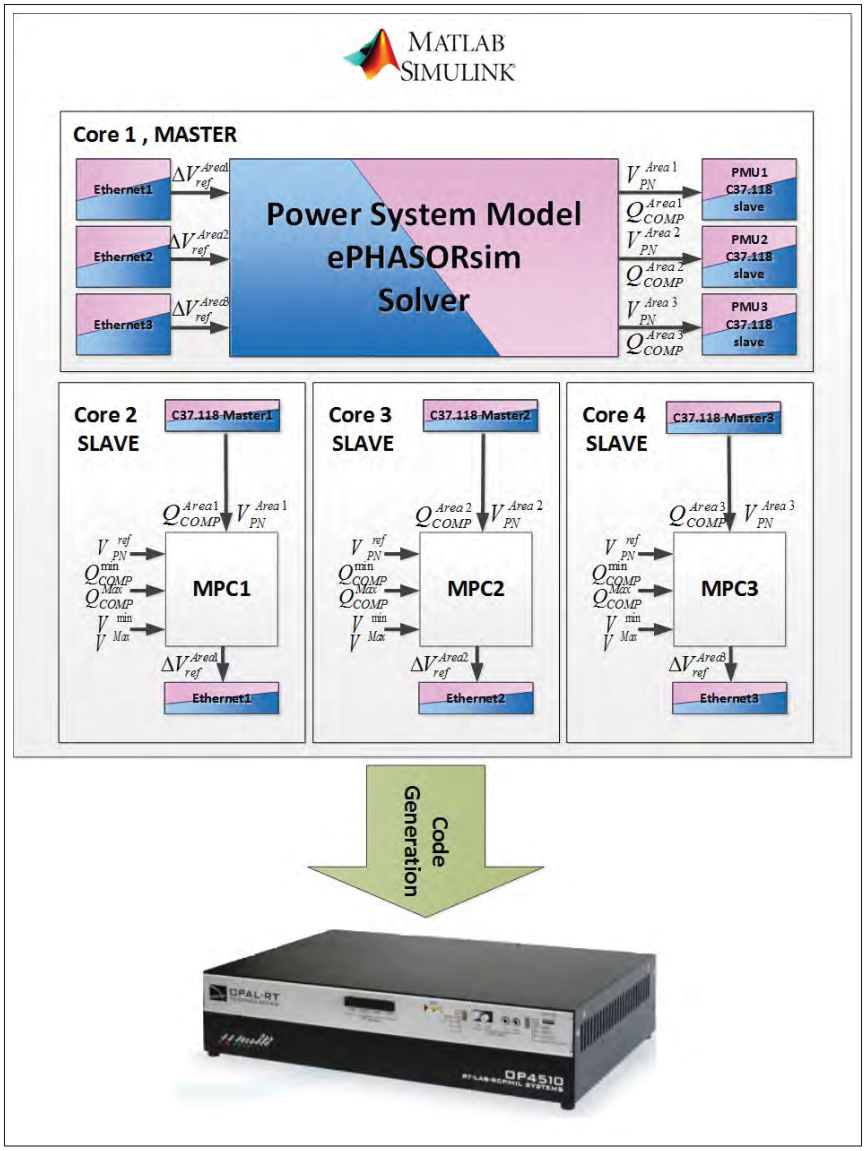

Figure 3.3 Configuration of the real-time test-bench for validation of DCSVC algorithm

ure 3.4 illustrates the HV transmission network, i.e. 230KV, 240KV and 500KV, depicted using GEPHI graph visualization tool Bastian *et al.* (2009). As can be seen, buses are shown using circles while the transmission lines are shown by edges. The length of the edges is proportional to the admittance of the lines which relatively decreases by increasing the geographical distance between the two connected mutual buses. The HV network has 580 buses which are spread between 34 geographically separated areas, distinguished by different node colors. The

selected pilot buses for each area are also shown with larger circles in Figure 3.4. The network and dynamic data are given in PSS/e ver.32 *.raw file and *.dyr formats and are read by ePHASORsim as input files. This network includes 3072 two winding transformers, 2400 constant power loads, 902 GENROU type synchronous machines, 308 EXST1 type exciters, 261 turbine governors of type TGOV1 and 261 power system stabilizer of type STAB1.

Figure 3.4 High Voltage transmission network for 5000 bus power grid. Larger circles represents selected pilot nodes. Different colors represent different areas

3.3.1 Pilot bus selection

For this network, voltage control zones are considered the same as areas shown in Figure 3.4. Sensitivity analysis described in Corsi (2015) is therefore applied on each area to find its most sensitive bus as its pilot node. These nodes are also shown in Figure 3.4 using larger circles. It is also assumed that the reactive compensators which participate in secondary voltage control

loop are installed on the pilot buses and their reactive power injection is controlled by the DCSVC algorithm.

3.3.2 System identification

To identify the LTI model of each area, the following steps are taken: Each area of the partitioned power system is considered as an isolated grid in which the tie-lines are replaced with PQ loads equal to the amount of active and reactive power transferred to the neighbor areas. In the next step, small perturbations are applied to reference signal of reactive power compensators V_{ref}^{ij}, and also reactive power part of the PQ loads who represent the tie-lines, Q_{tie}^{ij}. The effect of these disturbances is then measured as voltage on the pilot buses, V_{PN}^{ij} and also injected reactive power by compensators, Q_{COMP}^{ij}. Finally $\left[V_{ref}^{ij}, Q_{tie}^{ij}\right]$ is considered as input vector and $\left[V_{PN}^{ij}, Q_{COMP}^{ij}\right]$ as output vector.

After preparing input-output data set, the LTI state space model is identified using sub-space method described in Ljung (1998). This leads to 34 state-space models considering voltage at pilot buses as output and reactive power injection by reactive compensators as inputs. Reactive power injection on tie-lines from neighbor areas are also considered as measured disturbance. The fitness values of identification data for each LTI model of the 34 areas are shown in Figure 3.5.

As can be seen from Figure 3.5, the fitness value for identification data for all areas are greater than 88% which shows a good fit of the model to this data set.

3.3.3 Tuning the parameters of proposed controller

To tune the parameters of the proposed DMPC controller, i.e., prediction horizon, p, control horizon, m, controller weights, i.e. R & Q matrices, the following criteria are considered:

1. Settling time of the closed loop system is less than 60 sec., i.e. voltage on the pilot nodes should converge to steady state with 1% p.u. error in less than 100 sec;

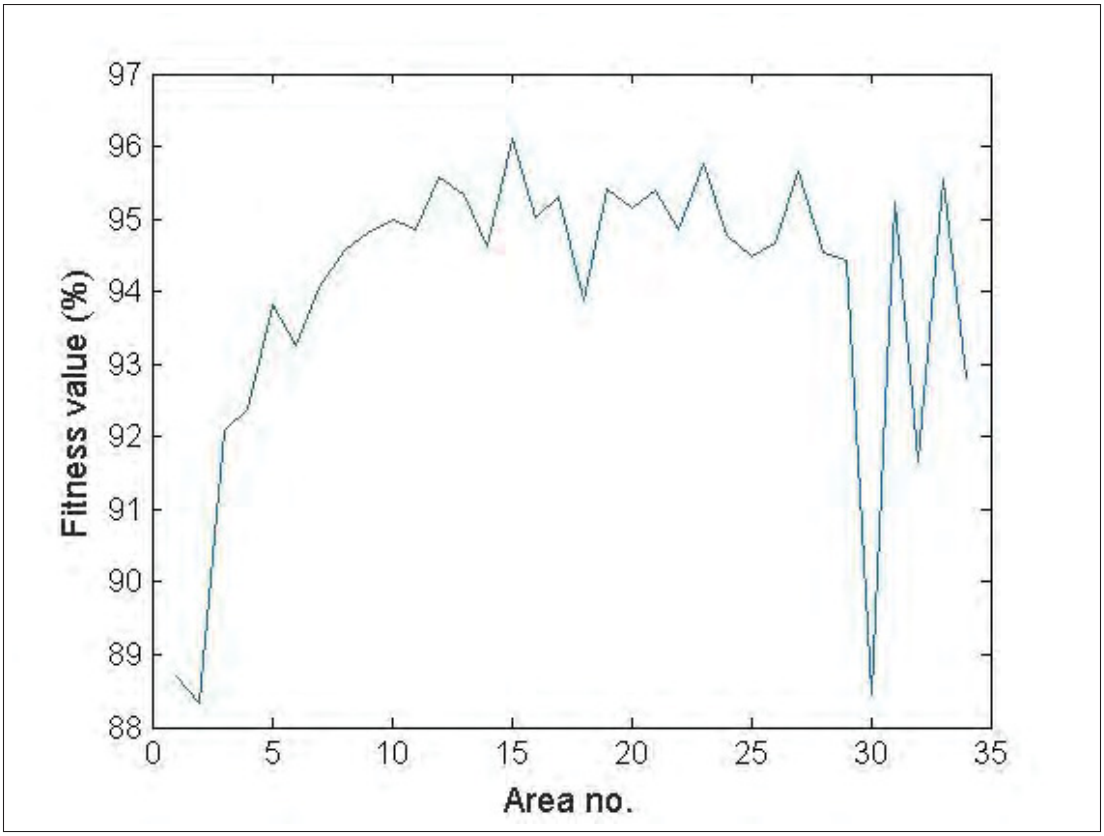

Figure 3.5 Fitness value of identified models of network areas for identification data

2. Voltage overshoot is smaller than 3% p.u.

The dynamic properties of a power system are dependent on the parameters of different dynamic components in the network as well as the admittance matrix of the power grid. In this way, for each network, the controller parameters are tuned in a way that the step response respects the criteria mentioned above.

For the 5000 bus power grid, the parameters are tuned based on a trial and error approach in which prediction horizon is 20 sec. and the control horizon is 10 sec. Moreover the output weighting matrix, R, is considered to be an identity matrix while the input weighting matrix, Q, is equal to scaled identity matrix by a factor of 0.001.

3.3.4 Validation of the proposed algorithm

The effectiveness of the DCSVC controller on 5000 bus power grid is validated through the following simulation scenarios:

3.3.4.1 Scenario 1- Sudden load variation

To validate the robustness of the proposed DCSVC, all active and reactive loads in the grid are suddenly increased by 10% at $t = 10sec.$. Figure 3.6 shows the simulation results for cases with and without DCSVC. As can be observed from Figure 3.6.a, the proposed DCSVC is able to maintain the voltage deviation of pilot buses within 0.5% after transients. However, the results with no DCSVC show that without any secondary voltage controller the steady state voltage error could not be compensated. Figure 3.6.b also illustrates the injected reactive power by compensator located at pilot buses.

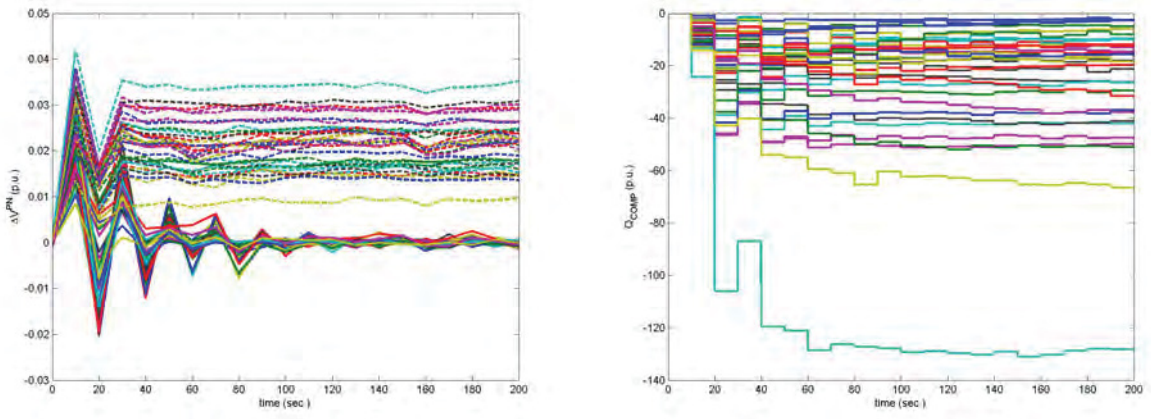

a) Voltage error on pilot buses

b) Injected reactive power by Compensators

Figure 3.6 Scenario1-DCSVC (solid line) vs. No DCSVC (dashed line) cases

3.3.4.2 Scenario 2- Change the reference value of the pilot bus

In another scenario, the reference of all the 34 pilot nodes are suddenly increased by 3% at 1 sec. to evaluate the tracking feature of the DCSVC. As can be seen from Figure 3.7.a, the proposed method is able to reduce the voltage deviation, i.e., the difference between the reference voltage and measured voltage on pilot nodes, to less than 0.5% on all pilot nodes while without having any DCSVC the primary controllers on pilot buses are not able to track the new voltage set-point. The steady state error of 3% can be seen in this case without any DCSVC. Figure 3.6.b also shows the injected reactive power by the compensators to change the voltage on pilot nodes.

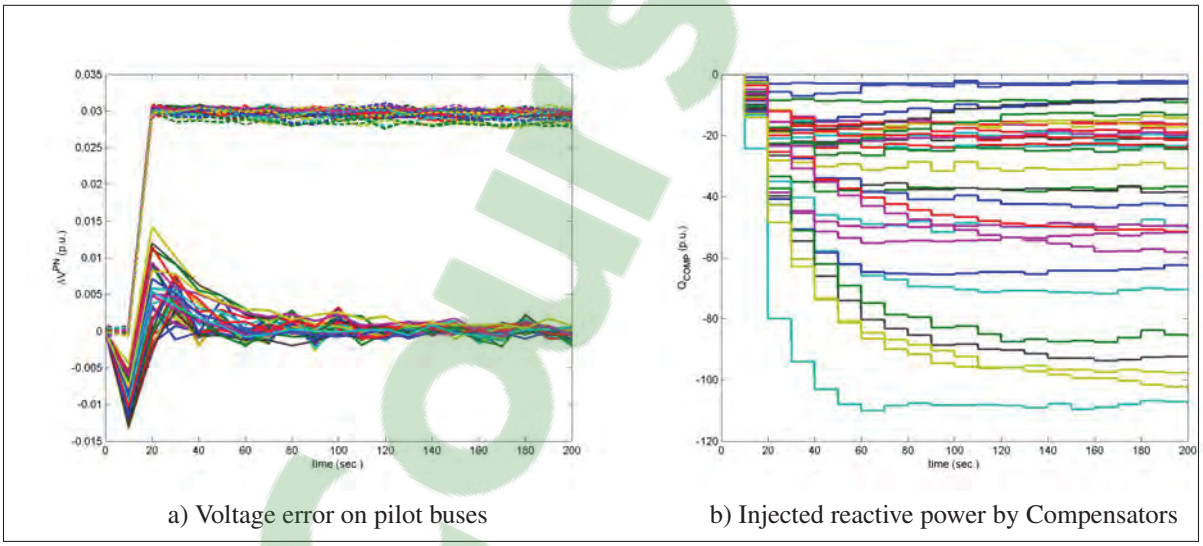

a) Voltage error on pilot buses b) Injected reactive power by Compensators

Figure 3.7 Scenario2-DCSVC (solid line) vs. No DCSVC (dashed line) cases

3.3.4.3 Scenario 3- Impact of communication delays

The communication delay in power systems is dependent on the communication channel specifications as well as protocols that are used to send & receive the data. This delay may vary from few milliseconds to hundreds of milliseconds. Since the time constant of the CSVC algorithm is much larger than such a natural delay, its effect on the closed loop stability can be neglected. However, with the rising concerns regarding to cybersecurity of power grids,

the existence of malicious attacks may lead to larger time delays in the order of few seconds Chen & Sun (2014).

To investigate the effect of such a threat on the performance of the proposed DCSVC algorithm, a delay of 10sec. is considered on the communication channel between the controller and the power system for Scenario 1. Although the discrete model of Equation 3.1 is delay free, the effect of communication delays can be considered by adding new poles located at $z = 0$. In this way, the state space model of Equation 3.1 is modified as follows:

$$
\begin{aligned}
& x_d^1(k+1) = u(k) \\
& \cdots \\
& x_d^{n-1}(k+1) = x_d^{n-2}(k) \\
& x_d^n(k+1) = x_d^{n-1}(k) \\
& x(k+1) = Ax(k) + B_u x_d^n(k) + B_v v(k) + d(k) \\
& y_m(k) = C_m x(k) + D_{vm} v(k) \\
& y_u(k) = C_u x(k) + D_{vu} v(k)
\end{aligned}
\tag{3.7}
$$

In this formulation, new states, $x_d^1, \cdots, x_d^n$ are added to model n-steps of input delay.

Figure 3.8 compares the simulation results for the two cases of MPC controllers, one with modeled delay as Equation 3.7 and the other without any delay model based on Equation 3.1.

As can be seen in this figure, for the case without any modeled delay, the DMPC controller can not compensate the oscillations caused by the delay. However, considering delay model by DMPC has led to a better performance in which the oscillations are damped out to less than 2% p.u. in less than 60 seconds.

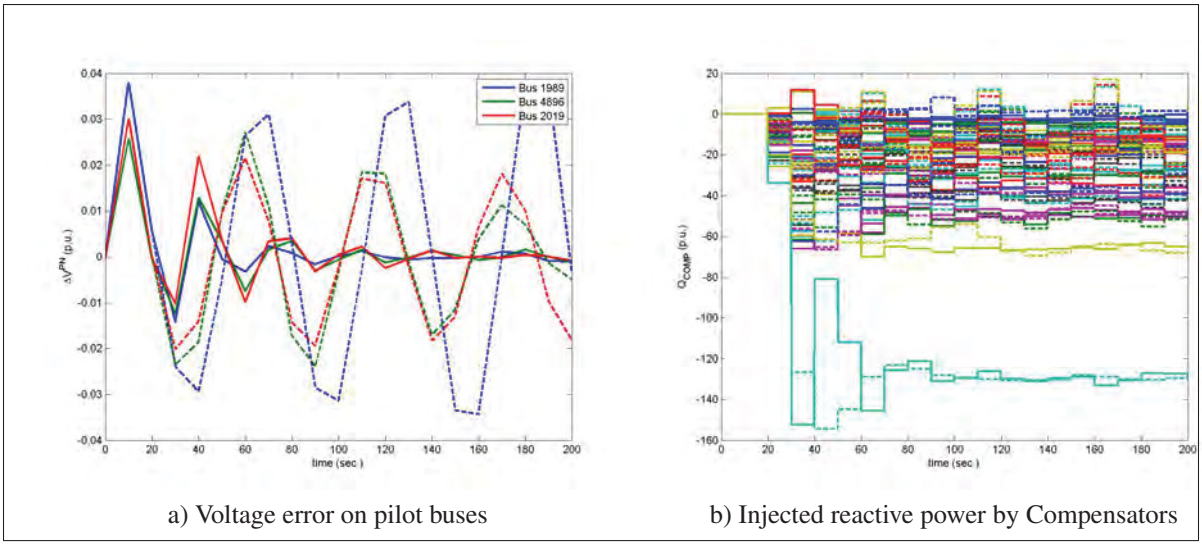

a) Voltage error on pilot buses b) Injected reactive power by Compensators

Figure 3.8 Scenario3-DCSVC (solid line) vs. No DCSVC (dashed line) cases

3.3.4.4 Real-time performance

The real-time performance of the DCSVCs is measured for Scenario 1. The maximum computation time of DCSVCs, per one control interval, i.e. 10 seconds, is 5 milliseconds. This means that for 5000 bus test-case, the proposed DCSVC can be easily implemented in real-time.

3.3.4.5 Convergence of the MPC algorithm

The convergence of the QP solver used in this paper and described in Schmid & Biegler (1994) depends mainly on whether all of the constraints are satisfied or whether some of them are violated. As described in Schmid & Biegler (1994), the algorithm starts from an initial guess of optimal solution which is the closed form solution of the unconstrained problem. If all the constraints are satisfied using this solution, then it will be considered as optimal value. Otherwise, an iterative process starts to determine the active constraint set satisfying the standard optimality conditions. If the algorithm detects any unfeasibility, the iterative process terminates and the MPC uses the last successful optimal value as the solution. Such an unfeasible situation usually occurs when the number of control variables is smaller than number of outputs or when all the control variables reach their limits.

In particular, for the secondary voltage control problem, the topology of the power system may affect the convergence of the algorithm. Indeed, an unfeasible situation, in which the optimization problem does not converge, may occur when the number of the compensator devices is smaller than the number of pilot buses. The same issue may rise for the case in which the reactive power required to compensate the voltage at a pilot node cannot be provided by the corresponding compensator devices in the grid due to their saturation.

3.4 Conclusion and Future Works

A decentralized MPC scheme for coordinated secondary voltage control of large-scale multi-area highly interconnected power networks has been proposed in this paper. The controllers were designed in a decentralized way for each area which modifies reference signal of reactive power compensator devices. The interactions between neighboring areas were considered as measured reactive power deviation on tie-lines between these areas. This value is defined as a measured disturbance for MPC in each area. The proposed algorithm was tested on realistic power grid with 5000 buses and its stability and robustness are verified via different simulation scenarios. Moreover, a real-time test bench was presented to validate the performance of the proposed method and it was shown that the method is computationally feasible and scalable to large scale power grids.

Although the proposed method can be generalized to other types of reactive compensators such as tap-changers, capacitor banks, synchronous condensers and other FACTS devices, certain considerations should be taken into account for switching based devices such as capacitor banks or tap-changers. The number of switching of such devices should be minimized as much as possible to avoid long-term damages. Moreover, due to the discrete nature of these devices, the optimization problem leads to a mixed integer linear or quadratic programming which can be solved using available methods.

Another possible improvement to the proposed method is to use physical modeling instead of black-box system identification to have more accurate and meaningful models. Having lin-

earized symbolic models of different components of the power system, one can easily formulate the MPC optimization problem symbolically which leads to a more flexible and performant approach which can easily be adapted for any power system.

On the other hand, considering different load models and their dynamics can lead to more accurate formulation of voltage stability problem. Considering the dynamics of the load in the MPC formulation can provide more accurate control when loads are constantly changing in the power grid.

Finally, the effect of unknown communication delays on the stability of the controller can be considered as a future work. Such an assumption is more realistic for delays caused by cyber attacks since it is not in control of the power system utilities and they may not have any statistic data to estimate the value.

3.5 Acknowledgment

We thank OPAL-RT Technologies for providing data for 5000 bus test-case, the Real-time simulator and also software licenses for ePHASORsim and RTLAB.5

CHAPTER 4

NONLINEAR SENSITIVITY-BASED COORDINATED CONTROL OF REACTIVE RESOURCES IN POWER GRIDS UNDER LARGE DISTURBANCES

Arvin Morattab[1], Maarouf Saad[1], Ouassima Akhrif[1], Serge Lefebvre[2], Asber Dalal[2]

[1] Department of Electrical Engineering, École de Technologie Supérieure,
1100 Notre-Dame Ouest, Montréal, Québec, Canada, H3C 1K3
[2] Institut de Recherche en Électricité du Québec (IREQ),
1800 Boulevard Lionel-Boulet, Varennes, Québec, Canada, J3X 1S1

Article submitted for publication, February 2018

Abstract

In this paper, a coordinated secondary voltage control strategy is proposed to improve mid-term and long-term voltages of power systems facing large disturbances. In this way, sensitivity analysis is used to first find the strongest buses of the network called pilot nodes and second to locate the control buses in which discrete type or continuous type controllers are installed. The coordinated secondary voltage controller is then designed based on the notion of nonlinear sensitivity model which relates reactive power injection/absorption or change of reference voltage of controllers to the voltage variation at pilot buses at different operating points of the network. The non-linear sensitivity model is identified using Neural Networks approach which is then used by SA optimization algorithm to solve a mixed discrete-continuous type optimization problem and find the suboptimal control input. The proposed algorithm is tested in real-time against coordinated secondary voltage control method based on linear sensitivity models and also traditional capacitor/inductor banks' control method which is based on local measurements. The effectiveness of the proposed algorithm is also verified through different simulation scenarios on the dynamic phasor domain model of standard IEEE 118 bus test case.

Introduction

One of the major challenges in voltage control of transmission networks in todays' power grid is how to deal with mid-term and long-term voltage control issues due to the higher utilization of transmission assets. Nowadays, in some of the utilities voltage is still controlled in a traditional way, i.e. voltage at specific buses is controlled within a proper range by switching in/out shunt capacitors or reactors based on local information and Q-V curve analysis Taylor *et al.* (1994). This method is easy to be implemented and the cost is low. However, the increased distance between generation and load units, delays in building new transmission projects and high penetration of distributed generations into transmission network lead the grid to work closer to its voltage and power limits in which the behavior of the network is highly non-linear Martins & Corsi (2007). On the other hand, due to increasing number of voltage control devices and meshed structure of transmission networks, the compensators' reactive power injection does not have a local effect on the voltage and it may affect voltages on many sensitive buses of the network. In this situation, local control of bus voltages may fail since it does not consider coupling between many compensators and different buses and in some cases compensators' actions may interfere with each other Narita & Hammam (1971a). This requires a coordinated Multi Input-Multi Output strategy in which the voltage control problem for coupled buses in a region is solved simultaneously. The wide area voltage control approach should have therefore a coordinated structure and should also take into account the nonlinearity and constraints of the power grid.

The idea of coordinated voltage control has first appeared in Hano *et al.* (1969); Narita & Hammam (1971a) and Narita & Hammam (1971b) in which a centralized real-time control strategy is presented for integrated voltage and reactive power control using an optimization algorithm consisting of terms related to voltage deviation at buses and reactive power loss through the lines in the objective function. In these papers, voltage-reactive power relation is also defined using linear sensitivity matrix. On the other hand, Narita & Hammam (1971a) proposes a method using several sets of sensitivity constants depending on different loading conditions of the network.

One of the implemented strategies of voltage control in transmission networks is hierarchical voltage control with emphasis on division of the control problem temporally and geographically into three primary, secondary and tertiary levels corresponding to local, regional and national concerns. In Nakamura & Okada (1969), the network is divided into several coherent areas and voltage in each area is controlled independently. The hierarchical voltage control has also been studied and developed in Italy Arcidiacono *et al.* (1977); Arcidiacono (1983) and France Paul *et al.* (1987); Lefebvre *et al.* (2000); Vu *et al.* (1996) starting in 1980s.

In Arcidiacono *et al.* (1977); Arcidiacono (1983), a hierarchical secondary voltage control algorithm is presented in which the power network is divided into many theoretically non-interacting zones and at each zone, the strongest bus to reactive power disturbances is selected as pilot node. Voltage at this bus is then measured and compared with a desired voltage dictated by tertiary level controller. Regional controller, which is basically a PI controller calculates the total amount of reactive power that is needed to compensate the voltage deviation and sends this signal to the regional participant generators. At generation level, a reactive power control loop, which is also a PI controller, calculates the new voltage set-point for the AVR, considering the generator's participation factor as well as its reactive power limits. As has been discussed further in Lefebvre *et al.* (2000); Vu *et al.* (1996), the assumption of one sensitive bus per control zone may not be realistic for a densely meshed network, such as French transmission grid. For these networks, they have proposed CSVC algorithm, which is basically an optimal, model based, multi-input/multi-output, regional controller. CSVC uses voltage measurements from many sensitive buses in a control zone and calculates new set-points for generators that take part in secondary voltage control loop considering their reactive power and voltage limits. CSVC uses a linear sensitivity model for Voltage-Reactive power and also for Voltage-Voltages and recalculation of these sensitivity matrices are triggered by an event or an incident (change of topology, unit tripping, major load change). Further details on the advantages of model based CSVC compared to the method presented in Arcidiacono *et al.* (1977); Arcidiacono (1983), can be found in Lefebvre *et al.* (2000); Vu *et al.* (1996).

Using linear models has also been proposed in other references Dragosavac *et al.* (2012, 2013); Flórez *et al.* (1994); Ilic-Spong *et al.* (1988); Sancha *et al.* (1996); Da Silva *et al.* (2013) in which the model is used in combination with different control strategies. Dragosavac *et al.* (2012, 2013) have considered a coordinated V-Q controller for a multi-machine SPP. The controller uses a feed-forward correction signal based on the application of the sensitivity matrix at a power plant level. In Flórez *et al.* (1994), a robust multivariable PI control algorithm which permits the coordination of discrete and continuous type reactive power sources is applied. The model of the network at secondary level was also defined by sensitivity matrices. In Ilic-Spong *et al.* (1988); Sancha *et al.* (1996), a sensitivity matrix as a model of the network to find pilot nodes and feedback control law for CSVC problem was used. Finally in Da Silva *et al.* (2013), a sensitivity-based methodology to identify the most effective plants and the associated impedance value to improve voltage profile and prevent system from collapse is presented.

However, when a power system is close to its critical point, or a large disturbance affects the network, the behavior of the system is highly non-linear and using a linear model for CSVC algorithm may fail or may not be as accurate as a non-linear one. At this point, the amount of injected/absorbed reactive power determined by linear model based CSVC might be under-/over estimated so that it may not be able to maintain the voltage within the acceptable limits. Using a nonlinear model of the system, on the other hand, can improve the model accuracy hence leading to a better voltage control. Such a nonlinear model can be either formulated analytically using conventional power flow equations or by using machine learning algorithms such as Neural Networks or fuzzy methods. Using former approach requires detailed model of the power network which is not necessary for CSVC purposes and requires nonlinear optimization techniques which are not computationally efficient for real-time closed loop control. In contrast, machine learning algorithms can extract acceptable model for CSVC problem from input-output data without knowing internal details about the model. The identified model can then be combined with evolutionary algorithms to find the optimal or suboptimal solution in a timely manner.

Evolutionary algorithms have found great acceptance in the area of control, due to their robustness and their capability to handle highly nonlinear and/or nonconvex problems. A survey on the implementation of evolutionary computations in controller design, parameter optimization, system identification, robust stability analysis, and other control engineering applications are presented in Fleming & Purshouse (2002). In the field of CSVC, a nonlinear fuzzy model of the network in which the inputs are load variations and the outputs are bus voltages is proposed in Mehrjerdi *et al.* (2013b). This model is combined with a fuzzy controller to form a decentralized CSVC. In Wen *et al.* (2004), a coordinated voltage control framework is developed based on nonlinear system equations using Euler state prediction and pseudo-gradient evolutionary programming. In Larsson (2000) and Negenborn (2007), NLMPC algorithm was applied to improve the network voltage profile. A hybrid QSS model of the power grid considering both its discrete and continuous dynamics was used. Despite the effectiveness of the NLMPC method compared to MPC for small-scale power networks, its tremendous computational burden is a major challenge when applied to large-scale power grids.

This paper is exclusively devoted to CSVC as a model based optimal controller for secondary voltage regulation and the focus of this work is on large-scale power systems in presence of large disturbances. In this way, pilot buses and controllers are first chosen based on sensitivity analysis method discussed in Corsi (2015). In the next step a non-linear NN model is identified as a nonlinear sensitivity model of the system for CSVC algorithm. The model maps reference voltage of continuous type regulators such as AVR as well as reactive power injection/absorption of discrete type compensation devices (such as capacitor/inductor banks) to voltage variations on pilot buses for different operating points of the system defined by voltage magnitudes at pilot nodes and loading conditions in the network. The loading level of the network is provided by measurement or by load estimations. Considering different loading conditions of the network during model identification and also defining loading level of the grid as an input, gives the controller a degree of adaptability to load changes over the power network.

The identified NN model is then used by SA technique to find the suboptimal coordination of continuous type (generators, FACTS devices, synchronous condenser,...) and also discrete

type (switched shunts, OLTC, ...) compensators to inject reactive power in order to compensate voltage deviations. As a secondary and tertiary goal, the optimization algorithm also takes into account reactive power minimization and equalization at each iteration.

Although the convergence of SA algorithm to global optima used by CSVC algorithm could not be guaranteed, suitable parameters for SA lead to suboptimal solutions which can still improve voltage profile considerably while benefiting from the following advantages of the algorithm: 1-Due to the discrete values of reactive power injection of compensators, coordinated control of Capacitors/Inductors banks is formulated as an IP problem. It has been shown in Černý (1985) that using SA algorithm for IP problems such as traveling salesman leads to a close to optimal solution with a fast convergence. 2- Unlike gradient based optimization methods, SA approach is independent of mathematical model of the system and can easily cope with black box models such as the identified NN sensitivity model.

The following assumptions are made throughout this paper:

- It is assumed that the iterative sensitivity analysis to re-evaluate the number of pilot buses and their location is handled by the tertiary level controller which is not the main focus of this paper. In this way, the number of pilot buses and their locations are considered fixed and they are not affected by the disturbances;
- It is assumed that the nonlinear NN based sensitivity model is identified off-line and remains unchanged during its operation. Although the model benefits from a degree of adaptability to the loading level of the network due to the definition of such an input for the NN, there is no adaptive mechanism by which the parameters of the NN updates. Updating the model is usually done by the tertiary level controller which is out of the scope of this paper;
- The time step of the proposed secondary level controller is defined so that within one time step, the primary level controllers such as AVRs could stabilize the transient voltage dynamics and hence there would be no interference between the primary and secondary level controllers.

Moreover, the novelties of this paper can be enumerated as below:

- Propose a novel nonlinear sensitivity model based on Neural Networks which maps reactive power injection by compensators to the corresponding voltage variation on pilot nodes considering different demand levels of the network;
- Propose a novel closed loop suboptimal secondary voltage controller which uses SA to solve Mixed discrete-continuous type optimization problem with NN based sensitivity model as nonlinear constraint and quadratic objective function at each time step of the controller;
- Propose a novel technique to generate rich data for training Neural Network as the nonlinear sensitivity model.

This paper is organized as follows: The structure of the control design is explained in Section 4.1. Section 4.2 discusses pilot bus selection and also control buses allocation using sensitivity analysis. In Section 4.3, the identification procedure toward NN model of nonlinear sensitivity function is presented for IEEE-118 bus power network. Next in Section 4.4, the obtained NN model is combined with SA optimization block to test the proposed control strategy on a dynamic setup of IEEE-118 bus network modeled using ePHASORsim's phasor domain simulator from OPAL-RT Technologies Jalili-Marandi *et al.* (2013). The validation process is done through different simulation scenarios on OPAL-RT's real-time simulator. The proposed method is also compared with linear sensitivity based CSVC approach as well as traditional approach which uses local connected bus measurements to switch capacitor/inductor banks. All three methods use the same controller structure, however, the model of the network in each case is different. Finally, Section 4.5 concludes the paper and future works are discussed.

4.1 Proposed Control Strategy

The proposed control strategy is a model based optimal controller. The model of the network is defined as a nonlinear sensitivity function $\hat{H}$, which, for current loading level of the network, P^{load} and Q^{load}, and current voltage at pilot buses, V^{PN}, relates the reactive power injection by discrete compensator, ΔQ^{dctrl}, and the change in the reference voltage of continuous type compensator, ΔV^{cctrl}, to voltage variation at pilot buses, ΔV^{PN}. This relation is defined in Equation 4.1.

$$\Delta V^{PN} = \hat{H}(\Delta Q^{dctrl}, \Delta V^{cctrl}, V^{PN}, P^{load}, Q^{load}) \tag{4.1}$$

Equation 4.1 is approximated using Neural Networks approach in this paper and discussed in detail in section 4.3.

The core of the proposed controller is based on SA algorithm which runs for many iterations at each time step to find the optimal control signal. To distinguish between values of the variables during each iteration of the SA algorithm and also the measured signals or calculated control signal at k^{th} time step of the controller the following rules are used throughout this paper:

- A variable shown simply as x indicates the calculated value of a variable at k^{th} time step of the controller and at m^{th} iterations of the SA algorithm;
- A variable shown as $x(k)$ indicates the measured or calculated value of the variable at k^{th} time step of the controller, at the beginning (for measured variables) or at the end (for calculated variables) of all iterations of the SA algorithm.

Suppose that nd discrete type compensators (such as capacitor/inductor banks) and nc continuous type (such as generators, synchronous condensers, FACTS devices, ...), and n pilot buses, are allocated over the network to take part in CSVC. We assume that the control signal for discrete type compensators is reactive power injection and for continuous type is change of reference voltage. In this way the control vector for discrete type compensators is defined as $\Delta Q^{dctrl} = \left[\Delta Q_1^{dctrl}, \cdots, \Delta Q_{nd}^{dctrl}\right]$ and it is randomly generated at each iteration of SA algorithm based on the method explained in 4.1.1. ΔQ_i^{dctrl} is the amount of injected/absorbed reactive power by ith discrete controller and it takes values from the finite set of $\left\{\Delta Q_i^{-p}, \cdots, \Delta Q_i^{-1}, 0, \Delta Q_i^{+1}, \cdots, \Delta Q_i^{+q}\right\}$ where superscripts $-p$ and $+q$ stand for the negative and positive reactive power changes respectively. Negative sign for p indicates absorption and positive sign for q indicates injection of reactive power. On the other hand, for continuous type controllers, the control signals are defined as $\Delta V^{cctrl} = \left[\Delta V_1^{cctrl}, \cdots, \Delta V_{nc}^{cctrl}\right]$ which is also randomly generated at each iteration of the SA algorithm based on the method explained

in 4.1.1. For simplicity the input vector of NN model is defined as $\Delta U = \left[\Delta Q^{dctrl}, \Delta V^{cctrl}\right]$ and the output vector is defined as $\Delta V_{PN} = \left[\Delta V_1^{PN}, \cdots, \Delta V_n^{PN}\right]$. Finally, we define V_{min}^{PN} and V_{max}^{PN} as allowable limits of voltage at pilot nodes, V_{min}^{dctrl} and V_{max}^{dctrl} as allowable limits of voltage at buses where discrete type controllers are connected, V_{min}^{cctrl} and V_{max}^{cctrl} as allowable limits of voltage at buses where continuous type controllers are connected, Q_{min}^{cctrl} and Q_{max}^{cctrl} as reactive power limits for continuous type controllers and Q_{min}^{dctrl} and Q_{max}^{dctrl} as reactive power limits for discrete type controllers.

Moreover, the sensitivity matrices, S^{cctrl} and S^{dctrl}, are used in Equation 4.4, which maps linearly voltage deviation to reactive power deviation. These matrices are defined as follows:

$$\Delta Q^{cctrl} = S^{cctrl} \Delta V^{cctrl} \tag{4.2}$$

$$\Delta Q^{dctrl} = S^{dctrl} \Delta V^{dctrl} \tag{4.3}$$

S_{ii}^{cctrl} used in Equation 4.4 is i^{th} diagonal term of the S^{cctrl}.

Based on these definitions, the optimization problem is formulated as follows:

$$\begin{aligned} \min_{\Delta U} J = & \left\| \Delta V^{PN} - \Delta V_d^{PN}(k) \right\| + \Delta U^T R \Delta U + \\ & \sum_{\substack{i=1 \\ i \neq j}}^{n_d} \sum_{j=1}^{n_d} \alpha_{ij} \left\| \Delta Q_i^{dctrl} - \Delta Q_j^{dctrl} \right\| + \\ & \sum_{\substack{i=1 \\ i \neq j}}^{n_c} \sum_{j=1}^{n_c} \beta_{ij} \left\| \frac{\Delta V_i^{cctrl}}{S_{ii}^{cctrl}} - \frac{\Delta V_j^{cctrl}}{S_{jj}^{cctrl}} \right\| \end{aligned} \tag{4.4a}$$

s.t:

$$V_{min}^{cctrl} < V^{cctrl}(k) + \Delta V^{cctrl} < V_{max}^{cctrl} \tag{4.4b}$$

$$V_{min}^{dctrl} < V^{dctrl}(k) + S^{dctrl}\Delta Q^{dctrl} < V_{max}^{dctrl} \tag{4.4c}$$

$$Q_{min}^{dctrl} < Q^{dctrl}(k) + \Delta Q^{dctrl} < Q_{max}^{dctrl} \tag{4.4d}$$

$$Q_{min}^{cctrl} < Q^{cctrl}(k) + (S^{cctrl})^{-1}\Delta V^{cctrl} < Q_{max}^{cctrl} \tag{4.4e}$$

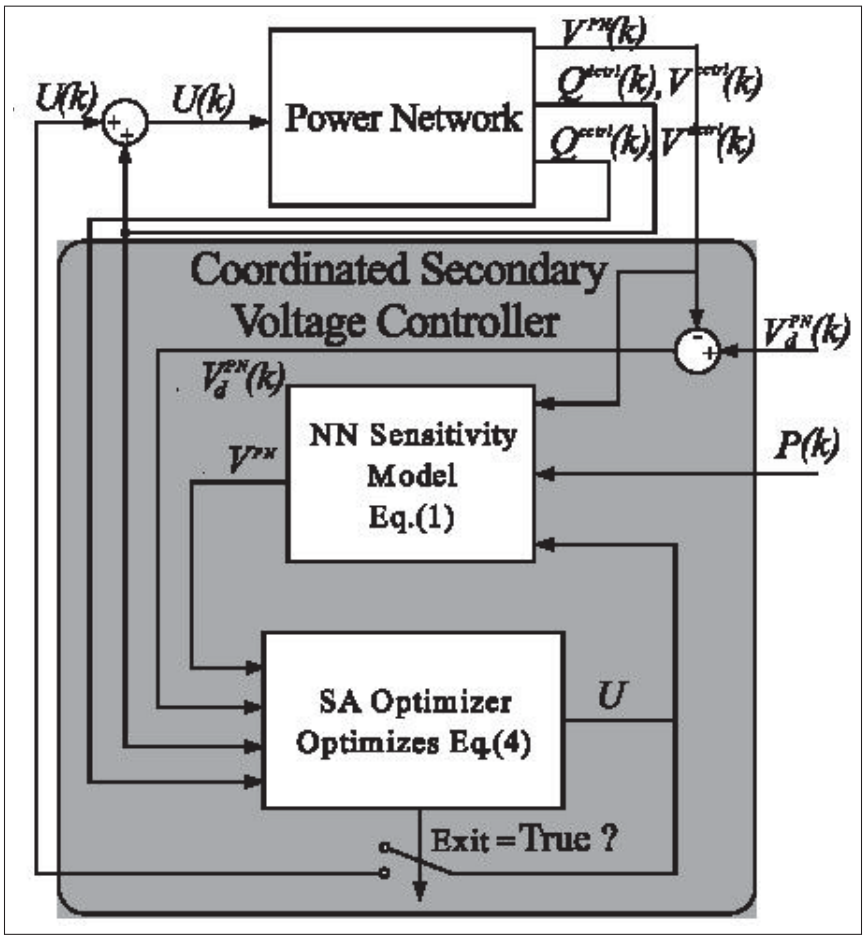

Figure 4.1 Block diagram of the proposed controller

In this formulation, the objective function consists of four terms. The first term represents the Euclidean norm of the error between output of the nonlinear sensitivity model defined in Equation 4.1, and desired voltage deviation ΔV_d^{PN}. Since the number of compensators is usually greater than the number of pilot buses, we can use the remaining degrees of freedom to achieve

other goals. In this way the second term is defined as a weighted Euclidean norm to minimize control effort which leads to the minimization of reactive power injection/absorption. As has been discussed in Bhattacharya & Zhong (2001); Zhong *et al.* (2004); Mozafari *et al.* (2007) minimizing reactive power indirectly reduces the costs regarding to reactive power dispatch as ancillary services and also increases reactive power reserve of the power grid. In this term, R is a diagonal weighting matrix which is chosen by trial and error. Equal weights for injected reactive power gives the same importance to different compensators during the optimization process. The diagonal elements are considered to be smaller than 1 to give a higher priority to minimizing pilot bus voltage error.

Furthermore, the third and fourth terms in the objective function enforce reactive power equalization between all of the resources to pick up the same proportion of total reactive power demand. The energy equalization term has the third priority compared to the two other terms corresponding to voltage control and energy minimization. In this way, the equalization weights, α_{ij} and β_{ij} should be chosen smaller than the weights of the two other terms.

It should be noted that the weighting coefficients R, α_{ij} and β_{ij} are assumed to be fixed in this paper. However, they might required to be reevaluated in case of major change in the network topology.

Equations 4.4b and 4.4c are constraints to maintain the voltage at both continuous and discrete type controller buses. Furthermore, Equations 4.4d and 4.4e are constraints suppressed by physical limitation to inject reactive power by continuous and discrete type controllers. As is discussed in 4.1.1, all the constraints are handled inside neighbor selection algorithm at each iteration of SA.

Figure 4.1 illustrates the proposed closed loop CSVC strategy to find the optimal control variable $\Delta U^{(k)}$ at k^{th} time step of the controller. As can be seen from this figure, the controller consists of two main blocks, i.e. the NN sensitivity model block and the optimizer. The measured outputs, i.e. voltage at pilot buses $V^{PN}(k)$, current loading level, $P(k)$, current injected reactive power by continuous and discrete type compensators, $Q_{cctrl}(k)$ and $Q_{dctrl}(k)$ corre-

spondingly, and finally, current voltage magnitude at all control buses are measured from the Power network and sent to the CSVC. The measured voltage and reactive power of the controllers are sent to the SA optimizer to check for constraint violations at each iteration of SA algorithm. The rest is fed into the NN nonlinear sensitivity model of Equation 4.1. The output of the model corresponding to these measured signals and also the control input from the optimizer, ΔU, is the estimated voltage variation of the pilot buses, ΔV^{PN}. Reactive power and voltage limits are also sent to the optimizer. The optimization block iterates with the NN model to solve the optimization problem of Equation 4.4. At each iteration, an exit condition is checked. If the exit condition is met, the iterations are terminated and the last calculated ΔU is considered as the suboptimal control solution. The optimal control signal is then added to the current measured $\left[Q^{dctrl}(k), V^{cctrl}\right]$ vector and the outcome, $U(k)$, is applied to the power grid. These calculations are repeated at each time step of the controller based on the new measurements.

4.1.1 SA optimization process

Figure 4.2 illustrates the flowchart of SA algorithm used to find the suboptimal control vector, ΔU. The total number of iterations, T, is set to T0 and the SA algorithm starts with an initial guess of optimal solution, a zero vector in this case. At each iteration, the SA algorithm attempts to replace the current solution by a randomly selected solution candidate, ΔU_{new} which is generated by neighbor selection algorithm. This generated solution candidate is usually close to the current solution. In the proposed method, ΔU_{new} is generated by random perturbation of one of the elements of ΔU. This perturbation is applied differently depending on the type of the randomly selected element, either discrete or continuous. If the selected element corresponds to a discrete type compensator, the current value is randomly decreased or increased by one discrete step. However if it corresponds to continuous type compensators, the perturbation is done by adding a random number in $[-0.05, 0.05]$ to the current value of the element. After perturbing ΔU, the next step is to check the constraints of the optimization problem which are defined in Equations 4.4b, 4.4c, 4.4d and 4.4e. If any of these constraints are not satisfied,

ΔU_{new} is reset to ΔU and the neighbor selection is repeated so that finally all constraints are met.

After choosing the solution candidate, ΔU_{new}, corresponding ΔV_{new}^{PN} is calculated from the NN and afterwards the objective function, J_{new} is evaluated for the new solution. If the objective function's value for the new point is smaller than the previous solution, the new point is then considered as suboptimal solution. If this is not the case, i.e. the current solution is bigger than the previous one, there is still a chance that it is accepted as a new solution with a probability called acceptance probability. Such a possibility to move in opposite direction of objective function's minimization potentially saves the method from getting stuck at local optima. Acceptance probability depends on both the difference between objective function's value for current and previous solutions, as well as iteration value, T. The iteration number gradually decreases at each cycle of the algorithm which leads to declination of acceptance probability and henceforward the algorithm's tendency to find the global minimum. The iterations continue until the iteration number is equal to zero. The final value of ΔU is then considered as the suboptimal control signal for current time step of the proposed control algorithm.

4.2 Pilot buses selection and control buses allocation for CSVC algorithm

Many approaches exist in the literature to allocate pilot buses and also control buses to participate in CSVC algorithm Corsi (2015); Amraee *et al.* (2012, 2010). In this paper, the method described in Corsi (2015) is used which is based on short-circuit capacities and sensitivity analysis of the network. In this method, the buses are sorted from the most to the least sensitive one. Afterwards the strongest buses are selected as pilot nodes based on an iterative process. The number of pilot buses are dependent on two predefined parameters. The first parameter, $\frac{1}{\gamma}$, defines the minimum admissible threshold value of the short circuit power for a pilot node. Any bus with short circuit power smaller than this threshold will not be considered as a pilot bus. The second parameter is called coupling coefficient threshold, ϵ_p, which defines the minimum admissible limit for coupling of remote buses to a pilot bus. Any remote bus with coupling value smaller than ϵ_p will not be considered in the same control area as the pilot bus.

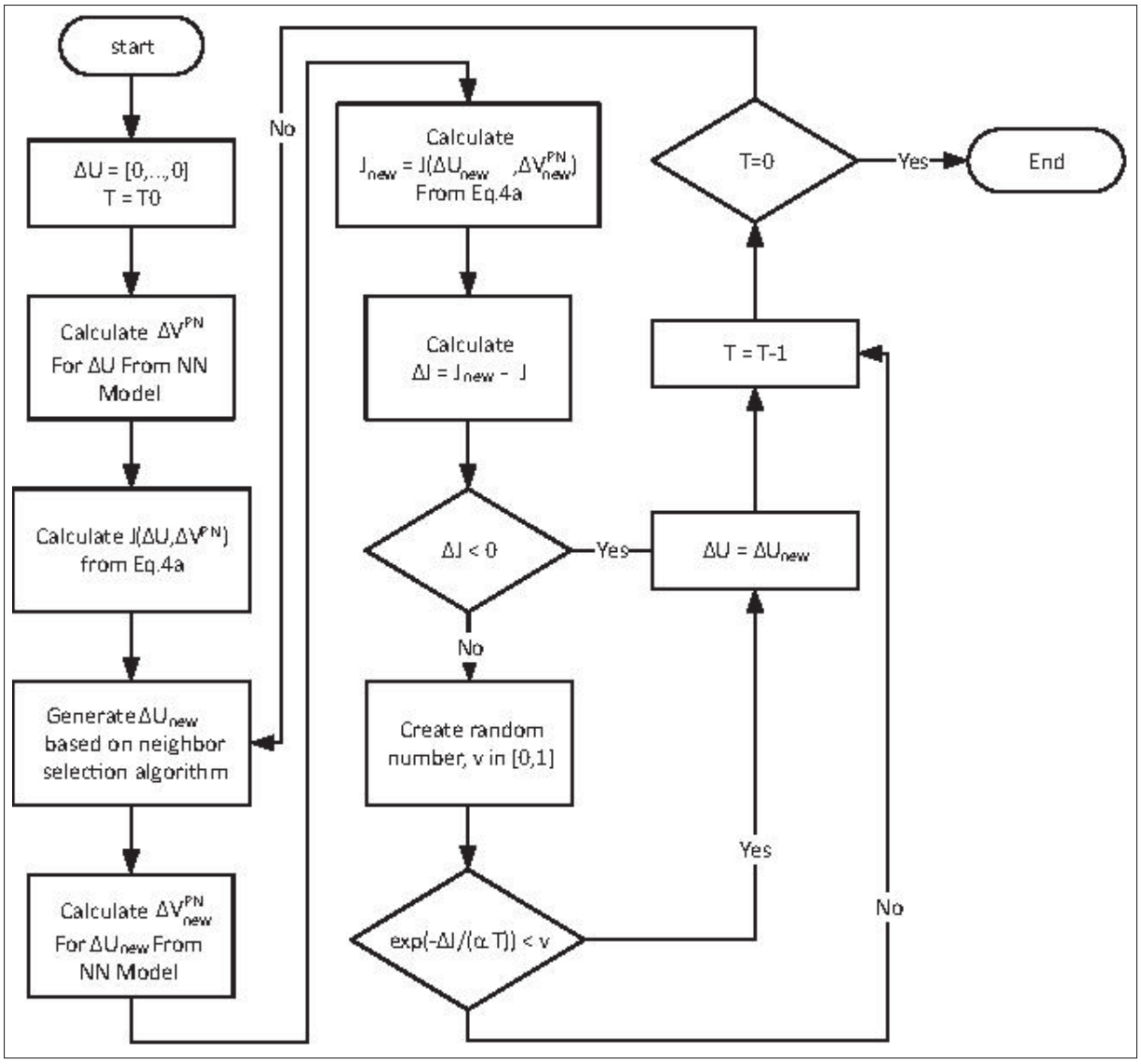

Figure 4.2 Block diagram of the proposed controller

As discussed in Corsi (2015), increasing ϵ_p leads to smaller control areas, which consequently increases the number of pilot nodes. This requires more measurement devices and more reactive compensators to be installed on the system hence increases the cost of secondary voltage control. Moreover the secondary control loops in neighbor areas might have more uncoordinated interactions which require more complex control strategies to take this into account. Another issue with large number of pilot nodes and smaller control areas is the frequent reselection of pilot nodes, even in the case of small network changes. On the contrary, reducing ϵ_p

reduces the number of pilot nodes and significantly de-couples their control areas. However, this might lead to a bad voltage profile on the buses which are electrically distant from the pilot node.

The procedure to find pilot and control buses is applied on the IEEE-118 bus power network shown in Figure 4.3. This network has 19 generators and 35 synchronous condensers. The loads are initially set to be ZIP loads with 40% as constant power, 30% as constant impedance and 30% as constant current load.

Although the proposed CSVC algorithm can include any type of continuous compensators (generators, synchronous condensers, FACTS, SVC, ...) as well as discrete type compensators (capacitor/inductor banks, OLTC, ...), to validate the proposed controller, only generators and capacitor/inductor banks are considered to participate in CSVC for the IEEE-118 bus case study. Moreover, since the proposed CSVC has a centralized control structure, the areas found during pilot bus selection algorithm are not considered as control areas and the CSVC considers the power grid as one control area.

The capacitor/inductor banks are assumed to be installed on the buses which are found by the algorithm and no compensator has already been installed on them. The parameters γ and ϵ_p are found by trial and error to have a good voltage profile on remote buses. In this way $\gamma = 1E-3$ and $\epsilon_p = 1E-6$. This choice of parameters leads to allocation of 6 buses as pilot nodes which are listed as buses 117, 21, 43, 52, 101 and 86. These pilot buses are shown with solid line. Moreover, the continuous control buses are located at buses 12, 49, 54, 85, 87 and 100 and discrete type controllers are located at buses 117, 20, 21, 22, 23, 43, 44, 45, 51, 52, 53 and 58. The control buses are shown with dashed lines in Figure 4.3.

4.3 Identification of Neural Network Nonlinear Sensitivity Model

The identification procedure toward obtaining Neural Network nonlinear sensitivity model is presented for IEEE 118-bus system of Figure 4.3. Pilot buses as well as discrete and continuous type compensators who participate in CSVC are assumed to be installed on the buses found in

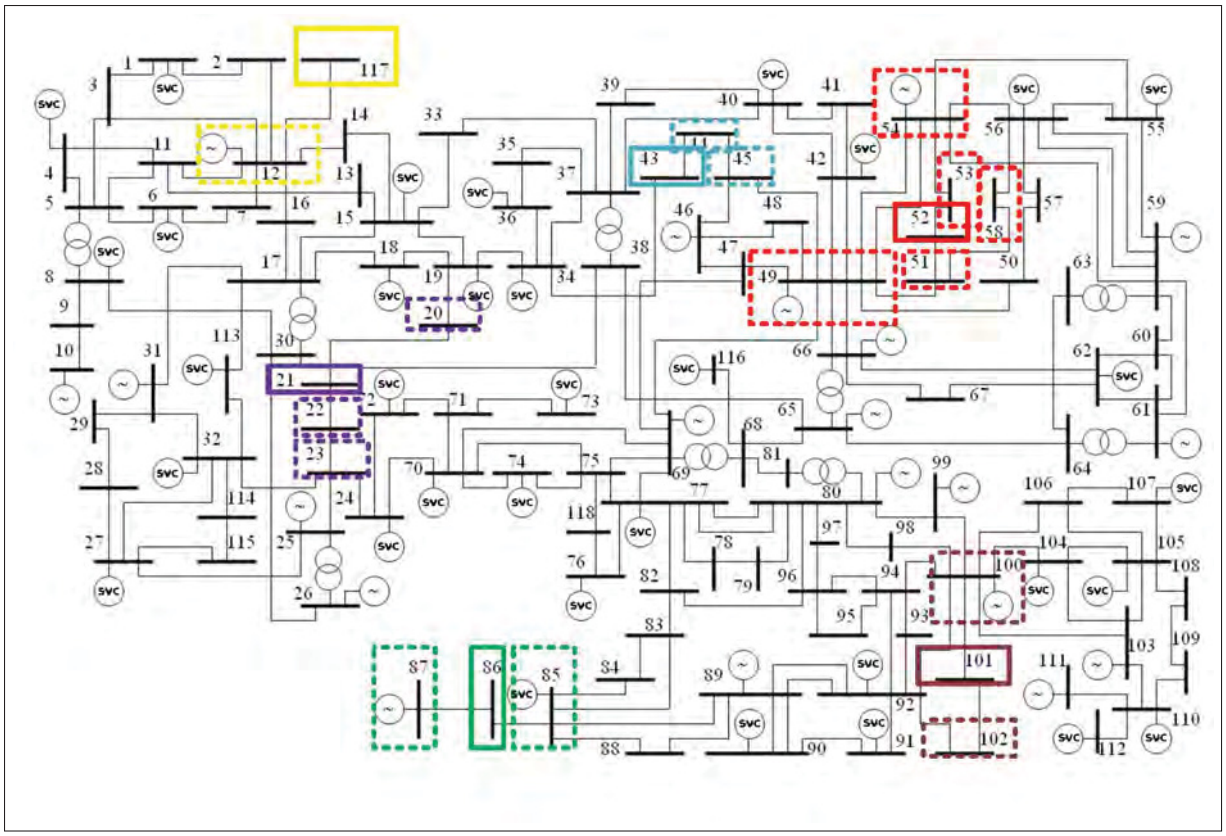

Figure 4.3 IEEE 118-bus power network. Pilot nodes (solid rectangle) and control bus (dashed rectangle)

4.2. Initial value of the control vector is considered to be zero, i.e. $U = 0$. All discrete type compensators are assumed to be capacitor/inductor banks which have 10 switching steps as capacitor and 2 step as inductor with a step size of 10 MVAR/step. Furthermore, the change of reference voltage for continuous type compensators is assumed to be within -0.05 and 0.05 range and it is discretized with discretization step of 0.001.

The identification process is done in two steps: input-output data generation and model fitting. The ideal input data set for data generation consists of all possible values of ΔU vector from the discrete domain defined in Section 4.1 with equal probability of occurrence for each disturbance level. However for a large-scale power grid with large number of controllers, each having many discrete values, this leads to a large amount of input-output data which requires larger memory and higher amount of computational effort during learning of the Neural

Network. As an alternative, the following information about the general operation of CSVC controller is quantified using probabilistic tools to generate less but richer data samples: 1- For negative disturbances, i.e. decrease of load, voltage increases, hence the compensators absorb reactive power. 2- For positive disturbances, i.e. increase of load, voltage decreases, hence compensators inject reactive power. 3- for higher disturbances, compensators inject/absorb higher reactive power.

From these informations, it can be noticed that the discrete step of a compensator can be related to the disturbance level. For the capacitor/inductor bank as a discrete type compensator, maximum number of steps as capacitor and maximum switching steps as inductor correspond to maximum positive, and maximum negative disturbance levels respectively. Moreover non-switched state of the compensator corresponds to zero disturbance level. Having these assumptions, a linear relation between the two variables is defined as follows:

$$\mu = \begin{cases} \dfrac{\Delta Q_i^{-p}}{N_n} i & N_n < i < 0 \\ \dfrac{\Delta Q_i^{+q}}{N_p} i & 0 < i < N_p \end{cases} \tag{4.5}$$

in which i is disturbance level, N_p and N_n are maximum positive and negative disturbance levels respectively, and ΔQ_i^{-p} and ΔQ_i^{+q} are maximum positive and negative switching steps. μ is corresponding switching step to the disturbance level, i.

To convert deterministic relation defined in Equation 4.5 into a stochastic relation, switching step is considered as a stochastic variable with the highest probability for μ. Also the corresponding (PMF) is defined as follows:

$$Pr(k) = \alpha e^{\frac{-(k-\mu)^2}{2}}, k \epsilon \{\Delta Q_i^{-p}, ..., \Delta Q_i^{+q}\} \tag{4.6}$$

in which α is the normalizing factor to have $\sum_{k=1}^{n} Pr(k) = 1$.

Figure 4.4 illustrates relation between mapping function defined in Equation 4.5 and the PMF defined in 4.6. This figure shows that each disturbance level is corresponding to one PMF with highest probability for μ . This PFM is then used for data generation process which is described later.

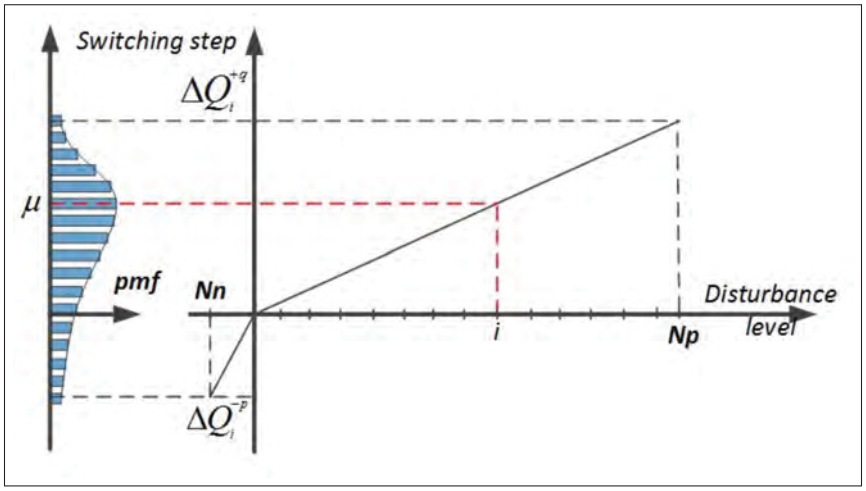

Figure 4.4 generating probability mass function for random capacitor/inductor switching

The same interpretation can also be done for continuous type controllers.

Before starting the data generation process, the maximum loadability limit of the network, dMAX, is calculated to safeguard power flow step from divergence in the data generation process described in Figure 4.5. In order to extract behavior of the system, especially when contingencies move the operating point of the system close to the nose of the QV curves, both active and reactive ZIP loads are increased gradually as disturbance and at each level, input data is generated based on PMF defined in Equation 4.5 and Equation 4.6. The input data is then given to steady state power flow model of the network and the corresponding voltage deviation is calculated after doing power flow. In case of divergence of the power flow, the process is repeated with new sets of inputs until it converges and finally the input-output data is saved into the data set.The whole process is repeated for N_p disturbance levels and N_s random values of ΔU vector based on PMF defined using Equations 4.5 and 4.6.

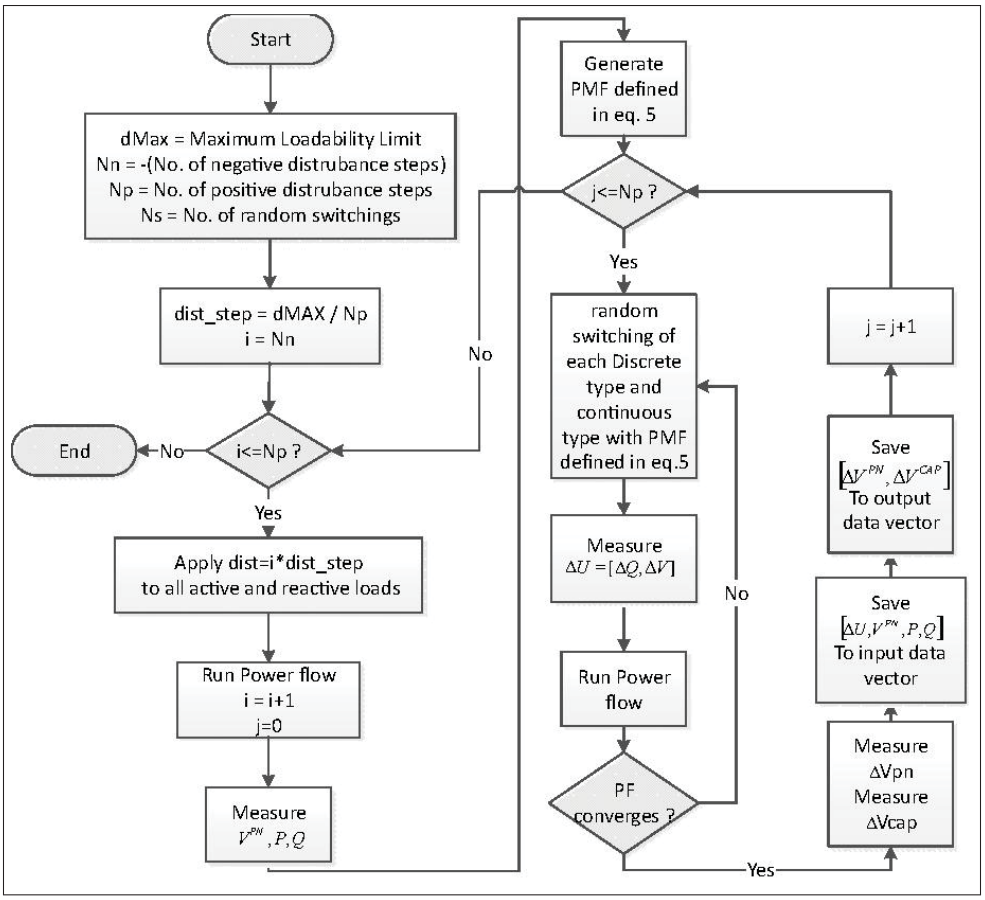

Figure 4.5 Algorithm for generating Input-Output data

After generating input-output data set, a two layers feed-forward NN with 100 neurons as hidden layer is chosen to fit data set. The network is also trained using Levenberg-Marquardt method for 70% of the generated In-Out data samples as training data and then validated and tested by the remaining 30%. Figure 4.6 shows error histogram for the identified NN model after 8 iterations. As can be seen from Figure 4.6, the error between outputs of the identified model and the output data for the same input instances are normally distributed around zero with standard deviation less than 0.001 which is acceptable for this problem.

4.4 Simulation Results for IEEE 118-bus power network

To validate the stability and robustness of the proposed controller, the closed loop system is tested on a real-time dynamic simulator from OPAL-RT technologies. The dynamic model of

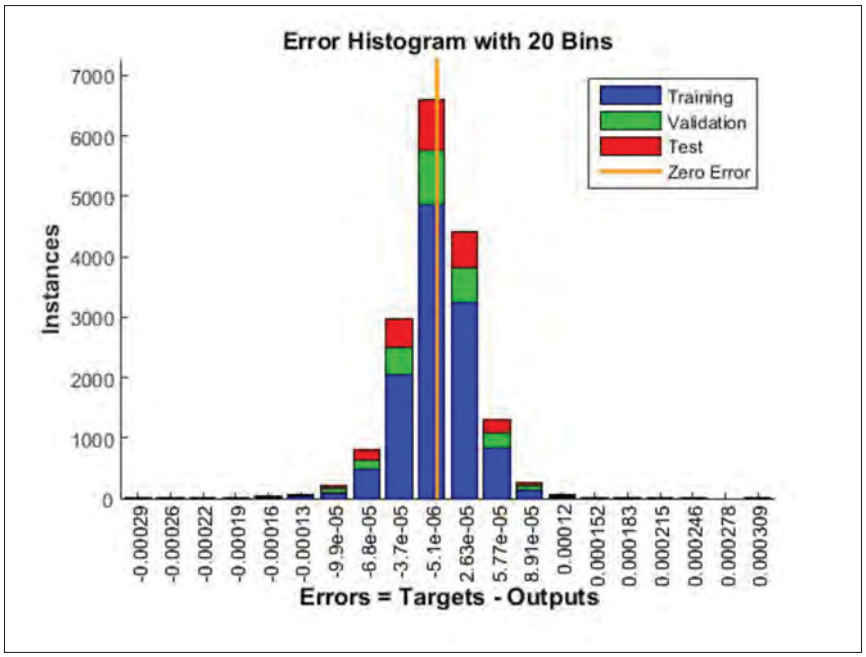

Figure 4.6 Error histogram for the identified NN sensitivity model of IEEE 118-bus test case

the power system is defined using ePHASORsim software for which the input data of power flow as well as dynamic parameters are provided in PSS/e format. The dynamic models used in this test-case are synchronous generators of type GENROU, static var compensator of type CSVGN5, excitation systems of type EXST1, maximum excitation limiters of type MAXEX2 and also turbine governors of type TGOV1. Power system stabilizers of type STAB1 are also connected to excitation systems on buses 26, 49 and 100. In addition, the network includes 35 static var compensator of type CSVGN5. Finally, constant power loads are considered to represent the capacitor/inductor banks.

Maximum voltage deviation on generator buses are considered to be $0.05p.u.$ and the minimum limit is assumed to be $-0.05p.u.$. Moreover, the capacitor/inductor banks can inject maximum of $100MVAR$ and absorb $-20MVAR$ with the switching step of $10MVAR$. On the other hand, voltage on the buses to which the compensators are connected should be between $0.9p.u.$ and $1.1p.u.$. Finally, synchronous generators as well as static var compensators have a reactive power capacity between $-100MVAR$ and $400MVAR$.

The parameters of the proposed CSVC used for validation are shown in Table 4.1.

Table 4.1 parameters of the proposed CSVC controller

Parameter	Value
Number of iterations of SA algorithm, T0, for each time step	1000
Diagonal weights of R for generators	0.1
Diagonal weights of R for capacitor/inductor banks	5E-4
Equalization weights for generators, α_{ij}	1E-5
Equalization weights for capacitor/inductor banks, β_{ij}	1E-6
Coefficient, α, in SA flowchart, Figure 4.2	0.0214

The proposed CSVC is tested under different scenarios against linear sensitivity based CSVC method and also traditional method based on local measurements and control. All three methods use the same control structure of Figure 4.1, except for the network sensitivity model which is different. The linear based CSVC uses a linear full matrix sensitivity model while the traditional controller employs a diagonal sensitivity which just maps local reactive power injection to local voltage. Also the linear sensitivity based CSVC method uses the same generators and capacitor/inductor banks as the proposed algorithm while the traditional control method only uses capacitor/inductors which are installed on the pilot buses. The time step of secondary voltage controller used in all three cases is 5 seconds.

In the following, the validation scenarios are discussed.

4.4.1 Senario 1: change of reference voltage on the pilot nodes:

In the first scenario, the tracking feature of the proposed CSVC is validated. In this way, the reference voltage of all pilot nodes are suddenly increased by 3% of per unit at t = 5 seconds.

Figure 4.7 shows the dynamics of the voltage deviation on pilot nodes as well as its steady state values. As can be seen from Figure 4.7a, after immediate reference change at t = 5 seconds,

voltage on pilot nodes does not change instantaneously due to a delay of 5 seconds exists in the control loop. Consequently, voltage error error shows a gap of $0.03p.u.$ in the timespan $5 - 10$ seconds. However, at $t = 10$ seconds, all control approaches except the traditional method take action, which leads the voltage error to reduce gradually. However for the traditional control approach, as seen in Figures 4.7a & 4.7b, the voltage error on pilot buses remain unchanged since none of the capacitor's installed on the pilots take actions as shown in Figures 4.8b & 4.8c. This is caused by the large switching step of capacitor/inductor banks and also the lack of continuous type compensators to reduce the error by adjusting the control command with smaller changes.

Comparing the results shown in Figure 4.7b for the proposed method and linear based CSVC method, one can see that the steady state voltage error for both controllers are quite the same with a slightly better performance of the proposed method. However, from Figure 4.7a it can be seen that the settling time of the proposed method is significantly smaller due to the fact that the nonlinear NN based model in the proposed CSVC calculates the required reactive power more precisely at each time step hence the introduced steady state error after applying the control command is smaller. Moreover oscillatory behavior seen specifically on the voltage error of bus 43 for the linear based CSVC method does not exist in the proposed method.

Figure 4.8 illustrates the corresponding calculated reference voltage change for AVR connected to the excitation system of the generators as well as reactive power injection by capacitor/reactor banks. As depicted in Figure 4.8a, the reference voltage of AVRs start to increase with a 5 seconds of delay right after fault for both proposed CSVC and linear sensitivity based CSVC. However, in the latter, the reference voltage for the AVRs connected to the synchronous machine at bus 54 saturates at its maximum, i.e. $5\% p.u.$.

Finally, Figure 4.9a illustrates voltage on the buses to which participant generators, static var compensator and capacitor banks are connected and Figure 4.9b shows the injected reactive power by participant generators and static var compensators. As can be seen for both proposed

CSVC and linear sensitivity based CSVC, terminal voltages and reactive powers are within the desired limits.

4.4.2 Senario 2: sudden load change:

In this scenario, all the constant impedance loads are suddenly increased by100% at t = 10 seconds, while constant power and constant current loads are increased by 40% and 20% respectively. Reference voltages on pilot buses are considered constant and they are equal to before contingency values. Figure 4.10 shows the dynamics of the voltage deviation on pilot nodes as well as its steady state values. As can be seen in this figure, few milliseconds after disturbance, voltage on pilot buses suddenly drops by $0.3p.u.$. However, the primary level controllers take action immediately and are able to reduce the error to less than $0.1p.u.$ just in 5 seconds. The steady state error, however, is compensated by the secondary level controllers starting the first time step, at t = 5 seconds. The dynamic simulations also show a similar response of the proposed CSVC and the other two methods. Figure 4.10b also illustrates the steady state error of voltage of the pilot nodes. As can be seen in this scenario, the proposed CSVC has a similar error to the other two methods.

Figure 4.11 also shows the calculated control signals for both generators and capacitor/inductor banks. Figure 4.11a illustrates that the reference voltage change for AVR of the machine at buses 12 and 54 saturate at 25 seconds for the linear based CSVC. However, for the proposed method only the AVR reference of the machine at bus 12 saturates.

Finally, Figure 4.12a illustrates voltage on the buses to which participant generators, static var compensator and capacitor banks are connected and Figure 4.12b shows the injected reactive power by participant generators and static var compensators. As can be seen in Figure 4.12a, at the time of fault voltage on some control buses drop as low as $0.7p.u.$. However due to the fast reaction of the primary level controllers, they recover back to $0.87p.u.$ in just 5 seconds after fault. At t = 10 seconds, both proposed CSVC and linear sensitivity based CSVC take action and bring back the voltage at control buses within the limit while they try to maintain

the voltage on pilot buses. Figure 4.12b also shows that reactive power of generators are kept within the desired limits except for the time of fault, t = 10 seconds and for the time period $[16.5, 19.75]$ seconds. In both cases, reactive power injected by the synchronous generator located at bus 100, goes beyond $400MVAR$ limits. The latter is caused by the fast reaction of the AVR connected to this machine. However few milliseconds after fault, the reactive power lowers down to less than the maximum limit. The later violation, on the other hand, occurs between two time steps of the CSVC and it is not detected by the algorithm. On the other hand, the CSVC is able to detect reactive power violation of the generator located at bus 49 at t = 15 seconds. Consequently, the CSVC reduces reference voltage of the connected AVR to lower the reactive power to less than the maximum limit.

4.4.3 Senario 3: bus trip:

In this scenario, buses 15, 80, 94 & 49 are tripped from the network at t = 10 seconds. Tripping these buses disconnects all lines, transformers, generators connected to them and leads to a topology change in the network. Moreover, one of the tripped buses, i.e. bus 49, has a participant generator in CSVC attached to it which is also tripped as a result of the bus trip.

Figure 4.13 shows the dynamics of the voltage deviation on pilot nodes as well as its steady state values. Moreover Figure 4.14 illustrates the dynamics of the control variables for both generators and capacitor/inductor banks versus time and also steady state values of capacitors/inductors switching steps.

As can be seen in Figure 4.10a, despite major topology change, the proposed controller is able to compensate voltage error even faster than the other two methods.

The simulations are run on Opal-RT's OP-4510 Real-time simulator with Intel Xeon E3 4-core 3.5 GHz CPU. Figure 4.15 illustrates the optimization results of the SA algorithm for scenario 3 in which the algorithm is run for 1000 iterations at each time step of the controller. Thus each 1000 iterations belong to one time step of the controller. As can be seen in this figure, the objective function value is able to converge at each time step of the controller to a suboptimal

solution in less than 100 iterations. However, it is run for 1000 iterations to achieve close to optimal results. In this simulation, the calculation to find the suboptimal solution is done in 500 milliseconds which is much smaller than the time step of the proposed CSVC loop, i.e. 5 seconds. In this way, the computational delay is negligible and the proposed controller can be applied in real time for such a network.

4.5 Conclusion and Future Works

In this paper, a new CSVC strategy is proposed which coordinates discrete and continuous type compensators in transmission system to improve voltage profile at pilot buses of the network when facing large disturbances. The controller consists of two parts: The identified nonlinear sensitivity model of the network and an optimizer. The nonlinear sensitivity model is identified using Neural Networks based on Input-Output data generated from random disturbances on the network. The optimizer utilizes SA algorithm and is combined with NN model to find the optimal switching of the capacitor/inductor banks after sensing any disturbance. The effectiveness of the proposed algorithm is tested by applying the controller on IEEE 118-bus power system while perturbing the network by different levels of disturbance. The simulation results show that the proposed controller is able to bring voltage back into the desired limits for different disturbance cases. Beside voltage control the algorithm also minimizes the reactive power injected to the network. Comparing the simulation results of the proposed method with linear CSVC method and also the traditional approach showed that taking into account the nonlinear model of the system leads to a faster convergence of the method. However both linear based CSVC and the proposed methods had the same steady state voltage error. Moreover it was observed that the traditional method is not able to track the reference voltage change while the other two can compensate the tracking error.

Future works toward improvement of the proposed controller can be considered as follows. As has been discussed in Section 4.4 the NN model is identified off-line, and remains unchanged during the implementation phase. One suggestion is to use adaptive learning methods in real-time to adapt the NN model with changes in the power network. On the other hand, the

proposed strategy was implemented as a centralized controller. This method can be modified to be applied in a decentralized way on the multi-area power networks. In this way, the interaction of areas with each other as well as coordination of the regional CSVC controllers may be considered in control design.

Finally, it was assumed in this paper that the pilot nodes are fixed. However, in case of major events or contingencies, these identified nodes might change. In this way, a comprehensive sensitivity analysis could be done to identify all the potential pilot nodes for different types of contingencies and network base cases. Afterwards, a nonlinear model can be identified assuming voltage of all these potential pilot nodes as outputs. In this way, for each operating condition, a subset of these nodes are controlled while assuming zero weighting coefficients for the voltage error term of other nodes which are not considered as pilot buses for this specific scenario.

4.6 Acknowledgment

The authors would like to thank Opal-RT Technologies for providing dynamic data for IEEE118 bus power system and also for the real-time simulator and ePHASORsim software license.

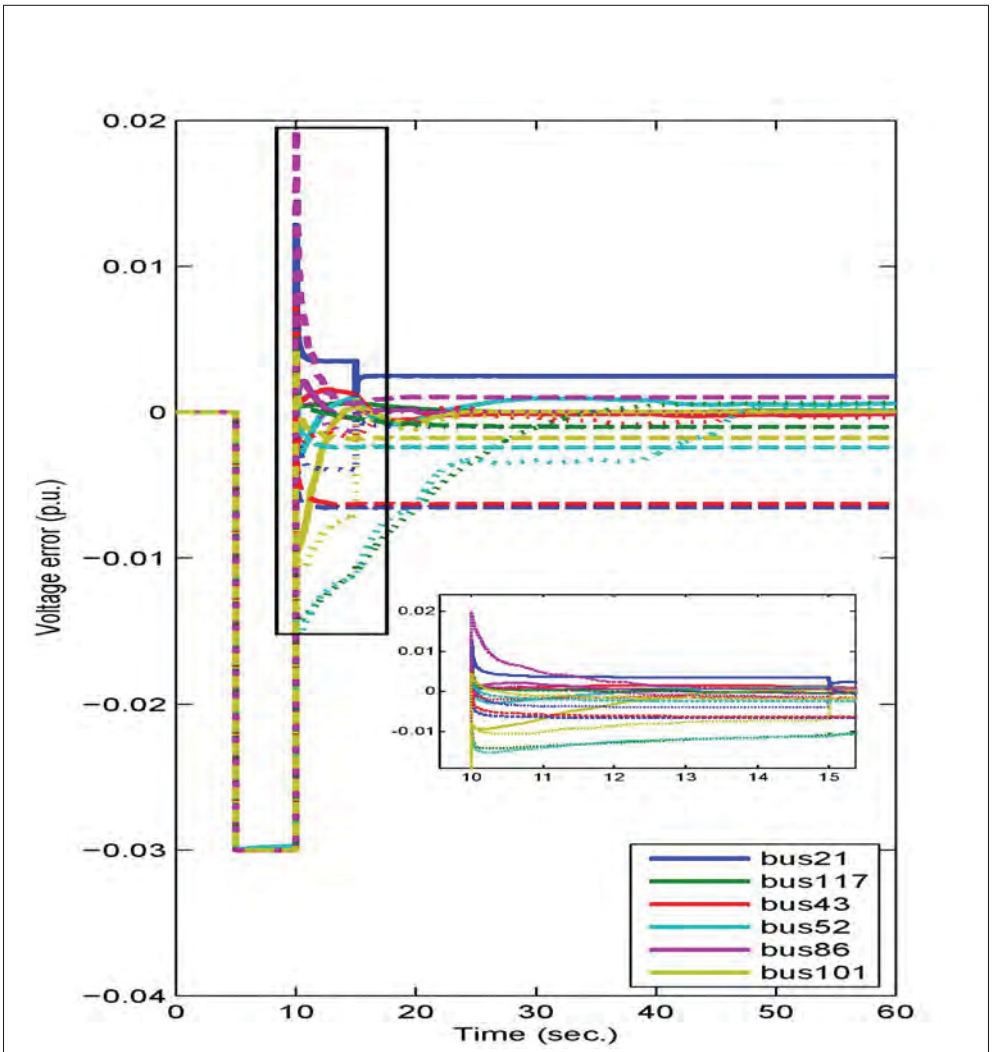

Figure 4.7 Scenario 1: Proposed method (solid line), Linear sensitivity based CSVC (dotted line) and Traditional method (dashed line)

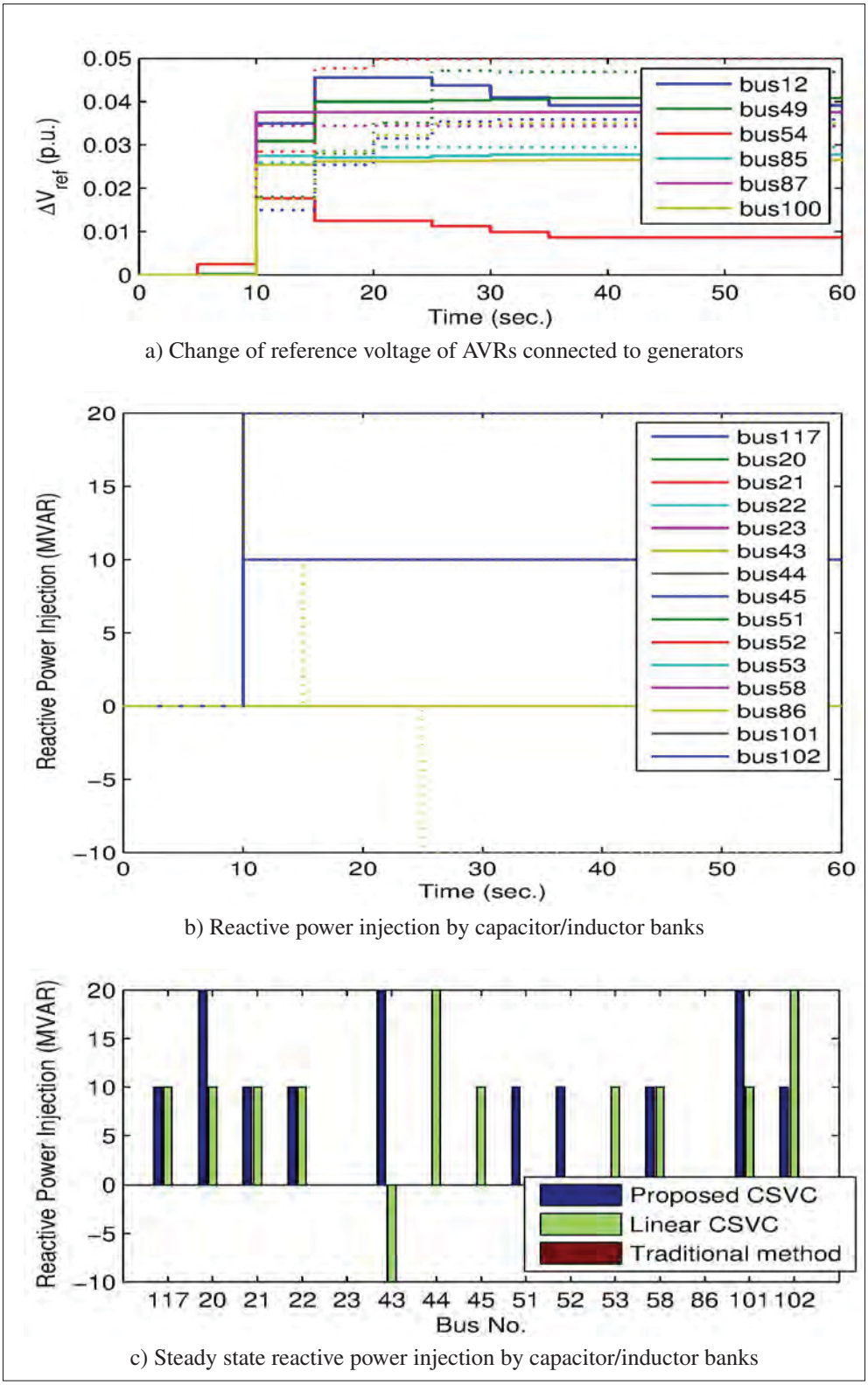

a) Change of reference voltage of AVRs connected to generators

b) Reactive power injection by capacitor/inductor banks

c) Steady state reactive power injection by capacitor/inductor banks

Figure 4.8 Scenario 1: Proposed method (solid line), Linear sensitivity based CSVC (dotted line) & Traditional method (dashed line)

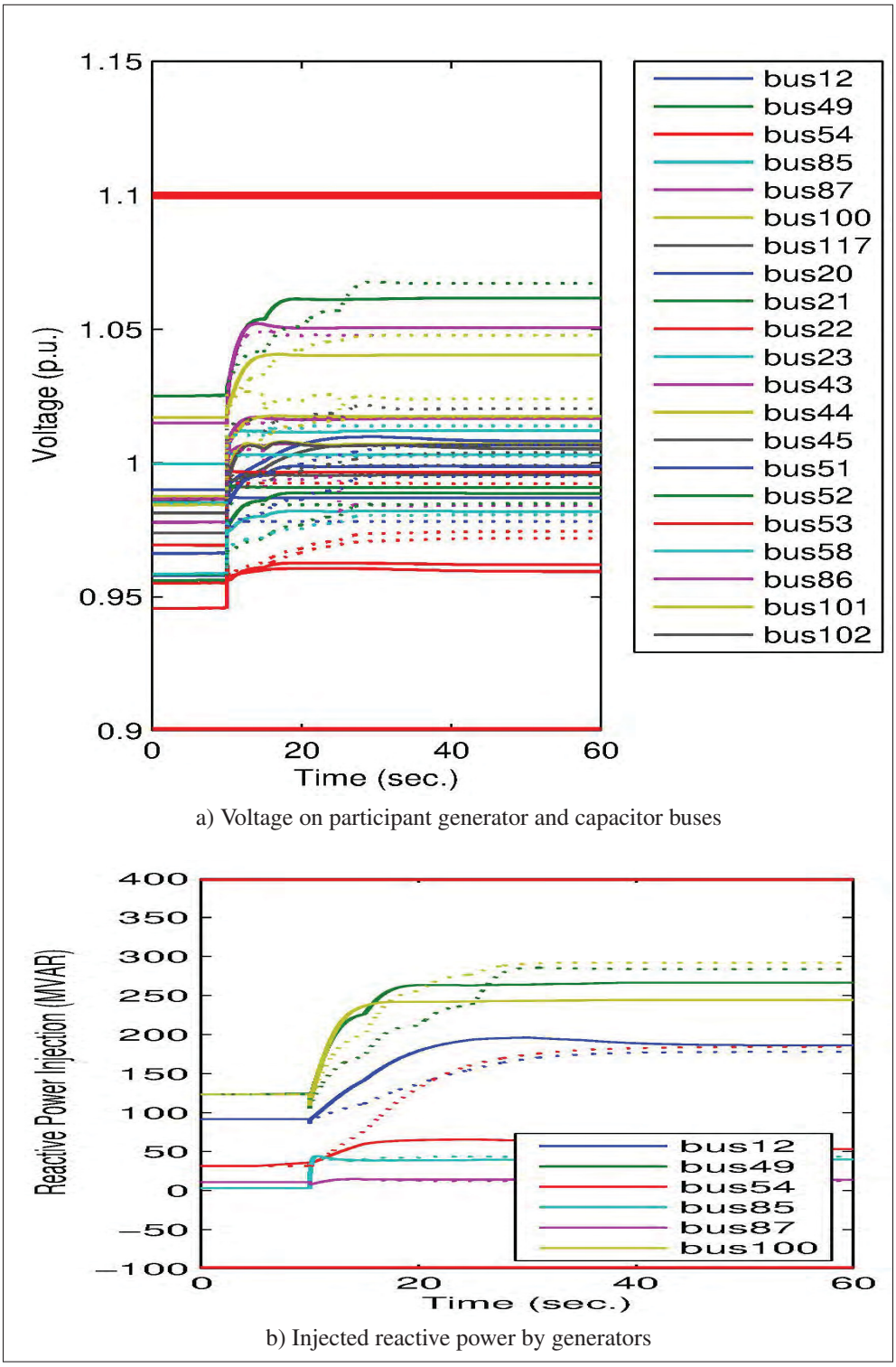

a) Voltage on participant generator and capacitor buses

b) Injected reactive power by generators

Figure 4.9 Scenario 1: Proposed method (solid line), Linear sensitivity based CSVC (dotted line) & Traditional method (dashed line)

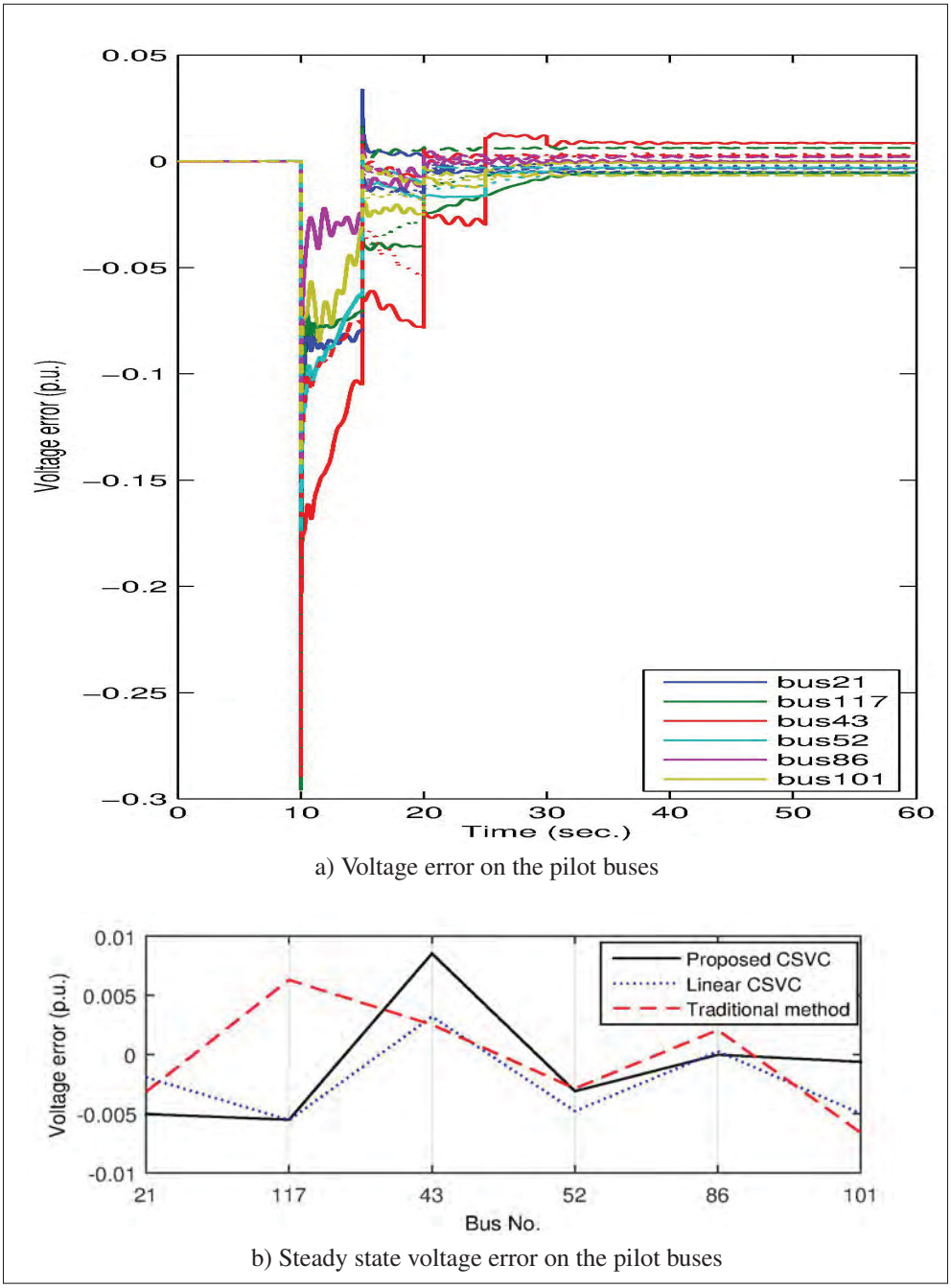

Figure 4.10 Scenario 2: Proposed method (solid line), Linear sensitivity based CSVC (dotted line) and Traditional method (dashed line)

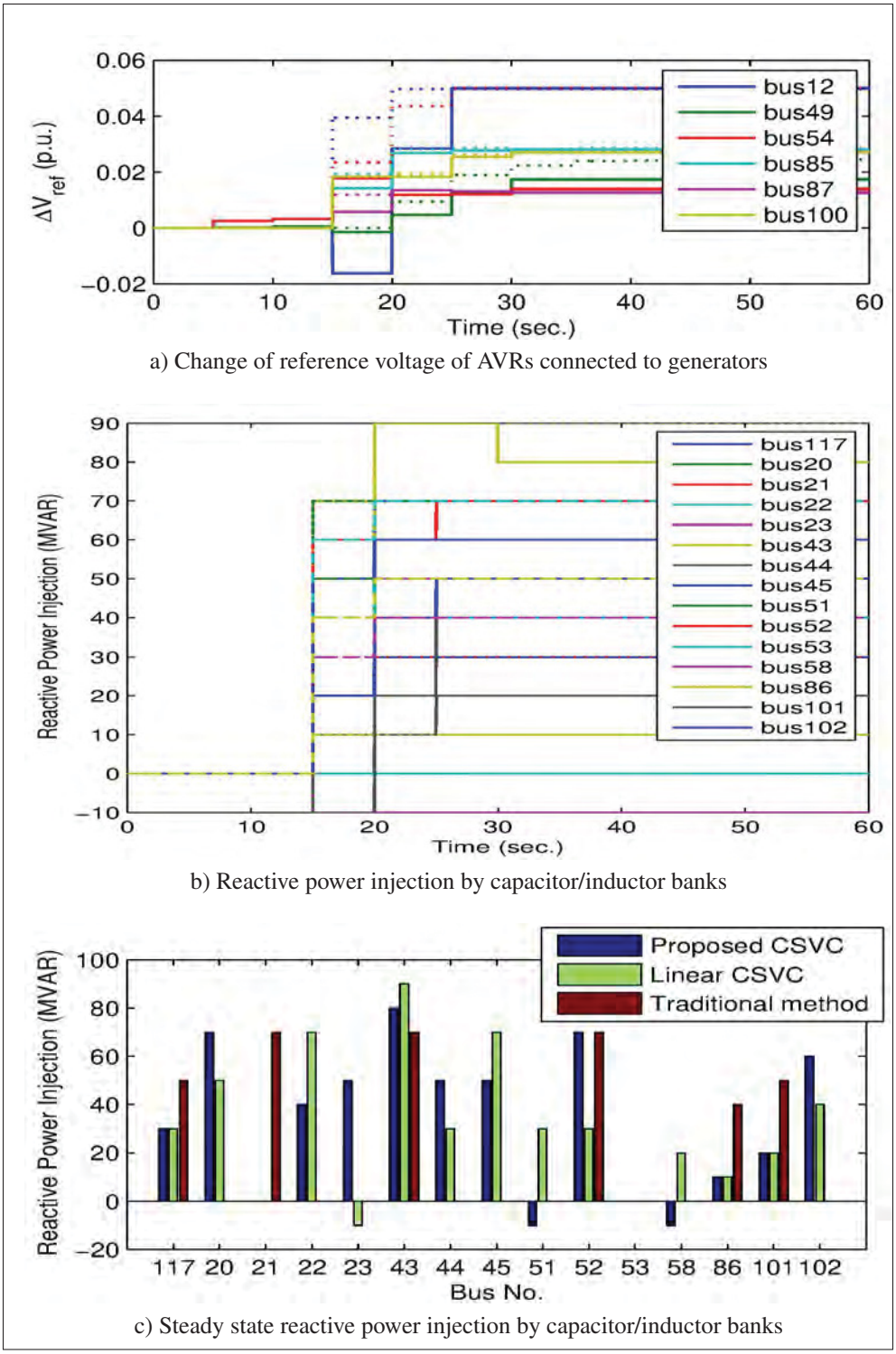

a) Change of reference voltage of AVRs connected to generators

b) Reactive power injection by capacitor/inductor banks

c) Steady state reactive power injection by capacitor/inductor banks

Figure 4.11 Scenario 2: Proposed method (solid line), Linear sensitivity based CSVC (dotted line) & Traditional method (dashed line)

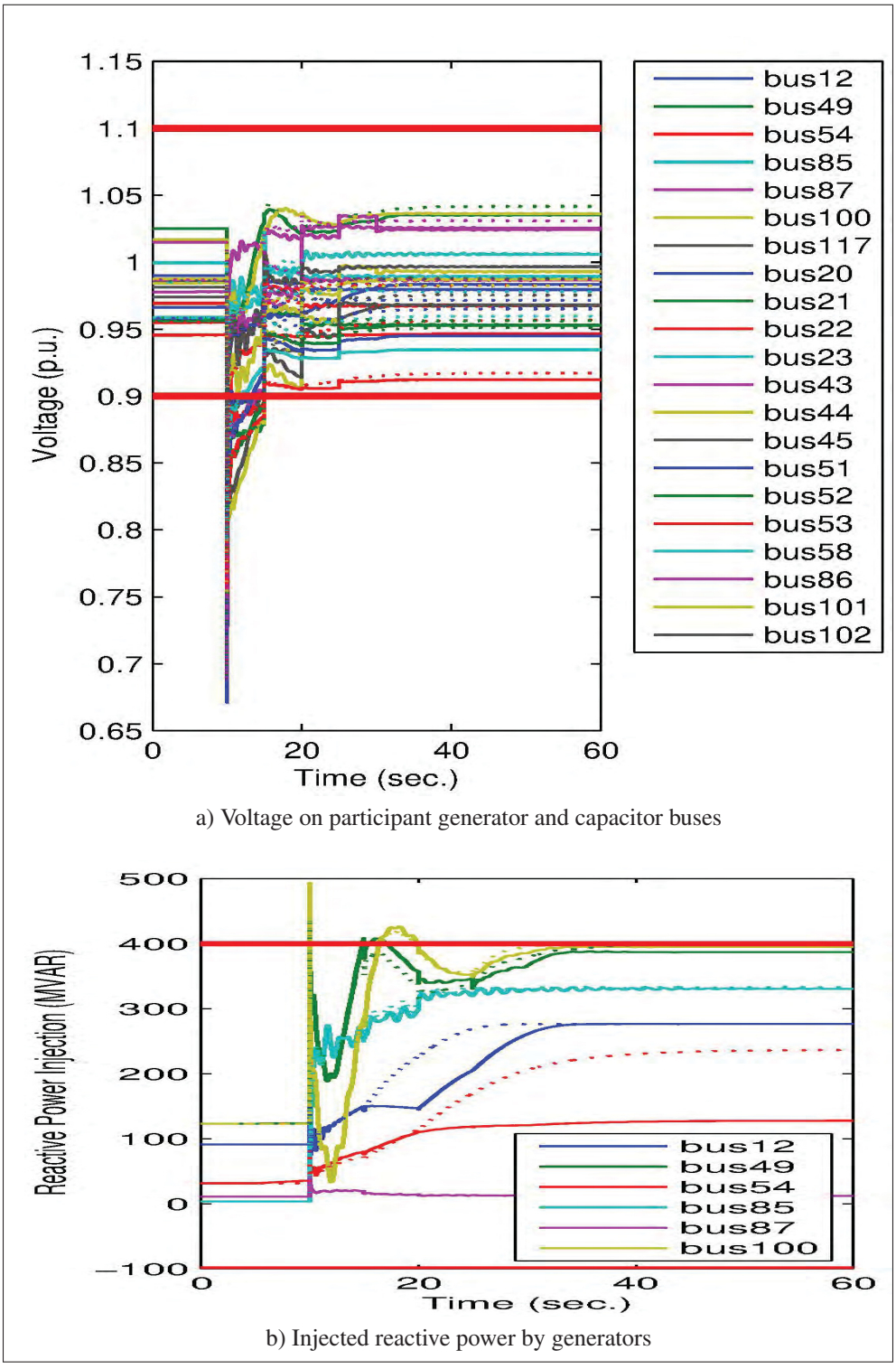

a) Voltage on participant generator and capacitor buses

b) Injected reactive power by generators

Figure 4.12 Scenario 2: (Proposed method (solid line), Linear sensitivity based CSVC (dotted line) & Traditional method (dashed line)

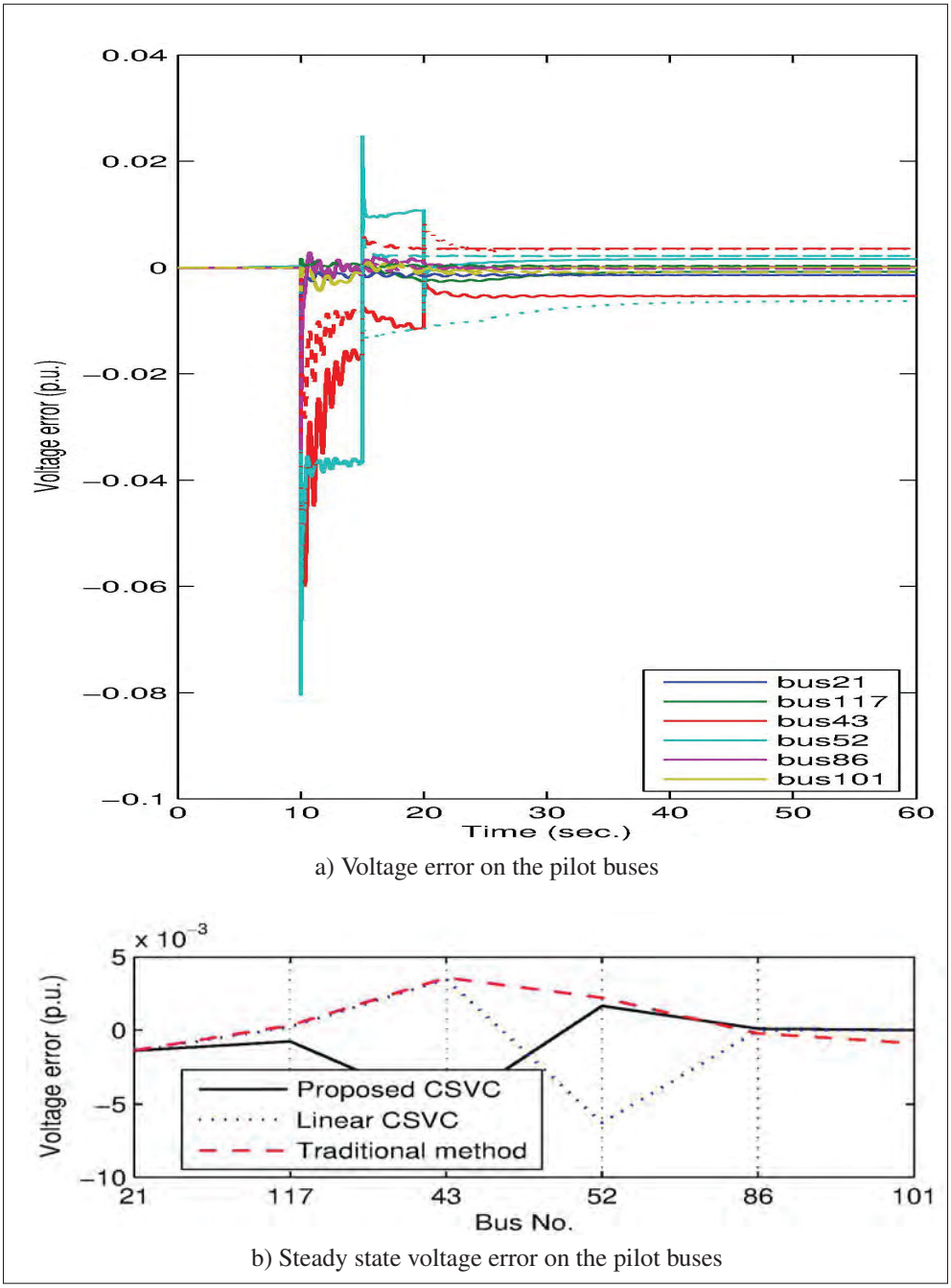

a) Voltage error on the pilot buses

b) Steady state voltage error on the pilot buses

Figure 4.13 Scenario 3: Proposed method (solid line), Linear sensitivity based CSVC (dotted line) and Traditional method (dashed line)

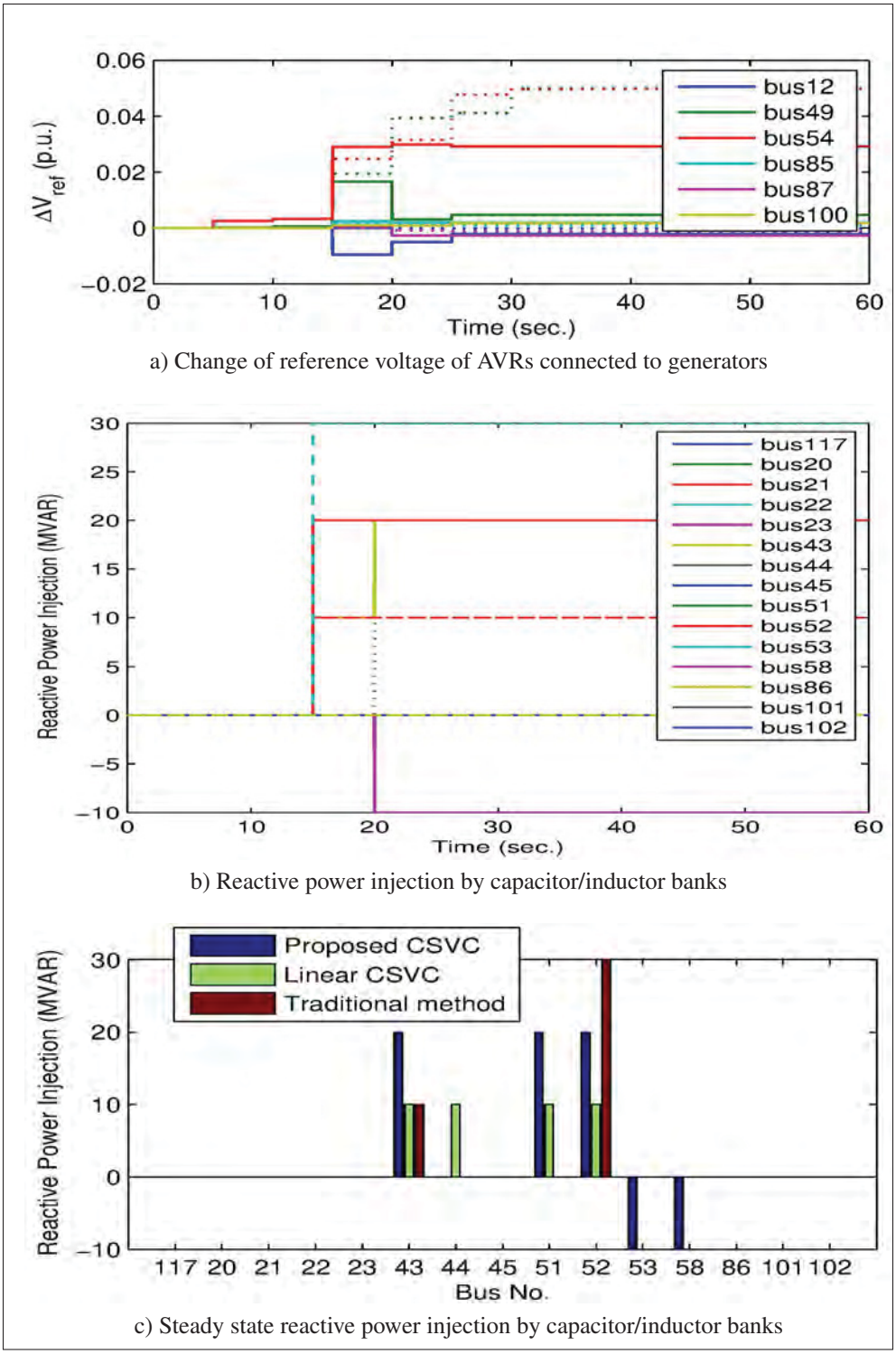

a) Change of reference voltage of AVRs connected to generators

b) Reactive power injection by capacitor/inductor banks

c) Steady state reactive power injection by capacitor/inductor banks

Figure 4.14 Scenario 3: Proposed method (solid line), Linear sensitivity based CSVC (dotted line) & Traditional method (dashed line)

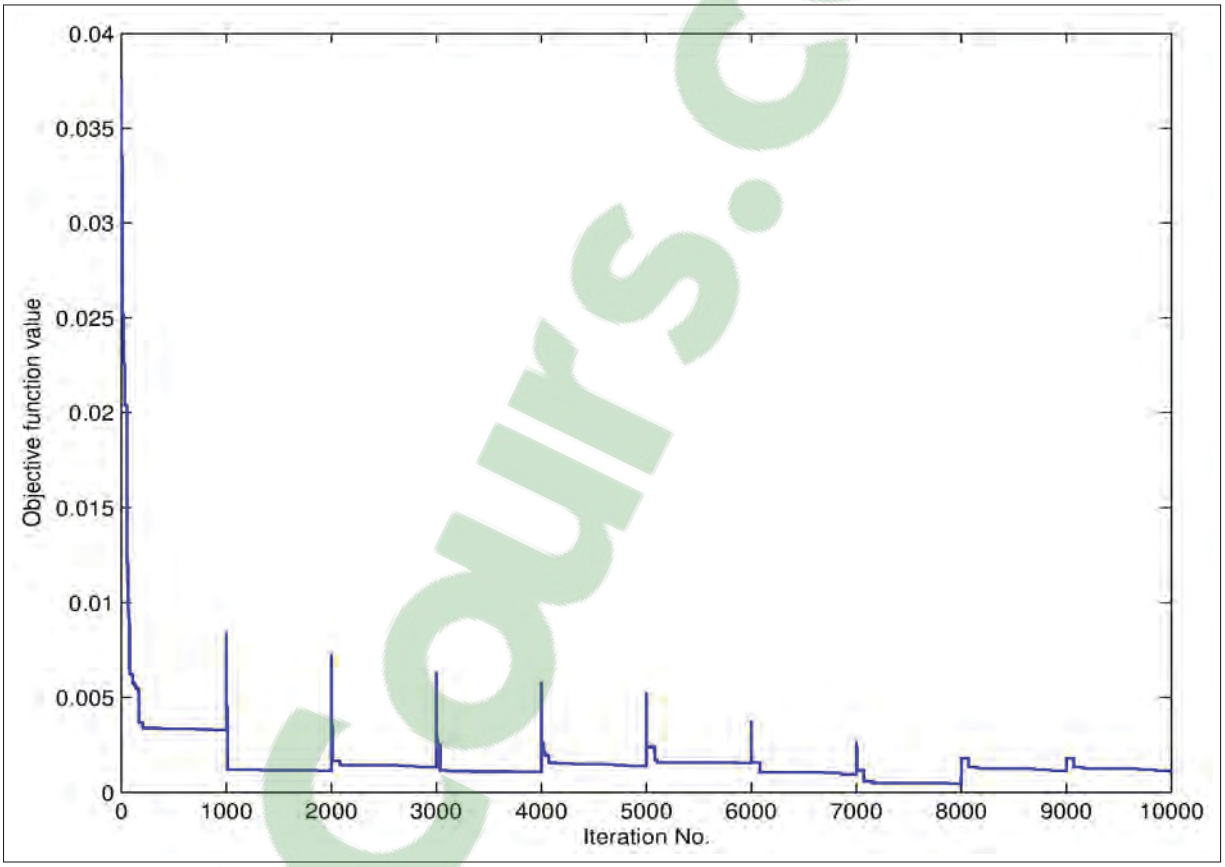

Figure 4.15 Evolution of the objective function at each time step of the controller

CHAPTER 5

SECONDARY VOLTAGE CONTROL WITH CONSENSUS BETWEEN REGIONAL CONTROLLERS

Arvin Morattab[1], Ouassima Akhrif[1], Maarouf Saad[1]

[1] Department of Electrical Engineering, École de Technologie Supérieure,
1100 Notre-Dame Ouest, Montréal, Québec, Canada, H3C 1K3

Article submitted for publication, February 2018

Abstract

SVC is a well-known control strategy to improve mid-term voltage stability in a region. It is based on partitioning the power system into electrically decoupled areas and controlling the voltage of pilot buses as representative nodes of each area in a decentralized way. In practice however, these control areas are not completely decoupled and some compensators in one area might affect a pilot bus of a neighbor area. In this case, a coordination is required between the regional SVCs to reach a consensus for the action of such compensators. This paper proposes a novel consensus based SVC strategy for coordination between neighbor areas of a power grid. In this way, for each group of regional SVCs with shared compensators, a higher level coordinator is defined which calculates the consensus values for all conflicting pairs based on a proposed consensus protocol. The consensus is reached in two iterations between SVCs and the coordinator. It is shown through simulations that the proposed strategy can diminish oscillations caused by uncoordinated regional SVCs while minimizing reactive power efforts. IEEE 118 bus test-case is used to validate the effectiveness and performance of the proposed algorithm on a real-time simulation test-bench in which the regional SVCs are run on separate computational cores. The communication between SVCs, measurement units and compensators are through standard IEEE C37.118 and DNP3 protocols.

Introduction

SVC is widely used nowadays in power system control centers as part of hierarchical control strategy to ameliorate voltage stability all over the power grid. Various implementations of SVC Corsi (2015) have been successfully employed in many countries such as France, Italy, Brazil, Romania, China and USA. Although voltage control is essentially a local problem, it has been proven that SVC, which emphasizes on voltage control in an area of the power system, can improve voltage stability by managing reactive power resources considering their limits to contribute to the voltage control of representative buses of each area, called pilot buses.

The first step toward SVC is to allocate pilot buses and to partition the power system into electrically decoupled coherent regions. There are many methods presented in the literature which discuss this issue Lagonotte *et al.* (1989); Conejo *et al.* (1994); Karakatsanis & Hatziargyriou (1994); Conejo & Aguilar (1998); Amraee *et al.* (2010); Trakas *et al.* (2014); Mezquita *et al.* (2015); Mehrjerdi *et al.* (2013b,c); Cotilla-Sanchez *et al.* (2013); Amadou *et al.* (2014); Chen *et al.* (2015); Alimisis & Taylor (2015). These methods are mostly centered around the idea of sensitivity analysis presented in Corsi (2015). The control buses are also identified for each control area using the same approach used for pilot nodes. Finally, the SVC control loop is established in each area as a two-level PI rule which measures the voltage on the pilot bus and sets the set-point of the PVC such as the AVR or static var compensators. This method lacks the coordination of SVC of two neighbor regions in the case when some compensators affect voltage of the two neighbor areas substantially.

To resolve this issue, Paul *et al.* (1987) presents Coordinated SVC in which the two interconnected areas form one region and a MIMO optimal controller is proposed to regulate voltage on the pilot buses.

Although this approach overcomes the problem of uncoordinated SVCs by unifying the two, it is not in favor of the deregulated structure of nowadays power grids in which the focus is on decentralization of the power system. In this way, a lot of research has been done to find decentralized control algorithms that consider coordination between neighbor areas. In this regard,

Mehrjerdi *et al.* (2013d) proposes a coordination strategy in which the interaction between areas is defined using a connection matrix. The effect of areas on each other is considered as the measured tie-line reactive power between the two neighbors. Moreover, Moradzadeh *et al.* (2013) uses distributed MPC algorithm for SVC in which each SVC considers the control action taken by its neighbors in the last time step to calculate its current control law. Also Morattab *et al.* (2017a) presents a decentralized MPC approach in which the effect of the neighbor areas is measured as tie-line reactive power and defined as a measured disturbance. While in these methods each regional SVC assumes the effect of its neighbors, there is no iteration between neighbor areas at one time step. The coordination of one area and its neighbor is basically based on the measured signals from the neighbors in the last time step.

In recent years, a growing amount of research has focused on multi-agent based cooperative SVC in transmission network in which the regional controllers reach a consensus at each time step Vaccaro *et al.* (2011); Loia *et al.* (2013); Bottura & Borghetti (2014); Su *et al.* (2016); Borghetti *et al.* (2017).

In this way, Vaccaro *et al.* (2011) proposes a decentralized non-hierarchical voltage regulation architecture in which the states of the neighbor areas dynamics are synchronized to the weighted average of the variables sensed by all the controllers in the smart grid. Moreover, Loia *et al.* (2013) proposes decentralized and non-hierarchal voltage control architecture based on cooperative fuzzy agents to achieve consensus. In addition, Bottura & Borghetti (2014) and Borghetti *et al.* (2017) discuss an asynchronous leaderless multi agent approach that coordinates the reactive power compensators. Finally, Su *et al.* (2016) formulates CSVC as a nonlinear successive ∞-norm minimization problem in which the load disturbances are estimated on-line.

The methods presented in Vaccaro *et al.* (2011) & Loia *et al.* (2013), define consensus as convergence to the average of the measurements and needs a quite large number of iterations, resulting therefore into a large number of exchange data. However, due to the local nature of voltage control problem, it is not required to reach a global consensus. In this way the

consensus could be just limited to the neighbor areas which are strongly coupled. On the other hand, the so-called gossip based approach presented in Bottura & Borghetti (2014) and Borghetti *et al.* (2017) requires some time to evaluate the priorities and come up with an action. By limiting the consensus strategy just to the strongly coupled neighbors, the required time for the gossip based method can be saved tremendously.

This paper presents a novel coordination technique in a multi area power systems between SVCs belonging to neighbor areas with common buses. Such a consensus is required especially when the overlapping buses include some compensators which can potentially affect the voltage of the pilot bus on all neighboring areas. These compensators are called shared compensators throughout this paper. In the proposed method, each regional SVC calculates the control set- point for the PVC of these shared compensators as well as its non-shared compensators. The calculated values for the former group by all SVCs of the overlapping areas might conflict with each other. These conflicting values alongside their corresponding solution of their local objective function are then communicated to a coordinator which resolves the conflicts by establishing a consensus protocol between all the participant SVCs. Such a decision is made by first a linear estimation of the pareto front of the optimization problems solved first locally and then calculating the consensus value for the PVC of the shared compensator by minimizing the weighted sum of all linearized objective value deviations of the overlapping areas. In the second iteration, the error caused by the consensus is corrected by communicating back the calculated consensus values to the regional SVCs and re-evaluating the set-points of the regional PVCs. as known.

The novelties of this paper are enumerated as follows:

- Propose a novel consensus strategy for multi-objective optimization problems;
- Propose a modified version of sensitivity analysis presented in Corsi (2015) in which control regions can overlap. Some compensators might be selected for SVC which belong to the shared area;

- Validate on a real-time simulator the iterative consensus algorithm with optimization based SVCs to show its feasibility to be implemented on real power systems.

The paper is organized as follows: Section 5.1 describes the proposed methodology in which the modified sensitivity analysis is presented which is then followed by the proposed consensus strategy. In Section 5.2, the case-study which is the IEEE 118 bus power system is presented. The results of applying modified sensitivity analysis to find pilot nodes, partitioning the network and allocation of the control buses is also discussed in this section. Section 5.3 presents the real-time test-bench on which the simulation scenarios, discussed in Section 5.4, are run and validated. Finally, Section 5.5 concludes the paper and discusses future works.

5.1 Methodology

5.1.1 Modified sensitivity analysis to partition the network

The classical sensitivity analysis method presented in Corsi (2015), relies on successive re-ordering of the sensitivity matrix relating reactive power injection to voltage deviation on all load buses of the grid. The first pilot node is considered as the bus with the strongest short circuit capacity and afterwards, all buses with their coupling coefficient to this node larger than a predefined threshold, are assumed to belong to the first control region. These buses are therefore excluded from subsequent pilot node searching procedure. This process repeats for the remaining buses until the short circuit capacity of the selected candidate is smaller than minimum requirement for a pilot bus. It should be noted that there might be some buses which are identified to belong to more than just one region. However, for such a bus, the coupling factor to the pilot nodes of all areas between which the bus is shared is compared and the bus is assumed to be owned or better to belong to the area with the highest coupling factor. Finally, the last step is to find the most effective compensators in each area, i.e. controllers which have the highest sensitivity to the regional pilot node.

The above assumptions that each bus can only belong to one control area, and that the identified controllers in each area have no impact on the pilot node of other areas simplifies the design of the classical SVC. However, there might be a bus, referred to in this paper as a shared bus, which has relatively the same coupling factor to two or more pilot nodes and can be identified as a control bus for both areas.

The modified version of the classical sensitivity analysis, as proposed in this paper, neglects the last step of network partitioning algorithms in which the coupling factor of the shared buses is compared for the two or more corresponding pilot nodes. By neglecting this step, the neighbor areas could share some buses, some of which can be identified as controller buses.

Figure 5.1 illustrates a partitioned network based on the modified sensitivity analysis which consists of m overlapping areas. In this figure, the pilot nodes and shared buses are shown using red and blue circle respectively and the rest of the buses are shown using black circles. Moreover, buses to which participant PVCs are connected are highlighted using green rectangles.

Since the compensators connected to shared buses affect the voltage on two or more pilot nodes simultaneously, it could potentially reduce the required power injection in some cases. However, using such controllers in decentralized control strategies requires a coordination between the regional SVCs.

5.1.2 Control methodology for Regional SVCs

Assume a multi-area power system with at least one group of m overlapping areas as shown in Figure 5.1. A typical area, $Area_i$, includes one pilot node with the voltage magnitude of V^i_{PN}, and some participant PVCs in SVC_i with their set-points defined as $\bar{u}^i$ vector. As can be seen in Figure 5.1, for each area, the participant PVCs are installed either on the shared buses, the local bus which is not shared with other areas or both. The corresponding set-point is defined as $\bar{u}^i_{sh}$ for the former group of PVCs and as $\bar{u}^i_{nsh}$ for the latter. In this way $\bar{u}^i = \left\{\bar{u}^i_{sh}, \bar{u}^i_{nsh}\right\}$.

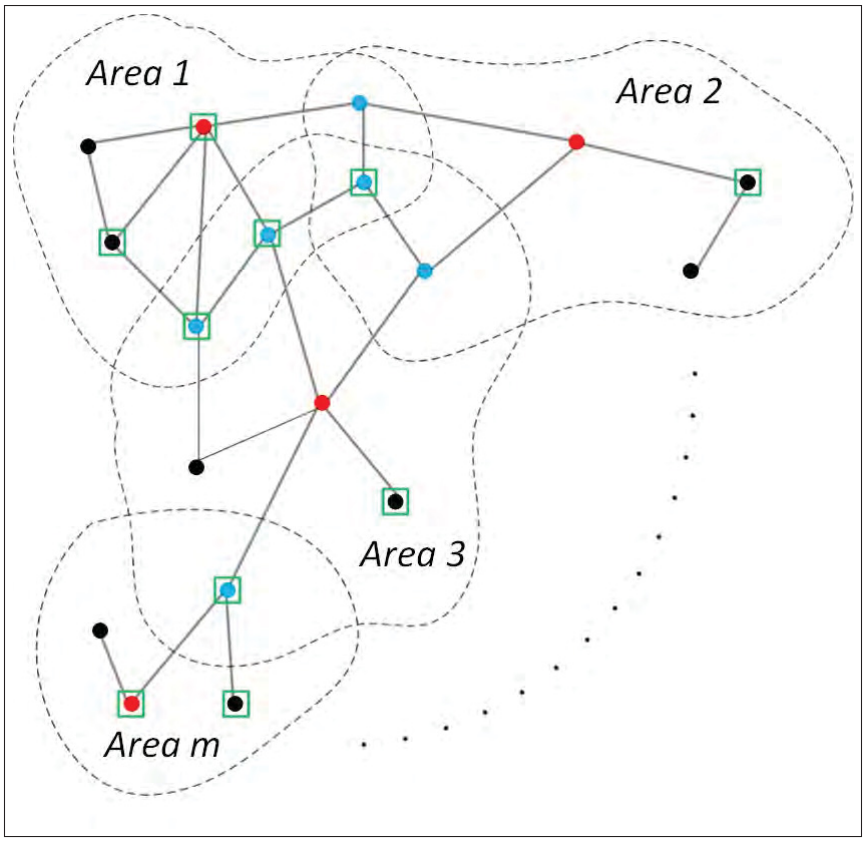

Figure 5.1 A group of overlapping areas partitioned using modified sensitivity analysis; pilot nodes (red nodes), shared buses (blue circles), nodes with participant compensator (highlighted using green rectangles)

A typical optimization problem solved by SVC_i is shown in Equations 5.1.

$$\Delta V^i_{PN} = f_i(\bar{u}^i_{nsh} - \bar{u}^i_{nsh}(k-1), \bar{u}^i_{sh} - \bar{u}^i_{sh}(k-1))$$

$$J^*_i = \min_{\bar{u}^i_{nsh}, \bar{u}^i_{sh}} J_i = \min_{\bar{u}^i_{nsh}, \bar{u}^i_{sh}} \left\| V^{di}_{PN} - V^i_{PN} - \Delta V^i_{PN} \right\| +$$

$$\left(\bar{u}^i_{nsh}\right)^T \bar{\alpha}^i_{nsh} \bar{u}^i_{nsh} + \left(\bar{u}^i_{sh}\right)^T \bar{\alpha}^i_{sh} \bar{u}^i_{sh} \tag{5.1}$$

$$s.t:$$

$$\bar{u}^i_{min} < \bar{u}^i < \bar{u}^i_{max}$$

In this formulation, f_i is a function which relates variation of shared and non-shared PVCs' set-points from their previous values, $\bar{u}^i_{sh}(k-1)$ and $\bar{u}^i_{nsh}(k-1)$ respectively, to the estimated voltage deviation on pilot node for $Area_i$, defined as ΔV^i_{PN}. Moreover, V^{di}_{PN} is the reference voltage of the pilot node of $Area_i$ which is dictated by the tertiary level controller. Also, $\bar{\alpha}^i_{sh}$ and $\bar{\alpha}^i_{nsh}$ are the weighting matrices for unknown control set-points, for the PVCs of both shared and non-shared compensators. Finally, $\bar{u}^i_{min}$ and $\bar{u}^i_{max}$ are minimum and maximum limits for the set-points of the PVCs in $Area_i$. Moreover, the computed optimal value for the set-points of shared and not-shared variables are defined as $\bar{u}^{i*}_{sh}$ and $\bar{u}^{i*}_{nsh}$ respectively.

The optimization problem formulated in Equations 5.1 is solved using the method presented in 4. An adapted version of this method is shown in Figure 5.2.

In this figure, the mathematical relation between control set-points and voltage of the pilot node, defined as functions f_i in Equations 5.1, is considered as a nonlinear NN. The optimization problem is then solved using SA through an iterative process between the model and the optimizer.

At each iteration, SA algorithm slightly disturbs the current value of set-point solution vector, $\bar{u}^i$. The solution is accepted if it first meets all the constraints and second reduces the objective function of the optimization problem. Otherwise, the SA algorithm uses the value from the last iteration. This process is repeated so that finally an exit criterion is met. This criterion could be defined either as a certain threshold for the objective function or the time limit in which the procedure must be completed. In this way, the last solution is considered as the sub-optimal control set-points and then sent to all PVCs in $Area_i$.

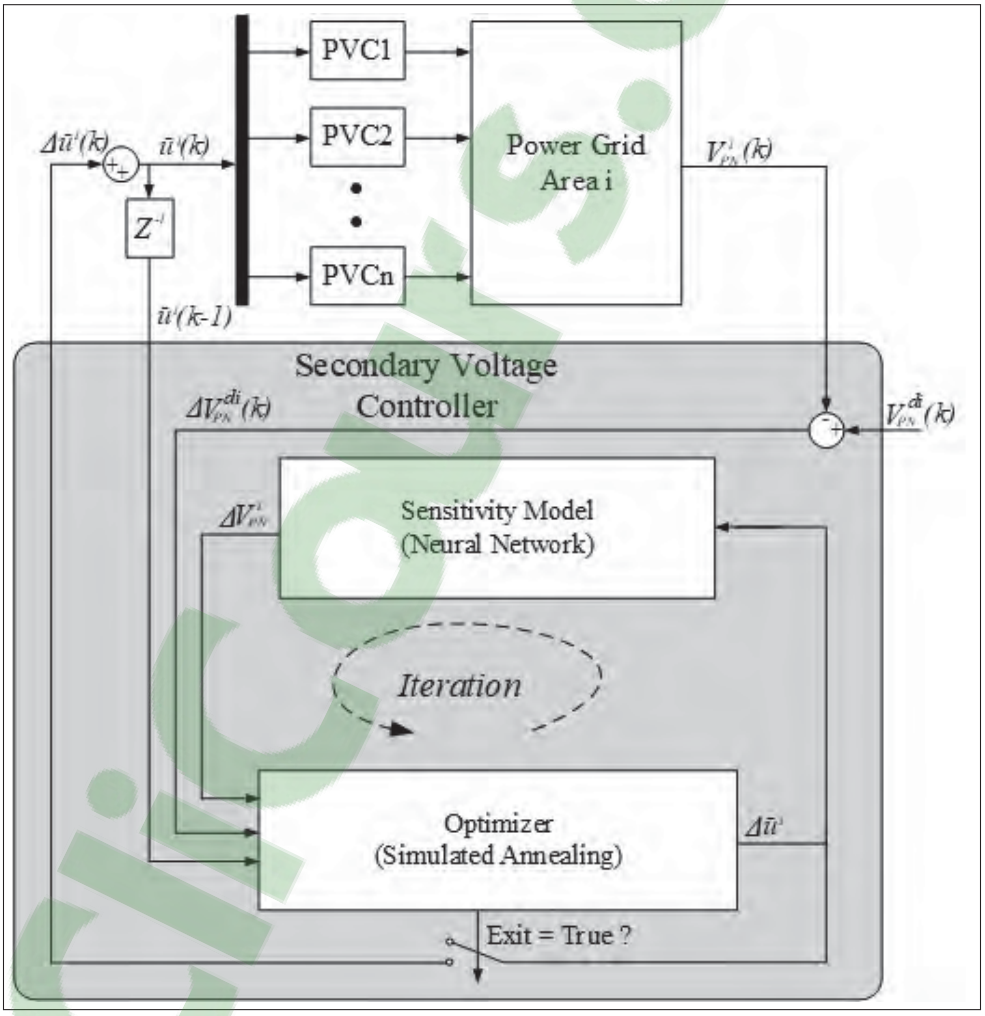

Figure 5.2 Secondary voltage control using neural network and SA

5.1.3 Architecture of the proposed consensus based SVC algorithm

Figure 5.3 illustrates the architecture of the proposed method. As can be seen in this figure, each regional SVC receives the measured voltage magnitude, V^i_{PN}, from the area's pilot node and sends back the calculated control set-points for PVCs, $\bar{u}^{i*}$, to the grid. On the other hand, all the regional SVCs of the overlapping areas communicate with a higher level coordinator which is responsible of reaching a consensus for the set-point value of the PVC for shared compensators.

A flow-chart describing the interaction between the power grid, SVCs and also the consensus coordinator to calculate regional PVC set-points at one time step of the controller is shown in Figure 5.4. The procedure here is described for one typical SVC, i.e. SVC_i, and it would be the same for the rest.

As shown in Figure 5.4, the procedure consists of two iterations for solving the regional SVC problem with a consensus step in the middle. In the first iteration, the regional SVC_i receives the measured voltage magnitude, V^i_{PN}, from the measurement unit installed on the network. Next the regional SVC calculates the set-points, $\bar{u}^i_{sh}$ and $\bar{u}^i_{nsh}$, for shared and non-shared PVCs respectively. This is done by solving the optimization problem described in Section 5.1.2. It should be noted that the calculated value for a specific shared compensator by one SVC, might be different from the one calculated by the other SVC. However, at the end, only one value should be sent to the corresponding PVC in the network. In this regard, in the next step, the calculated optimal set-points for the PVC of all the shared compensators, i.e. $\bar{u}^{i*}_{sh}$ for $i = 1, \cdots, m$, is sent to consensus coordinator unit which resolves the conflicts between the SVCs. For the proposed algorithm, additional information is required by the coordinator unit to calculate the consensus values. Namely, the optimal value of the objective function at the first iteration of SVC_i solution, J^*_i, as well as the linear sensitivity matrix of the objective function to the set-point of PVCs for shared compensators, defined as S_i. The methodology used by consensus coordinator is described in Section 5.1.4.

The calculated consensus value for the PVC of the shared compensator of $Area_i$, defined as $\bar{u}_c^i$, is different from the optimal values calculated in the first iteration, i.e $\bar{u}_{sh}^{i*}$. This difference leads to a deviation of regional objective function from its optimal value. To compensate for this, the consensus value for the set-point of the PVCs for shared compensators, $\bar{u}_c^i$, is communicated back to the regional SVCs where in the second iteration, local non-shared set-points, $\bar{u}_{nsh}^i$, are re-evaluated again assuming $\bar{u}_{sh}^i = \bar{u}_c^i$.

Finally, the calculated optimal values for $\bar{u}^{i*}$ are communicated back to the regional PVCs of $Area_i$.

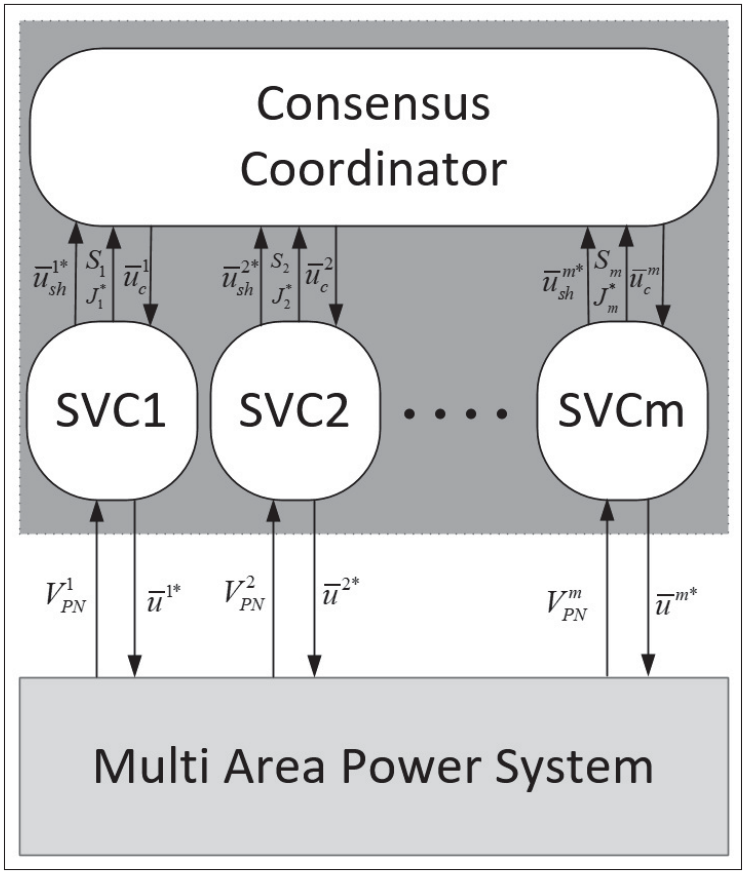

Figure 5.3 Architecture of the proposed consensus strategy

5.1.4 Consensus coordinator

The consensus coordinator, shown in Figure 5.3, solves the following optimization problem:

$$\begin{aligned} &\min_{\bar{u}_c} \ \sum_{i=1}^{m} \omega_i \left\| J_i - J_i^* \right\|^2 \\ &s.t: \\ &\bar{u}_c^{min} < \bar{u}_c < \bar{u}_c^{max} \end{aligned} \tag{5.2}$$

In this formulation $J_i - J_i^*$ is defined as the linearization of Equations 5.1 around the optimal solution, $\bar{u}_{sh}^{i*}$, found in the first iteration of the algorithm described in Figure 5.4. The linearized equations are as follows:

$$J_i - J_i^* = S_i(\bar{u}_c^i - \bar{u}_{sh}^{i*}) \quad i = 1, \cdots, m \tag{5.3}$$

In Equation 5.3, S_i is the sensitivity of J_i to $\bar{u}_{sh}^i$. This sensitivity matrix can be calculated by disturbing $\bar{u}_{sh}^i$ around the local minima points and measuring the objective functions' deviations. Moreover, $\bar{u}_c^i$ is a vector of consensus values for the set-point of shared compensators in $Area_i$ and $\bar{u}_c = \left[\bar{u}_c^1, \cdots, \bar{u}_c^m\right]$ is the vector of consensus values for all the shared compensators. Finally, ω_i is the weighting coefficient to prioritize the importance of each area for the consensus coordinator.

The corresponding consensus values for each area are then sent back to the regional SVCs to solve the second iteration of the SVC_i based on Figure 5.4.

5.1.5 Interpretation of consensus coordinator for two overlapping areas

The optimization problem formulated in Equation 5.1 is solved simultaneously by all SVC_i for $i = 1, \cdots, m$ in the first iteration of the proposed algorithm described in Figure 5.4. Instead of solving each problem individually for $Area_i$, if one tries to solve all these optimization problems together, it could be in fact considered as a multi-objective optimization problem in which $\bar{u}_{sh} = \left[\bar{u}^1_{sh}, \cdots, \bar{u}^m_{sh}\right]$ is considered as the set of all shared variables between all the regional optimization problems. This multi-objective optimization problem does not have a unique solution and instead there exists a set of pareto-optimal solutions.

As an example, for two overlapping areas with one shared compensator, a pareto-front curve is depicted in Figure 5.5 using a dashed arc which is defined as the locus of all pareto optimal solutions. As can be seen in this figure, starting from an initial solution, I, in the feasible region, shown as the shaded area, the solution of the local optimization problem by each regional SVC in the first iteration leads to different local minimas, E_1 and E_2, which are also on the pareto-front curve. The solutions for the shared variable, u^1_{sh} and u^2_{sh}, by each regional SVC is defined by u^{1*}_{sh} and u^{2*}_{sh} respectively. The corresponding optimal values for the objective functions are also defined as J^*_1 and J^*_2 respectively.

For two overlapping areas with one shared variable, u^1_c, the linearized equations would be as follows:

$$\begin{aligned} J_1 - J^*_1 &= S_1(u^1_c - u^{1*}_{sh}) \\ J_2 - J^*_2 &= S_2(u^1_c - u^{2*}_{sh}) \end{aligned} \tag{5.4}$$

In this way, any arbitrary value for u^1_c ranging from u^{1*}_{sh} to u^{2*}_{sh} corresponds to an equivalent point, C, on the line segment between E_1 and E_2 in Figure 5.5. This line segment can be interpreted as the linear approximation of the pareto-front curve.

Analogously, $\left\|J_1 - J_1^*\right\|^2$ and $\left\|J_2 - J_2^*\right\|^2$ correspond to the square of the length of sides, BC and AB respectively in the ABC right triangle shown in Figure 5.5. Also, based on the Pythagorean theorem, the consensus objective function in Equation 5.2, with the assumption of $\omega_1 = \omega_2 = 1$, is basically the square of the hypotenuse of ABC triangle, i.e. AC. In other words, solving the consensus optimization problem for the two overlapping areas with one shared compensator is equivalent to finding a point on E_1E_2 line which minimizes the distance between point A and the line segment E_1E_2. This optimal point, defined as C^*, is basically the intersection point between the line segment E_1E_2 and a perpendicular line from A.

5.2 Simulation case study: IEEE 118 bus network

IEEE118 bus power system, used as the test-case, is shown in Figure 5.6. This network has 19 generator units, including synchronous generators of type GENROU, excitation systems of type EXST1, maximum excitation limiters of type MAXEX2 and also turbine governors of type TGOV1. Power system stabilizers of type STAB1 are also connected to excitation systems on buses 26, 49 and 100. In addition, the network includes 35 static var compensators of type CSVGN5. The loads are considered to be ZIP loads with 40% as constant power, 30% as constant impedance and 30% as constant current load. Reactive power limit for all static var compensators as well as generators participating in SVC algorithm is considered to be the same and defined as: $Q_{min} = -300MVar$ & $Q_{max} = +300MVar$. Moreover the reactive power limits for participant capacitor/inductor banks are the same and they are defined as: $Q_{min} = -50MVar$ & $Q_{max} = +10MVar$. Base Power for the test case is $100MVA$ and the nominal frequency is $50Hz$.

The modified sensitivity analysis is used to find pilot nodes and also partition the network. Using the same parameter names for sensitivity analysis as Corsi (2015), the parameters γ and ϵ_p are found by trial and error to have a good voltage profile on remote buses. In this way $\gamma = 1E-3$ and $\epsilon_p = 1E-6$. This choice of parameters leads to allocation of 6 pilot nodes shown as shaded-fill rectangles in Figure 5.6 and are listed as buses 117, 21, 44, 52, 101 and 86. Each of these pilot nodes represents one corresponding control area with borders shown

using dashed lines in Figure 5.6. As can be seen, unlike the classical sensitivity method, the control areas have overlap in some buses. For example, Area 1 has one shared bus, bus 33, with Area 2 and also two shared buses with Area 3, buses 8 and 17. However the only shared bus which is identified as a control bus is bus 49 which is shown as shaded region between Area 2 and Area 4. In this way, the proposed consensus strategy is applied to coordinated Area 2 and Area 4.

The continuous type compensators are allocated at buses 12, 34, 49, 54, 85, 87 and 100 (static var compensators on buses 34 and 85 and synchronous generator on the rest). Moreover discrete type compensators which are basically capacitor/inductor banks are allocated at buses 117, 20, 21, 22, 23, 43, 44, 45, 51, 52, 53 and 58. All the control buses are shown using ovals in Figure 5.6.

5.3 Real-time test bench

The validation of the proposed control strategy is done on a real-time simulation target, OP4510, from OPAL-RT Technologies. Beside real-time capabilities to validate the performance of complex control strategies, OP4510 offers the possibility to implement simulations on multi-cores in parallel and also to support different industrial communication protocols used in real power systems. This makes it easy to validate distributed control architectures such as the proposed method. The software used to simulate the dynamics of the power system is ePHASORsim from OPAL-RT which is a phasor-domain solver Jalili-Marandi *et al.* (2013),Opal-RT (2018). It benefits from state of the art techniques to improve performance and accuracy of simulations for large-scale power grids. It also includes a rich built-in and Modelica based library of different power system components and also supports importing data from various power system stability analysis tools such as PSS/e and CYME.

Figure 5.7 illustrates the configuration of the test-bench to validate the proposed consensus strategy in real-time. The software interface to develop the test-bench is Simulink from MathWorks in which OPAL-RT's ePHASORsim block is used to define the power network. The data

is also sent through a communication channel with a Gaussian noise model in which the SNR is 100 dB. The communication protocol to send measured data from power gird (i.e. voltage on pilot buses) to the regional SVCs is IEEE C37.118 which is used by PMUs in real power grids. OPAL-RT's library supports both slave (sending) and master (receiving) C37.118 protocols. Moreover, the control commands from the DCSVCs are sent to the network using Ethernet protocol. As can be seen from Figure 5.7, a dedicated communication channel is defined to send and receive data from each area of the power grid. Such an architecture is also in-line with the requirements of multi-TSO power grids. To cope with the decentralized architecture of the proposed control strategy, regional SVCs as well as power network model are located in separate subsystems labeled as $Corei, MASTER/SLAVE$. The convention of master and slave subsystems are used by RT-LAB to inform the compiler during code generation process that each subsystem's generated code is transferred and run in a separate physical core on the target computer. In this way, computations on each core are done in parallel with the other cores and the performance of each subsystem can be measured separately without having any overloads caused by other subsystems. Although in this paper the method presented in 4 is adapted for SVC, the proposed test-bench can be used to run and validate any other decentralized control strategy.

5.4 Simulation Results

To validate the proposed control strategy, two different simulation scenarios are considered to be applied on IEEE 118 bus power system. The simulation results for the cases with and without consensus strategy are compared accordingly. It should be noted that for the case without consensus, the average calculated set-point by the neighbor SVCs is calculated. However, unlike the consensus strategy, this calculated value is directly applied to the corresponding PVC without having any iteration between SVCs and shared PVCs. In the following, each simulation scenario is discussed in detail.

5.4.1 Scenario 1- Sudden Load variation

In this scenario, all the constant impedance loads are suddenly increased by100% at t = 10 seconds, while constant power and constant current loads are increased by 40% and 20% respectively. Reference voltages on pilot buses are considered constant and they are equal to before contingency values. Figure 5.8 shows the dynamics of the voltage deviation on pilot nodes. As can be seen in this figure, few milliseconds after disturbance, voltage on pilot buses suddenly drops by $0.08p.u.$. However, the PVCs take action immediately and are able to reduce the error to less than $0.03p.u.$ in less than 10 seconds. The steady state error, however, is compensated by the SVC control loop starting the first time step, at t = 20 seconds. Comparing the voltage on pilot buses 44 and 52 for the cases with and without consensus strategy, one can see that steady state error for bus 44 gradually decreases with consensus between SVCs of Area 2 and Area 4 as well as PVC of the local controller. However for the case with no consensus the error remains constant. Moreover for the bus 52, the case without consensus has led to big overshoot at t = 20 seconds, while the consensus based controller is able to diminish such an overshoot.

Figure 5.9a also shows the calculated reference voltage deviation for AVR connected to the synchronous generators while Figure 5.9b illustrates the reactive power injection by capacitor/inductor banks.

5.4.2 Scenario 2- Reference Voltage change

In this scenario, the reference voltage of all pilot nodes are suddenly increased by $3\%p.u.$ at t = 5 seconds.

Figure 5.10 shows the dynamics of the voltage deviation on pilot nodes. As can be seen from this figure, after reference change at t = 5 seconds, voltage on pilot nodes does not change hence leads to sudden error of $0.03p.u.$. However, at t = 10 seconds, both controllers, with and without consensus take action which leads the voltage error to reduce gradually. However for the case without consensus strategy, it can be seen that the voltage on pilot bus 52 has a large

overshoot which diminishes after some oscillations while such a behavior is not seen form the controller with consensus strategy. On the other hand, same as scenario 1, the controller with consensus strategy is able to reduce the steady state error on bus 44 in less than 60 seconds while it remains constant for the case without consensus.

Figure 5.11a also shows the calculated reference voltage deviation for AVR connected to the synchronous generators and also Figure 5.11b illustrates the reactive power injection by capacitor/inductor banks.

5.4.3 Real-time performance validation

The simulations test-bench presented in 5.3 is used to validate real-time performance of the proposed controller. In this simulation, the maximum calculation time, between all SVCs, to find the suboptimal solution is 700 milliseconds which is much smaller than the time step of the SVC loop, i.e. 10 seconds. In this way, the computational delay is negligible and the proposed controller can be applied in real time for such a network.

5.5 Conclusion and Future Works

In this paper, a new sensitivity analysis method was used to (i) find the pilot nodes, (ii) partition the network and finally (iii) allocate the controllers. For the case where a control bus is identified to be a shared compensator, a consensus strategy is proposed in which the regional SVCs as well as the corresponding PVC reach an agreement in an iterative process. Simulation results showed that such a consensus strategy reduces the overshoots and oscillations due to the lack of coordination between regional SVCs. Moreover the consensus strategy was able to reduce the steady state error on the pilot buses corresponding to the areas with shared compensators.

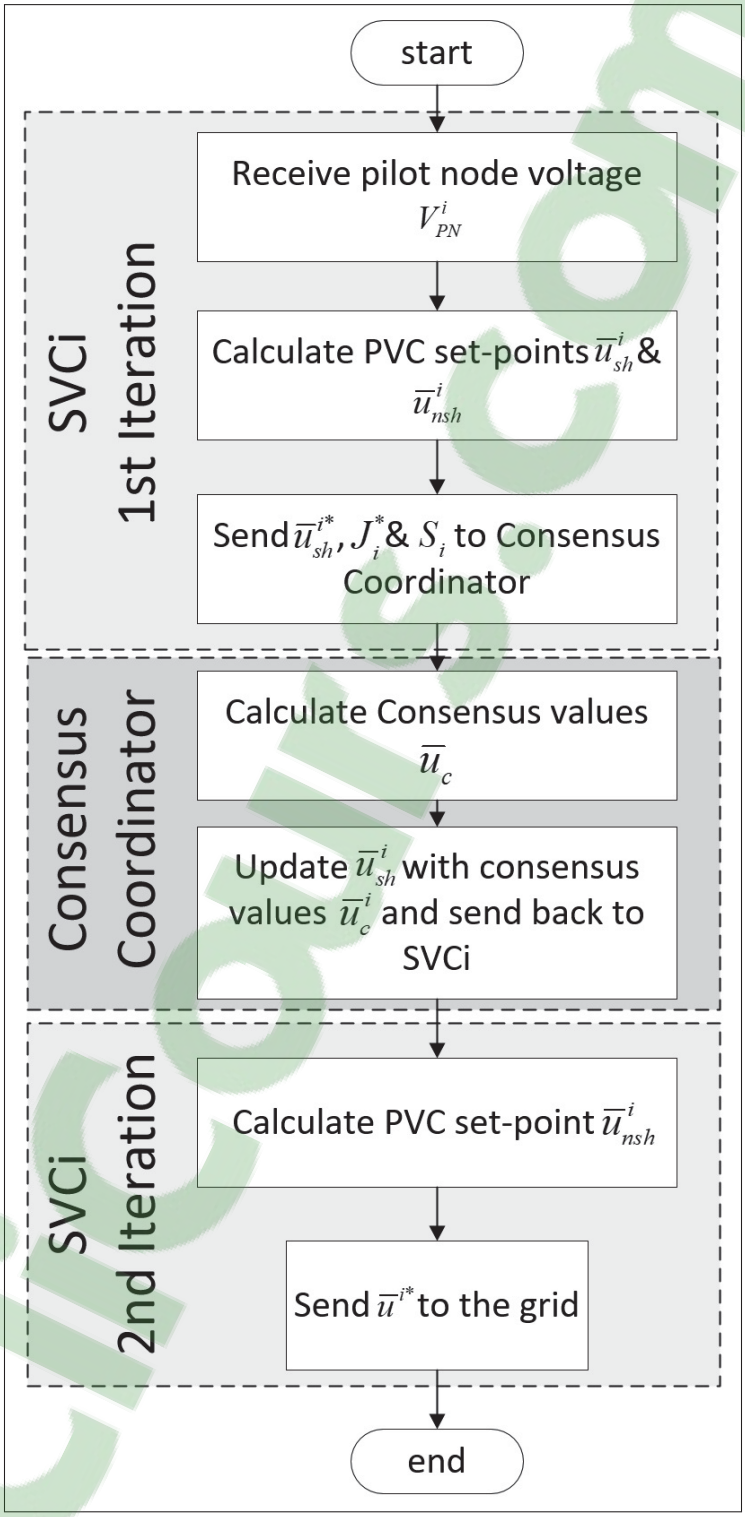

Figure 5.4 Flowchart describing the interaction of SVC of Area i and the consensus coordinator

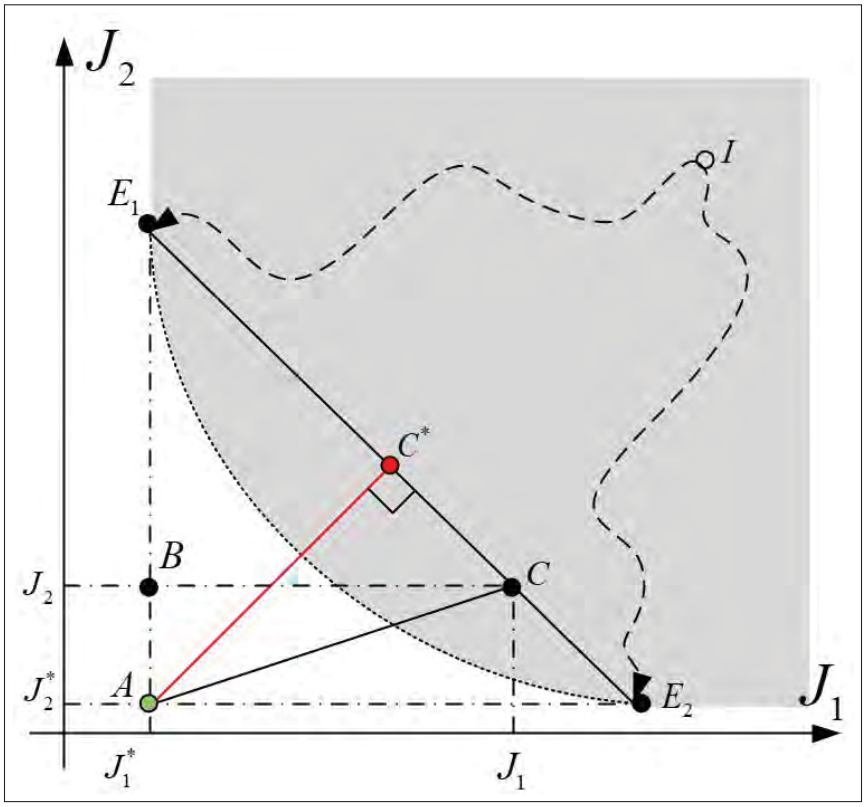

Figure 5.5 Pareto-front curve of a two-objective optimization problem with its linear estimation

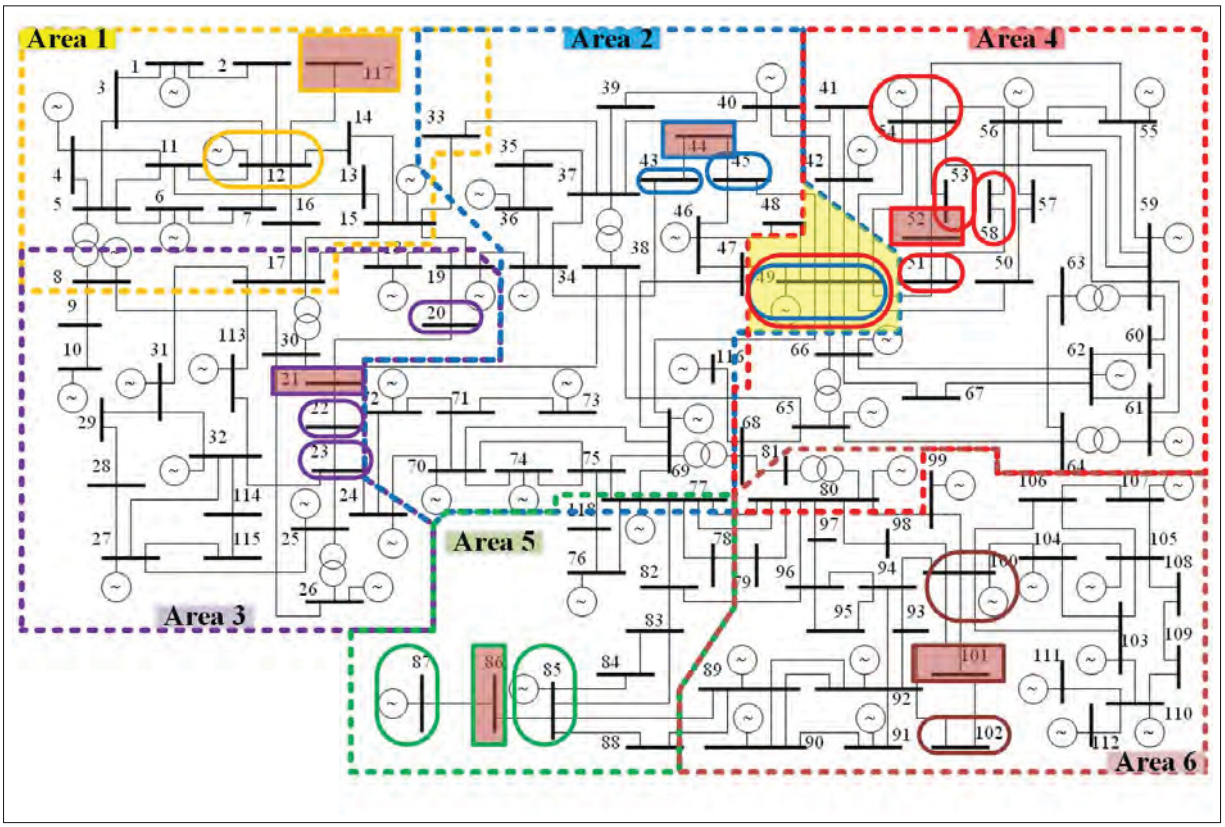

Figure 5.6 IEEE 118-bus power network. Pilot nodes (solid rectangle) and control bus (dashed rectangle)

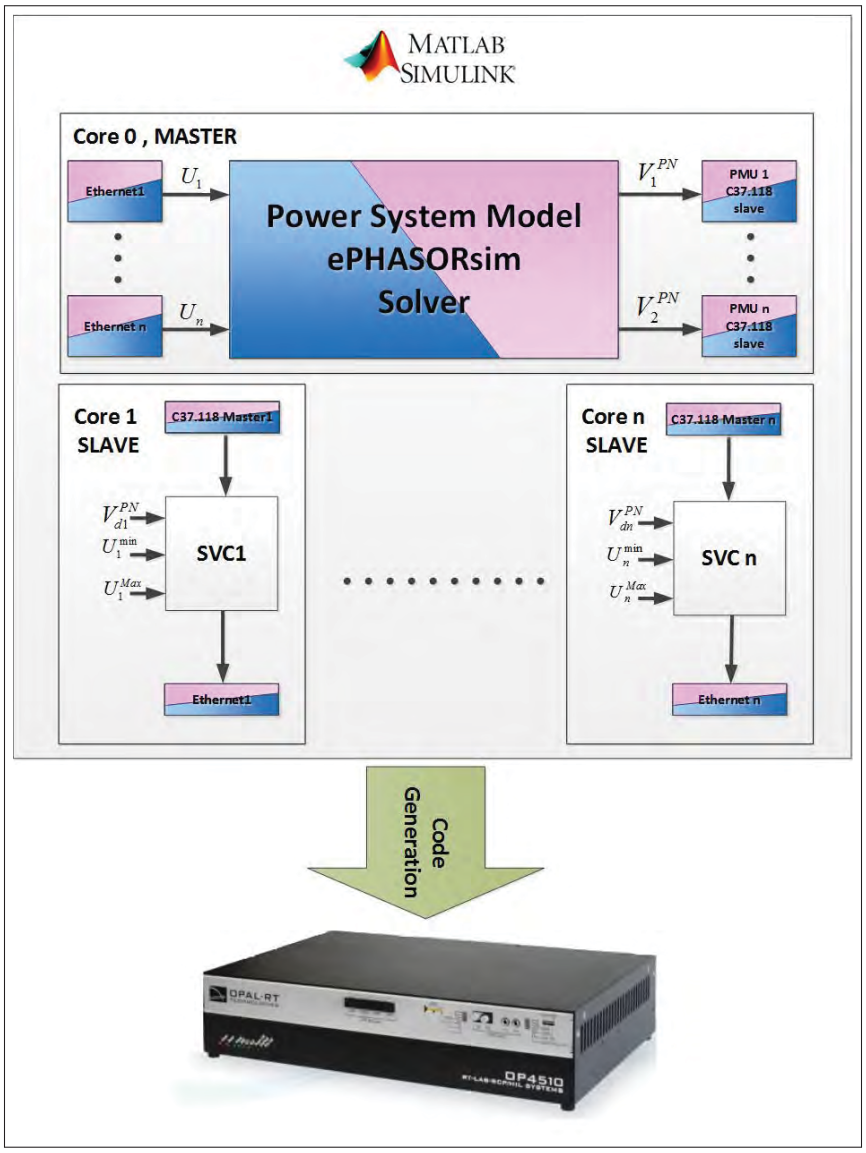

Figure 5.7 Configuration of the real-time test-bench for validation of DCSVC algorithm

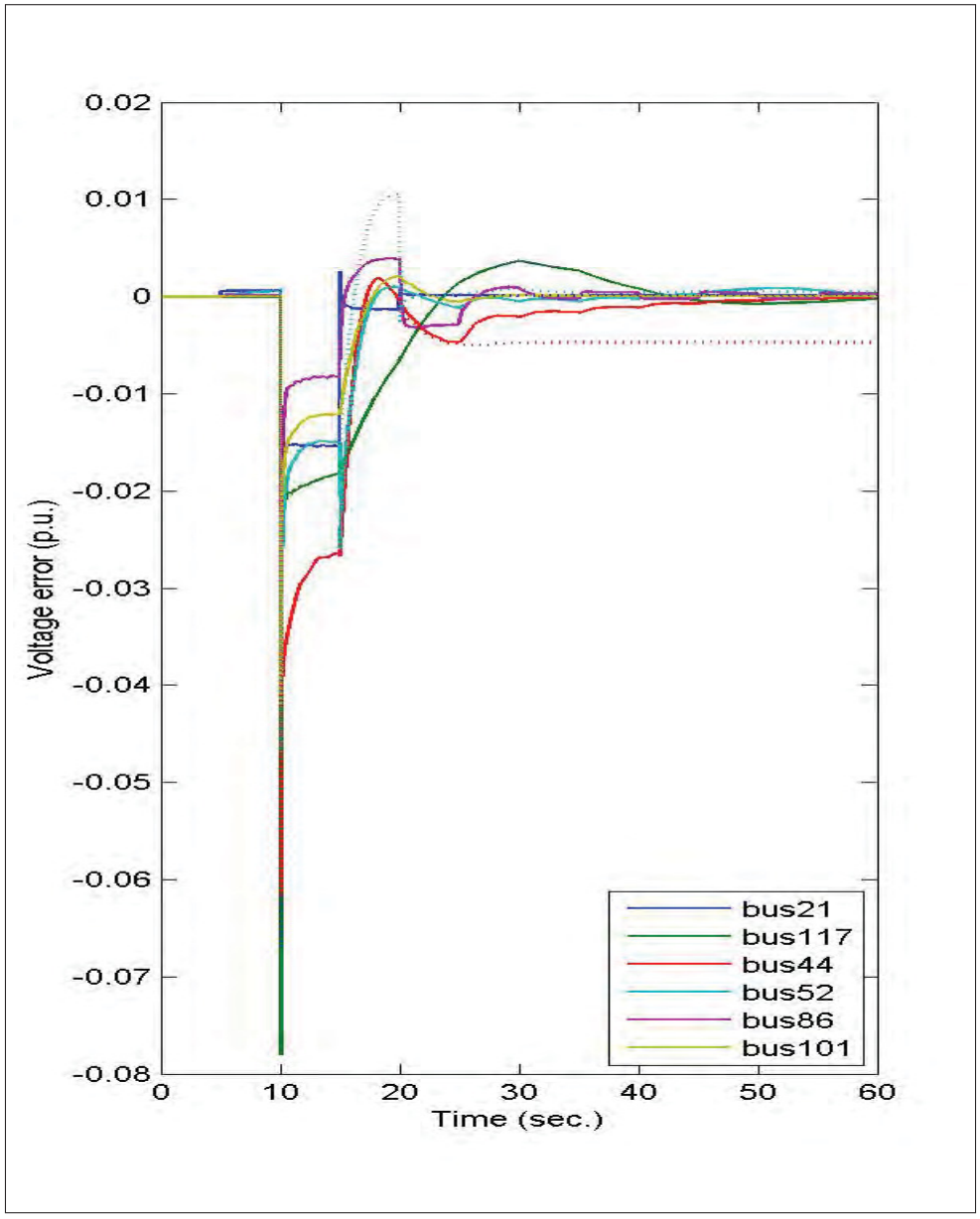

Figure 5.8 Scenario 1: Voltage error on the pilot buses. With consensus strategy (solid line), without consensus strategy (dotted line)

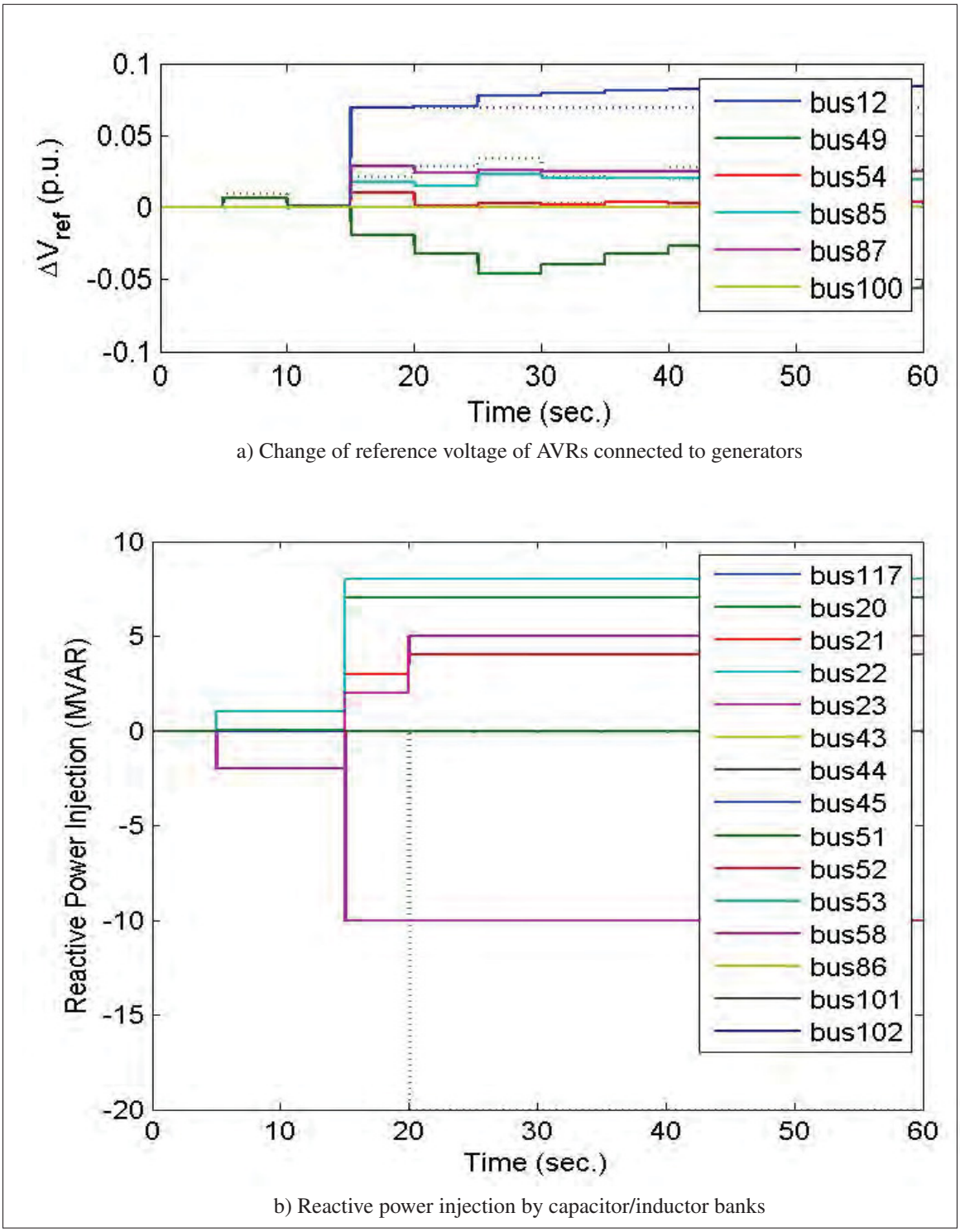

a) Change of reference voltage of AVRs connected to generators

b) Reactive power injection by capacitor/inductor banks

Figure 5.9 Scenario 1: With consensus strategy (solid line), Without consensus strategy (dotted line)

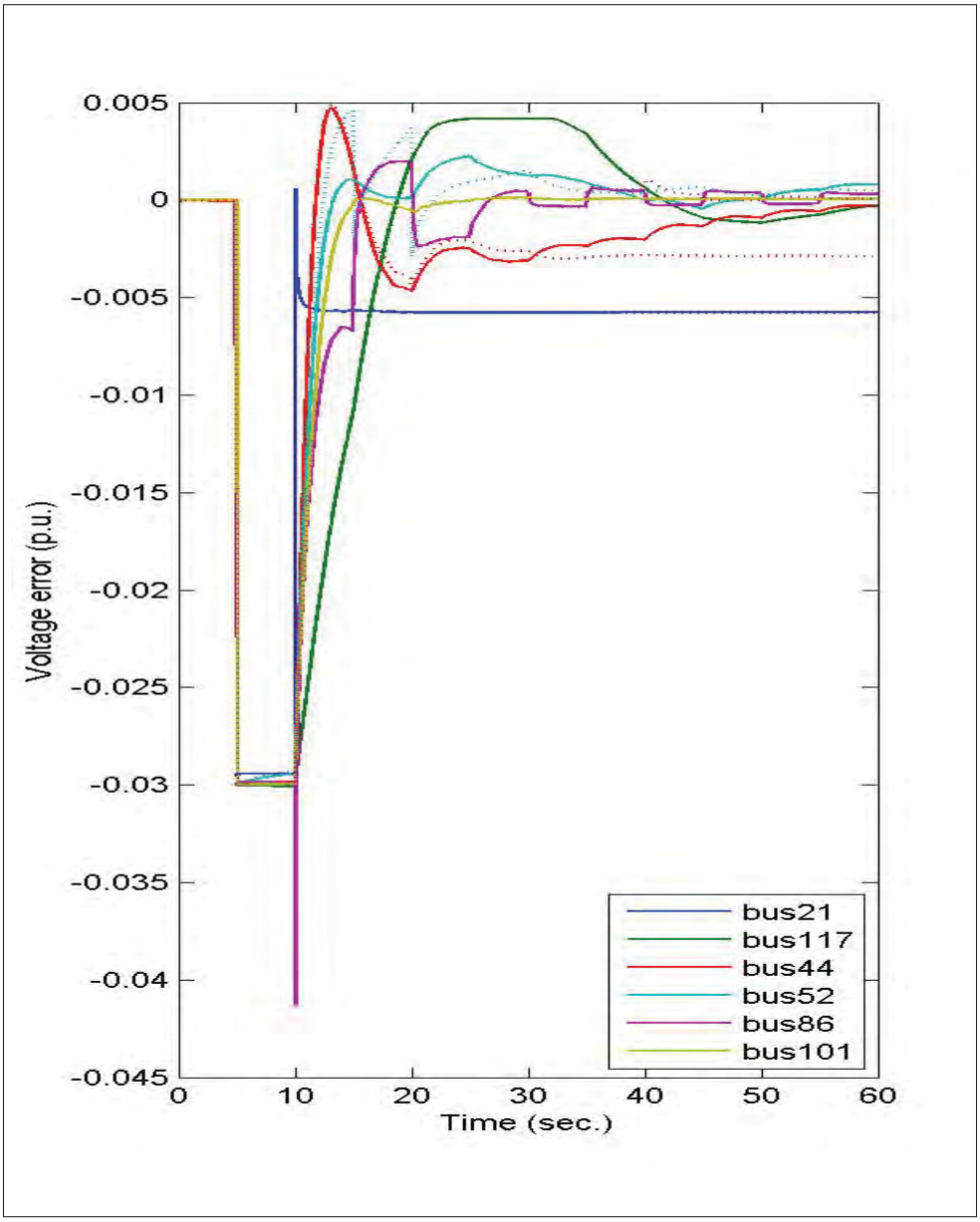

Figure 5.10 Scenario 2: Voltage error on the pilot buses. With consensus strategy (solid line), without consensus strategy (dotted line)

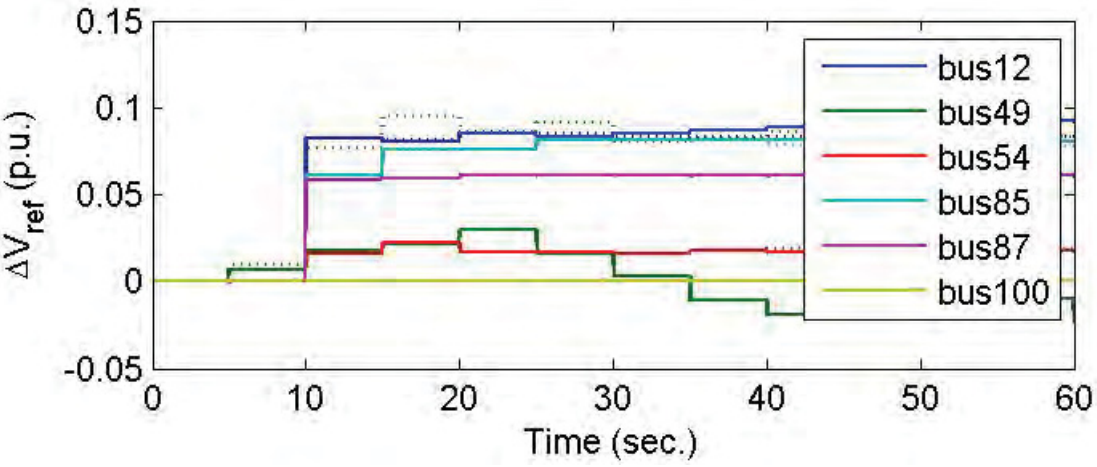

a) Change of reference voltage of AVRs connected to generators

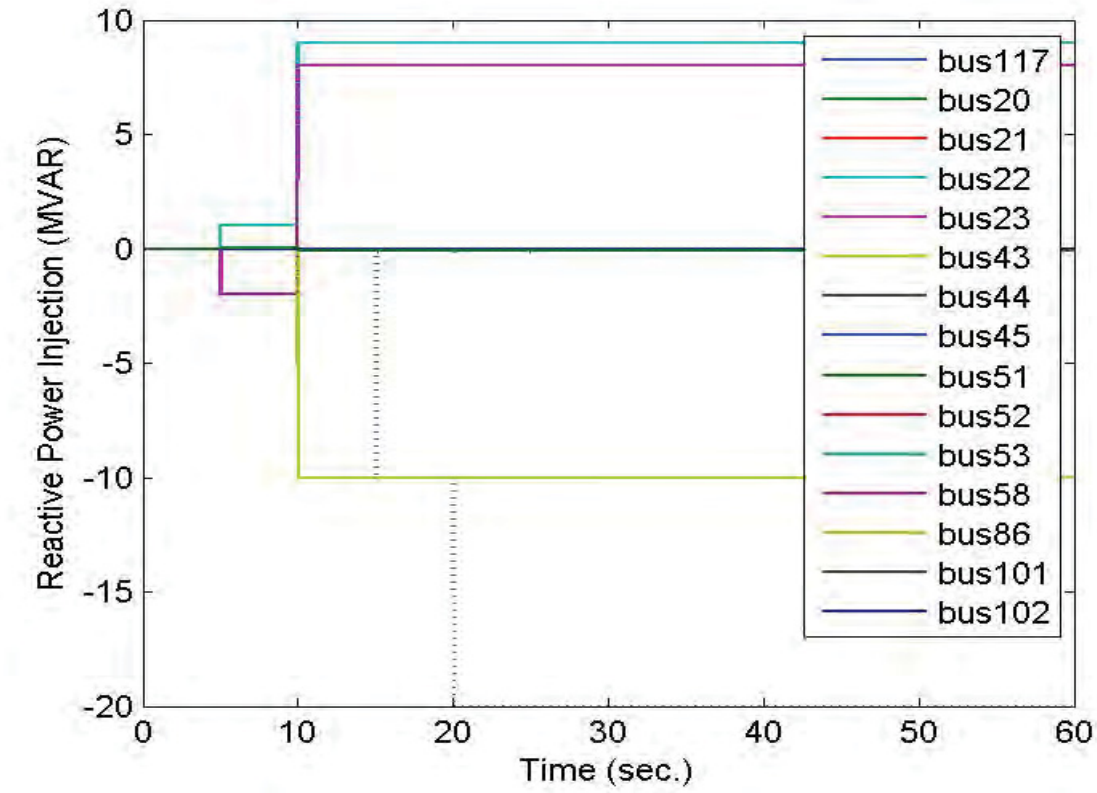

b) Reactive power injection by capacitor/inductor banks

Figure 5.11 Scenario 2: With consensus strategy (solid line), Without consensus strategy (dotted line)

CONCLUSION AND RECOMMENDATIONS

Conclusion

This thesis proposed novel approaches regarding to analysis and design of multi-agent coordinated SVC in transmission networks.

In the first chapter, an introduction to the fundamental concepts of voltage stability and control was presented. The chapter also discussed the classical SVC algorithm in which the advantages as disadvantages of the method were enumerated. CSVC method was then discussed as an alternative approach to overcome drawbacks of the SVC method.

Then in chapter 2 a timely review of the works related to SVC was done in which the literature was classified according to different aspects of the SVC problem. The chapter also analyzed recent literature based on which the methodologies and novelties of the this thesis were addressed.

Chapter 3 proposed a decentralized MPC scheme for coordinated secondary voltage control of large-scale multi-area highly interconnected power networks. The controllers were designed in a decentralized way for each area which modifies reference signal of reactive power compensator devices. The interactions between neighboring areas were considered as measured reactive power deviation on tie-lines between these areas. This value was defined as a measured disturbance for MPC in each area. The simulation results for the proposed method showed that the decentralized controllers are able to both regulate and track the desired voltage in presence of external disturbances. It was also shown that considering the delay model in each regional MPC model improves the stability of the closed loop system.

The proposed algorithm was also tested on a realistic power grid with 5000 buses in real-time considering the communication protocols and the model of the communication channel. The

real-time performance of the proposed method confirms that the proposed method is computationally feasible and scalable to large scale power grids.

Despite effectiveness of the proposed method, some difficulties were also observed. The proposed MPC method is based on the identified linear model of the system. In this way, the model might not be valid for extreme disturbance cases. Moreover, the control signals calculated by the proposed MPC method are continuous type by nature. Although one can discretize the continuous values and apply them to discrete type compensators, it might lead to oscillatory behavior of the closed loop system when the discrete steps are large. Using hybrid (mixed continuous and discrete) MPC approaches on the other hand requires a large amount of computational effort to solve the optimization problem.

To overcome these issues, in chapter 4, a new CSVC strategy was proposed which coordinates discrete and continuous type compensators in transmission system to improve voltage profile at pilot buses of the network when facing large disturbances. The controller consists of two parts: The identified nonlinear sensitivity model of the network and an optimizer. The nonlinear sensitivity model is identified using Neural Networks based on Input-Output data generated from random disturbances on the network. The optimizer utilizes SA algorithm and is combined with NN model to find the optimal switching of the capacitor/inductor banks after sensing any disturbance.

The comparison of the results of the proposed method with the linear model based CSVC and also traditional method in which only capacitor banks are utilized, shows that the proposed method has a faster response to load variation, sudden disturbances as well as change of the pilot nodes' reference voltage. The steady state error of the proposed method is also smaller than the traditional method and similar to the linear based CSVC. Beside voltage control, the proposed algorithm also minimizes the reactive power injected to the network.

Due to the local nature of the voltage control problem, solving a centralized optimization problem as proposed in chapter 4 might not be computationally beneficial for larger power systems with more control variables. On the other hand, while solving the optimization problem in a decentralized way, one should take into account the effect of the control actions on the neighbor areas to avoid any uncoordinated behavior.

This issue was investigated in chapter 5, in which a modified sensitivity analysis method was used to (i) find the pilot nodes, (ii) partition the network and finally (iii) allocate the controllers. For the case where a control bus is identified to be a shared compensator, a consensus strategy is proposed in which the regional SVCs as well as the corresponding PVC reach an agreement in an iterative process. Simulation results showed that such a consensus strategy reduces the overshoots and oscillations due to the lack of coordination between regional SVCs. Moreover the consensus strategy was able to reduce the steady state error on the pilot buses corresponding to the areas with shared compensators.

Future Works

Minimize the number of switching for discrete type compensators

Although the proposed method in chapter 3 can be generalized to other types of reactive compensators such as tap-changers, capacitor banks, synchronous condensers and other FACTS devices, certain considerations should be taken into account for switching based devices such as capacitor banks or tap-changers. The number of switching of such devices should be minimized as much as possible to avoid long-term damages. Moreover, due to the discrete nature of these devices, the optimization problem leads to a mixed integer linear or quadratic programming which can be solved using available methods.

Using physical modeling

Another possible improvement to the proposed method in chapter 3 is to use physical modeling instead of black-box system identification to have more accurate and meaningful models. Having linearized symbolic models of different components of the power system, one can easily formulate the MPC optimization problem symbolically which leads to a more flexible and performant approach which can easily be adapted for any power system.

Considering dynamics of the load

On the other hand, considering different load models and their dynamics can lead to more accurate formulation of voltage stability problem. Considering the dynamics of the load in the MPC formulation can provide more accurate control when loads are constantly changing in the power grid.

Considering the effect of unknown communication delays

The effect of unknown communication delays on the stability of the controller can be considered as a future work. Such an assumption is more realistic for delays caused by cyber attacks since it is not in control of the power system utilities and they may not have any statistic data to estimate the value.

Use adaptive learning methods for neural network

As was discussed in Section 4.4, the NN model is identified off-line, and remains unchanged during the implementation phase. One suggestion is to use adaptive learning methods in real-time to adapt the NN model with changes in the power network. On the other hand, the proposed strategy was implemented as a centralized controller.

APPENDIX I

MODEL PREDICTIVE COORDINATED SECONDARY VOLTAGE CONTROL OF POWER GRIDS

Arvin Morattab[1], Asber Dalal[2], Ouassima Akhrif[1], Maarouf Saad[1], Serge Lefebvre[2]

[1] Department of Electrical Engineering, École de Technologie Supérieure,
1100 Notre-Dame Ouest, Montréal, Québec, Canada, H3C 1K3
[2] Institut de Recherche en Électricité du Québec (IREQ),
1800 Boulevard Lionel-Boulet, Varennes, Québec, Canada, J3X 1S1

Abstract

In this paper MPC algorithm is applied to control, in a coordinated way, the voltage of some sensitive buses of the power network, called pilot nodes. A linear model of partitioned power system is first obtained by state-space system identification as the system model for MPC. Based on the measured voltage at pilot nodes, the centralized secondary MPC controller changes the reactive power injected to the pilot nodes so that voltage deviation of these buses is compensated and reaches its desired value defined by the tertiary level. The proposed method has been tested on the New England 39- bus network and compared with the case without any secondary voltage controller. The simulation results show the effectiveness of the proposed method.

Introduction

In a large scale power system, voltage control problem is usually divided spatially and temporally into three hierarchical levels which are primary, secondary and tertiary voltage control. While the primary controllers are taking care of local voltage stability of generator buses, the secondary controller tries to control voltage of sensitive buses of the network, called pilot nodes, by balancing of reactive power supply and demand over a control area. This reactive power can be injected to the power system through generation level by means of generators or through transmission level by means of VAR compensation devices such as capacitor banks, tap-changers, static var compensators etc.. At the top level of this hierarchy there is tertiary level controller which deals with the economic and security concerns of the overall power system. These levels work in different timescales so that their actions do not affect each other. Primary controller take action in a few seconds, secondary level in few minutes and for the tertiary level in 15 minutes.

The idea of CSVC was first introduced by Electricité de France in 1985 Vu *et al.* (1996). The proposed idea in Vu *et al.* (1996) and further discussed in Lefebvre *et al.* (2000); Richardot *et al.* (2006) is to apply a centralized multi-input multi-output optimal controller for a strongly interconnected power network in order to minimize an objective function that consists of bus voltage error, generated reactive power and terminal voltage error terms considering generators reactive power and voltage limits on terminal buses and also limits on voltage of sensitive nodes. Static model of the power network in terms of sensitivity matrices has been used in the cost function. Sancha *et al.* (1996); Wang (2001) has adopted the idea of static optimization in Vu *et al.* (1996) to cover different issues of voltage stability. Sancha *et al.* (1996) has considered distributed generations in CSVC algorithm while Wang (2001) has proposed a decentralization approach for CSVC of multi area power systems.

In addition to coordination of primary controllers in generators, many research works have considered coordination between reactive power compensators in transmission level. A multi-agent and fuzzy based control method is proposed in Wang *et al.* (2003) and Paul *et al.* (1987)

for coordination of AVRs, SVCs and STATCOM in the case of power system contingencies. Moreover Larsson (1999) has used a fuzzy rule based controller to coordinate cascade tap-changers in radial distribution feeders. The coordination of capacitor banks and tap-changers has been done in Larsson *et al.* (2002) using predictive control and tree search methods. MPC has also been considered as a suitable algorithm for reactive power management and voltage control. The MPC controller solves a constrained optimization problem based on predicted future behavior of the system over a prediction horizon and the first step of the optimal control sequence computed over a control horizon is applied on the system. Marinescu & Bourles (1999) has proposed a flexible secondary voltage control algorithm based on MPC in which both static and dynamic optimization sub-problems are used. In Zima & Andersson (2003), emergency voltage control is addressed using MPC based on sensitivity analysis calculated via system dynamic equations. In Larsson & Karlsson (2003), the coordination of generator voltages, tap changers, and load shedding is studied using tree search optimization techniques. In Wen *et al.* (2004), a coordinated voltage control framework is developed based on nonlinear system equations using Euler state prediction and pseudo gradient evolutionary programming. In Hiskens & Gong (2006), MPC of load is used to determine minimum amount of load shedding to restore system voltages. A centralized quadratic programming MPC formulation is considered in Beccuti *et al.* (2010) to optimally coordinate generator voltage references and load shedding and solved via Lagrangian decomposition. In Jin *et al.* (2010), a control switching strategy of shunt capacitors is presented by means of MPC to prevent voltage collapse and maintain a desired stability margin after a contingency. In Glavic *et al.* (2011) a receding-horizon multi-step optimization is proposed to correct nonviable transmission voltages and prevent long-term voltage instability. Explicit formulations are used to model evolution of load with time.

All papers described so far, except Marinescu & Bourles (1999), have considered the model of the system for CSVC problem either as a static algebraic equation using sensitivity matrix or as a logical rule based model. Despite the facilities which static models brings about for large scale power network calculations, from control theory point of view, setting up a dynamic

model to describe system behavior makes it possible to apply well-known control system analysis and design tools on CSVC problem.

To this end, in this paper, a dynamic state-space model was first obtained using linearized equations of power system and dynamic behaviors are deduced to design MPCSVC. The voltages at pilot nodes are measured and compared with desired values defined by tertiary controller. The resulting error signal is fed into the MPCSVC which generates the best possible control action. Unlike Marinescu & Bourles (1999) which uses generators to inject extra reactive power to compensate voltage deviation, this methods applies the control action on static var compensators which has been installed on the Pilot nodes.

The paper is organized as follows: Section 3 illustrates the CSVC problem followed by Section 4 which describes MPCSVC algorithm in details. In continuation of the paper, the procedure toward linear system identification for CSVC problem is discussed in Section 5. In Section 6 simulation results for typical power system are shown and the final section is devoted to conclude the remarks.

3. Coordinated secondary voltage control

The first step toward secondary voltage controller is to divide the large scale interconnected power network into several distinct areas so that if a disturbance happens in one area, it has the minimum effect on its neighbors. After network division, the next step is to find the nodes at each zone that are the most sensitive to disturbances on the reactive power.. The tertiary level controller plans the desired voltage values for these nodes and the secondary voltage controller maintains voltage in these buses as close as possible to its desired value by injecting reactive power in the pilot nodes themselves or changing reference voltage of primary controllers installed on the generators. Figure I-1 illustrates a typical CSVC for a multi-area power network. In Area1 in this figure, V_{PN}^{ij} is the measured voltage of the i^{th} Pilot Node in Area j which is directed to the centralized CSVC. The CSVC then compares these values with desired values defined by tertiary level controller, V_{PN}^{d}. Based on this error and physical limits such as reactive

power generation by generators and reactive compensation devices, the controller computes the amount of change in reference voltage of primary controller, ΔV_{refi}, and ΔQ_i for reactive power compensators on the pilot buses. Since the controller generates continuous control signals, we just consider continuous reactive power compensators such as SVCs on pilot nodes. Since the Areas are strongly interconnected, a centralized controller has been used as the CSVC in this work.

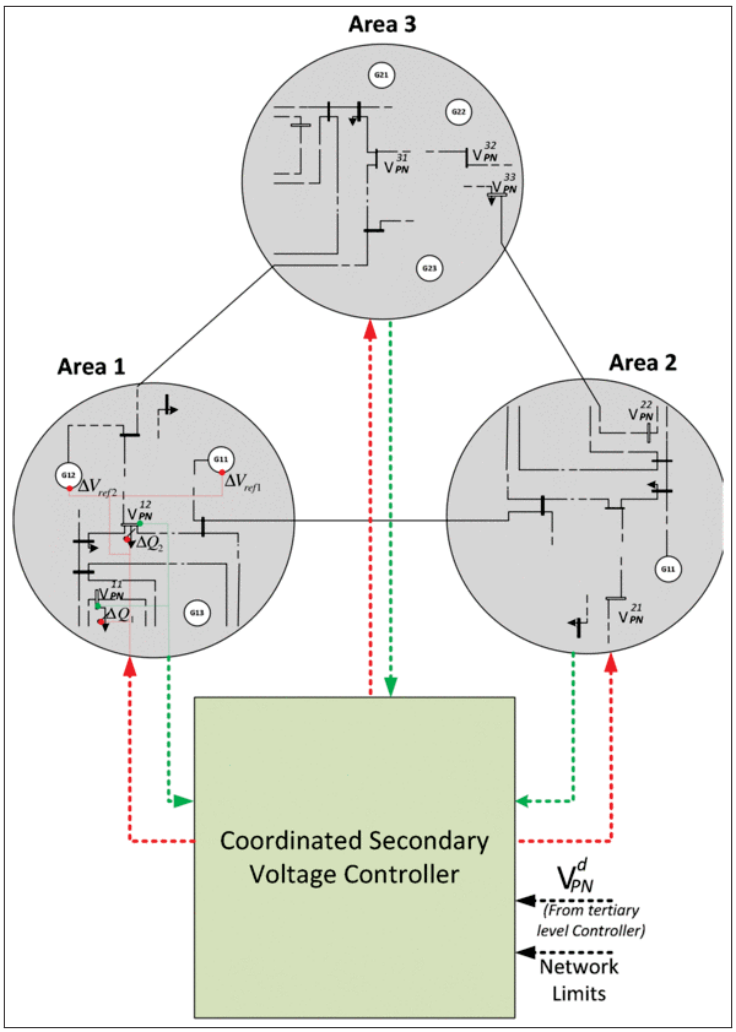

Figure-A I-1 Centralized Coordinated Secondary Voltage Controller for a Multi-Area Power Network

4. Model predictive coordinated secondary voltage control

4.1 Model Predictive control

MPC has been proved as an effective and accepted control strategy to stabilize dynamical systems in the presence of nonlinearities, uncertainties, constraints and delays, especially in process industries. A general MPC scheme is shown in Figure I-2. As could be seen, the MPC controller consists of two parts which are prediction and controller units. The prediction unit includes dynamical model of system and disturbance which forecast future behavior of system based on its current output, measured disturbance and control signal over a finite prediction horizon. The predicted output is exploited by control unit as known parameters in an optimization problem which minimizes an objective function in presence of system constraints. Solving of this problem leads to an optimal control sequence over a control horizon. The first element of this sequence is injected into the plant and the whole procedure is repeated in the next sampling interval with the prediction horizon moved one sampling interval forward.

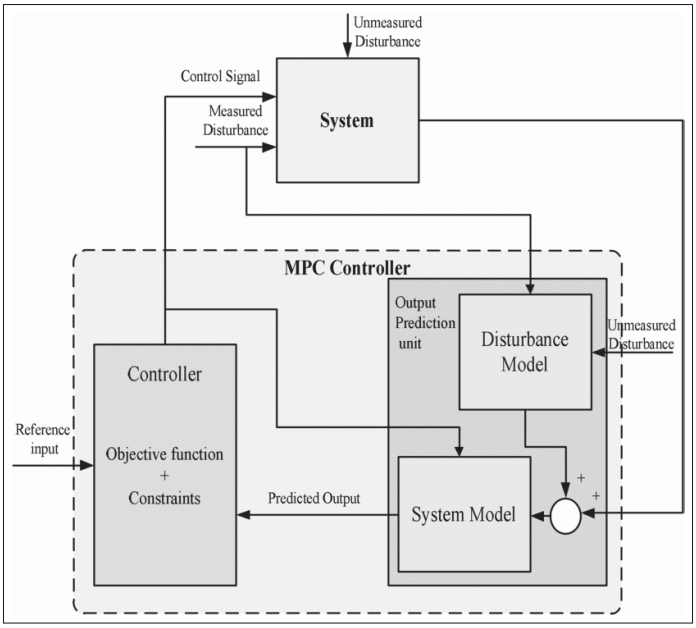

Figure-A I-2 A General MPC Scheme

This procedure can be classified into 4 steps as follows:

1. Obtain output and state measurements estimations of system at sampling interval k;

2. Predict the output signal $y(k+1 \mid k)$, over the prediction horizon p;

3. Solve the following optimization problem defined by an objective function and constraints. Solving this problem leads to finding an optimal control input vector $\{u_k, u_{k+1}, u_{k+2}, \cdots, u_{k+m}\}$ over control horizon m;

$$\min_{\Delta u(k),\ldots\Delta u(k+m-1)} \left\{ \sum_{j=0}^{m-1} \Delta u^T(k+j) R \Delta u(k+j) + \sum_{i=0}^{p-1} \Delta y^T(k+i) Q \Delta y(k+i) + \rho \varepsilon^2 \right\} \quad \text{(A I-1)}$$

Subject to:

$$\begin{aligned} & u_{min} \le u(k+j) \le u_{max} \\ & \Delta u_{min} \le \Delta u(k+j) \le \Delta u_{max} \qquad j = 0, \cdots, m-1 \\ & y_{min} - \varepsilon \le y(k+i|k) \le y_{max} + \varepsilon \quad i = 0, \cdots, p-1 \\ & \Delta u(k+l) = 0 \qquad\qquad\qquad l = m, \ldots, p-1 \\ & \varepsilon > 0 \end{aligned} \quad \text{(A I-2)}$$

In which: $u(k) = u(k-1) + \Delta u(k)$, $\Delta y(k) = y(k) - y_d(k)$ and ϵ is slack variable. The slack variable is used to soften constraints on output signal and prevents infeasibilities of the optimization problem. In addition, Q and R are nonnegative output and input weighting coefficients respectively and $u_{min}, u_{max}, \Delta u_{min}, \Delta u_{max}, y_{min}$ and y_{max} are lower/upper enforced upper and lower bounds;

4. Apply the first element, u_k, from the optimal control vector until new measurements are available;

5. At sampling interval $k+1$, return to step 1 and repeat the procedure.

4.2 MPCSVC algorithm

The MPC algorithm described above can be well fitted to the CSVC problem just by replacing the Controller block in Figure I-1 with the MPC block in Figure I-2. In this case, error signal,

i.e. $V_{PN}^{ij} - V_{PN}^{d}$, will be the input signal for the MPC. Using load prediction methods we can describe the load changes as measured disturbance, and if it is not predictable (sudden faults in the system) described as unmeasured disturbance. The usual method to cancel the effect of the measured disturbances is to use feed-forward controller in the MPC design. Linear or nonlinear model of the system can be obtained using online or offline identification methods. As it will be discussed later, a linear model of the system is identified offline in the normal operating point of the system. Since the system is large scale and also the primary level dynamics are not considered in secondary level, model reduction methods (for example using balanced realization) can be used to reduce the order of the system to include just the slow dynamics.

5. Generation of training data and linear model estimation

5.1 Identification method

A linear time invariant dynamic model with three inputs and three outputs, with change of reactive power, Formula, as input and voltage deviation at pilot nodes from its desired value, Formula, as outputs is identified using Prony method from input-output data of power network dynamic simulator, ST600, developed by IREQ.

One of the key issues of using MPC methods is how to identify the model of the system by which the controller can predict the future behavior of the physical dynamic system. The identified model can be described using transfer functions, state space model, neural network,.... Considering a linear time invariant Multi-Input Multi Output (MIMO) model, a state space dynamical models can be good choices which are models that use state variables to describe a system by a set of first-order differential, rather than by one or more nth-order differential or difference equations [18], [19].

The identification algorithm finds coefficients of the system (A, B, C and D). Realization of the system is made on discrete system (F, G, C) instead of continuous system (A, B, C) as

following equations:

$$x(k+1) = Fx(k) + Gw(k)$$
$$y(k) = Cx(k) + Du(k) \qquad \text{(A I-3)}$$

Where $F = e^{AT}$ and $G = A^{-1}(F - I)B$. D is simplified and obtained by regression between Y and U. The problem of state-space system identification has received considerable attention in recent years. In state-space realization methods the Hankel matrix plays a critical role because a state-space model can be obtained from a factorization of the Hankel matrix via its singular value decomposition. Much efforts have been devoted to obtaining the Markov parameters from input-output data by time or frequency domain approaches Jang *et al.* (1998).

Once the Markov parameters are determined, they become entries in the Hankel matrix for state-space identification.

The model to be identified is IEEE-39 bus power network which is divided into three areas based on fuzzy C-mean method described in Mezquita *et al.* (2011). Figure I-3 shows the divided 39-bus test case. Bus No. 26, 7 and 15 are chosen as pilot nodes for Areal, Area2 and Area3 respectively.

5.2 Perturbations to obtain F,G,C and D

To obtain input/output data, disturbances are randomly added individually on two different buses in each region (Table I-1) for each set of test. Disturbances are fixed as 30 Mvar. In 60 second 30Mvar inductance is added. Then at 260 second, another inductance is added in the same region but another bus (30 Mvar), but first inductance is removed.

Figures I-4, I-5 and I-6 show bus voltages obtained by system and estimated model for three sample buses 7, 15 and 26 in three different regions. Bus voltages are measured in 50 sec and as can be seen in these figures, there are some error between system and estimated model in transient time, but in steady state these errors go to zero. The same procedure could be done to obtain dynamic model considering arbitrary set of pilot buses.

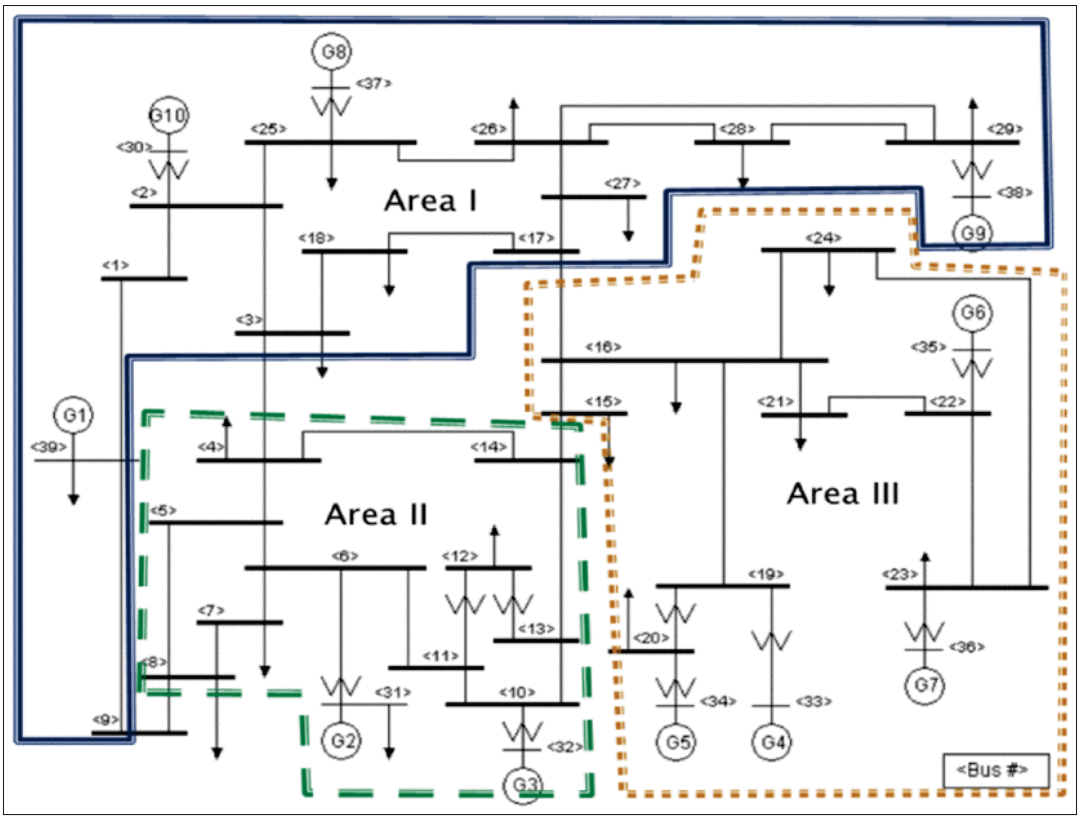

Figure-A I-3 3 Area IEEE-39BUS power network

Table-A I-1 Selected buses to add disturbances (IEEE 39-bus)

Test set No.	Region 1	Region 2	Region 3
1	[18, 27]	[5, 14]	[15, 21]
2	[28, 3]	[7, 13]	[20, 24]
3	[1, 10]	[8, 10]	[16, 22]
4	[2, 26]	[4, 12]	[23, 19]
5	[1, 17]	[6, 11]	[16, 19]

6. Simulation results

To obtain the dynamic model, the method discussed in section 4 is used considering bus No. 29, 11 and 21 as pilot nodes for Area1, Area2 and Area3 respectively. Having no track of how unmeasured disturbance behaves, the possible choice would be adding integral of white noise as output disturbance to measured outputs of the system. After gaining the model, MPC

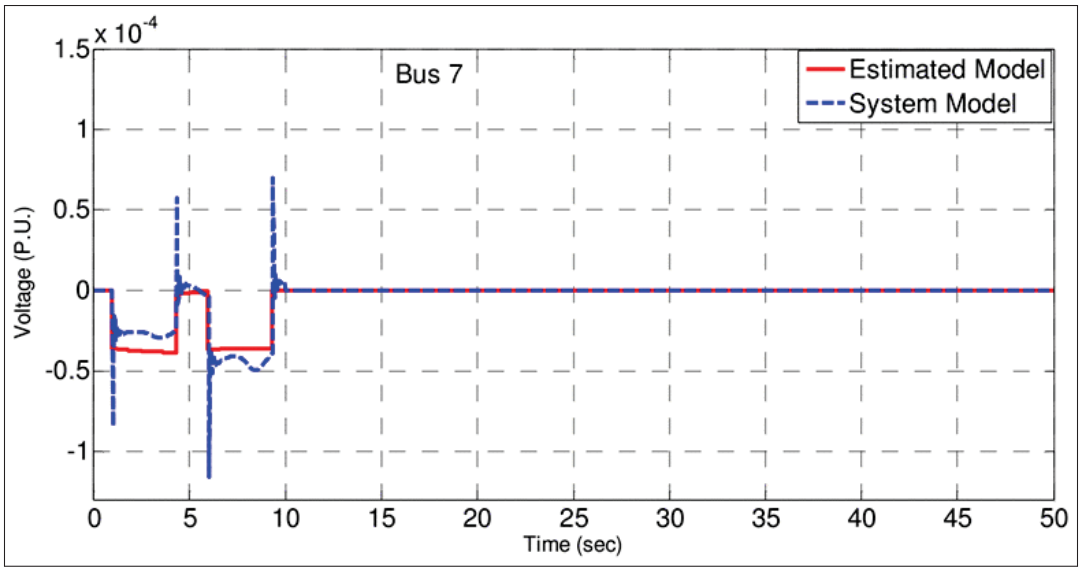

Figure-A I-4 System and estimation model for Bus 7 (region 2)

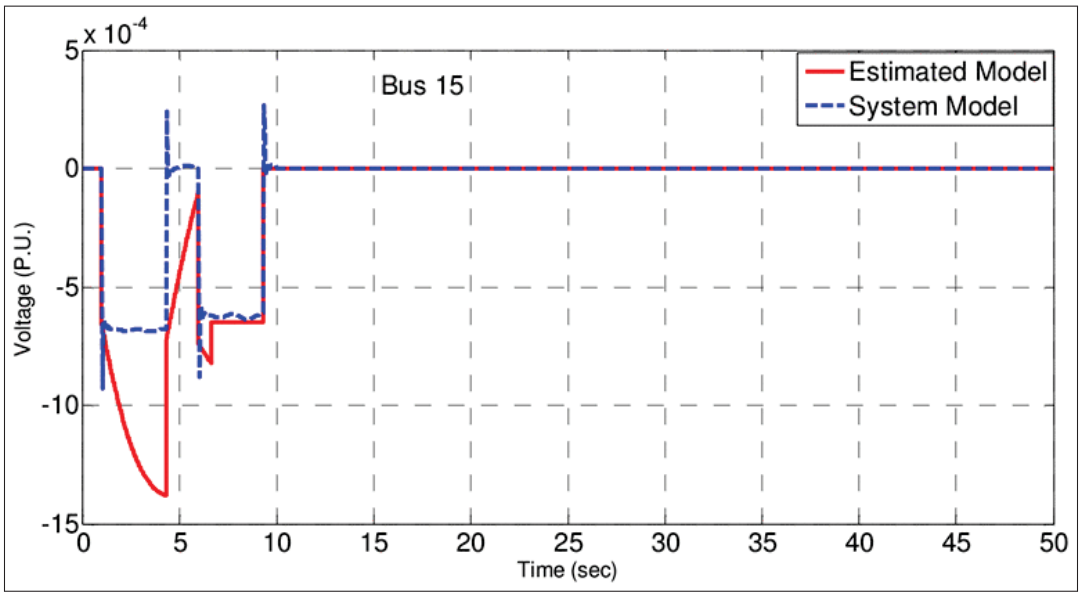

Figure-A I-5 System and estimation model for Bus 15 (region 3)

controller will be designed. To design MPC controller best possible controller parameters based on trial and error has been chosen. In this case, sampling interval of 1 second, control horizon of 2 samples (m = 2) and a prediction horizon of 10 samples (p = 10), are selected as appropriate length to achieve good control performance with manageable computations in

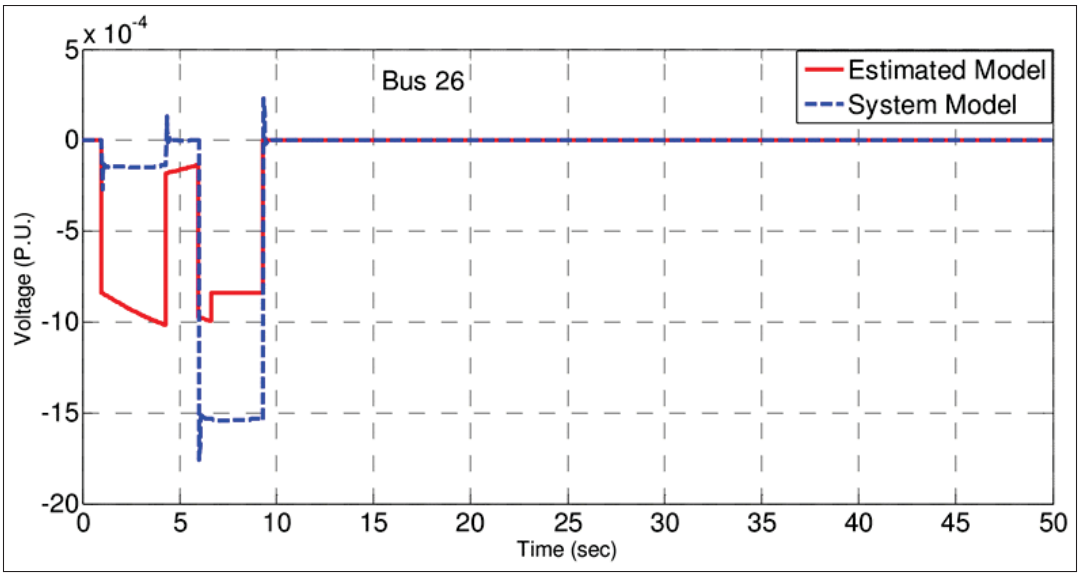

Figure-A I-6 System and estimation model for Bus 26 (region 1)

real-time. Furthermore, weights on system's input, output and state variables are chosen at their best chosen at their best quantities. Moreover reactive power generation limit by each static var compensator has been considered in MPC controller. Table I-2 shows these limits for three pilot buses.

Table-A I-2 static var compensator reactive power generation limits on pilot buses

Bus No.	**Max ΔQ (MVAR)**	**Min ΔQ (MVAR)**
11	90	-90
21	90	-90
29	30	-30

Two different scenarios are proposed here to validate the performance of the MPC controller. In the first scenario sudden active power load changes is applied on some nodes of the power network as unmeasured disturbance while in the second scenario disturbance is considered as sudden change of injected reactive power on some buses of the power network. Complete description of two scenarios has been brought in Table I-3.

Table-A I-3 Simulation scenarios to validate MPC algorithm

Scenario 1			**Scenario 2**		
Time (s)	**Bus No.**	ΔP **(MW)**	**Time (s)**	**Bus No.**	ΔQ **(MVar)**
1	19	10	1	11	-40
1	21	10	7.66	19	40
9.33	9	-10	9.33	18	-40
9.33	11	-10	12.66	2	20
16	11	-100			

Figure I-7 and Figure I-8 illustrate simulation results for two scenarios. As can be seen from two figures the MPCSVC controller has compensated voltage deviation cussed by disturbances on the system in less than 2 minutes in comparison to the case when there is no secondary voltage controller.

Figure I-7d shows the generated reactive power by static var compensatros. As can bee seen generated reactive power has reached its limit, -90 MVar, on bus 29 at t=80 sec.

Figure I-9 shows the comparison of voltage change before and after the disturbance for Scenario1 between two cases, with and without MPCSVC. As can be seen in this figure the controller has improved the steady state voltage profile for all PQ buses of the network.

7. Conclusion

An MPC strategy was presented in this paper as coordinated secondary voltage controller to regulate voltage at pilot buses. A state space model was first identified for MPC controller. Then the proposed controller was applied on three areas, 39 bus, power system considering both reactive and active disturbances on the system. Simulation results show that the proposed method has improved the voltage profile of the network in an efficient way in comparison to the case without any secondary level controller.

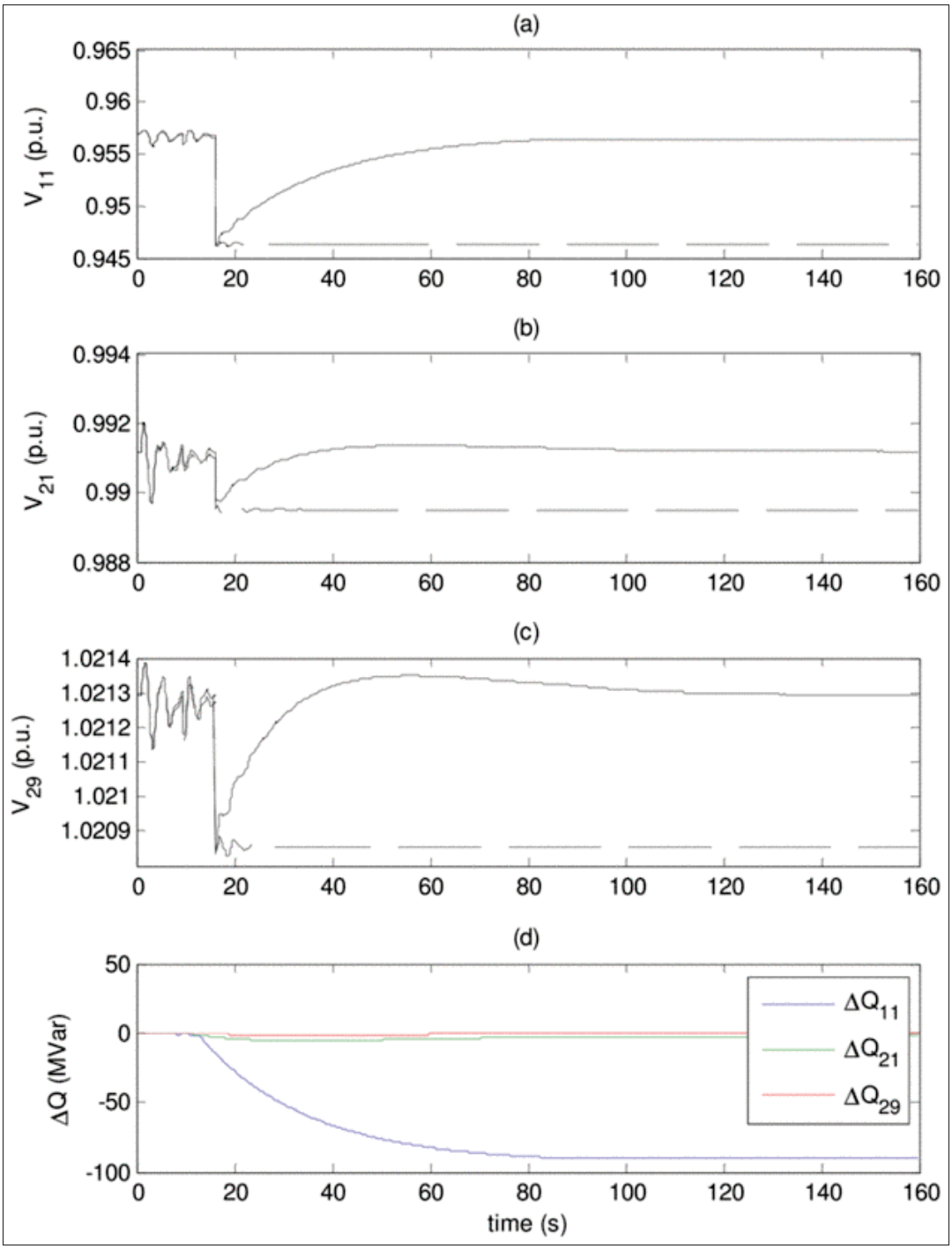

Figure-A I-7 Simulation Results for Scenario 1: (a,b,c) Voltage Profile at pilot nodes. Solid line: MPCSVC, dashed line: No Control. (d) Reactive power changes on pilot nodes by static var compensators

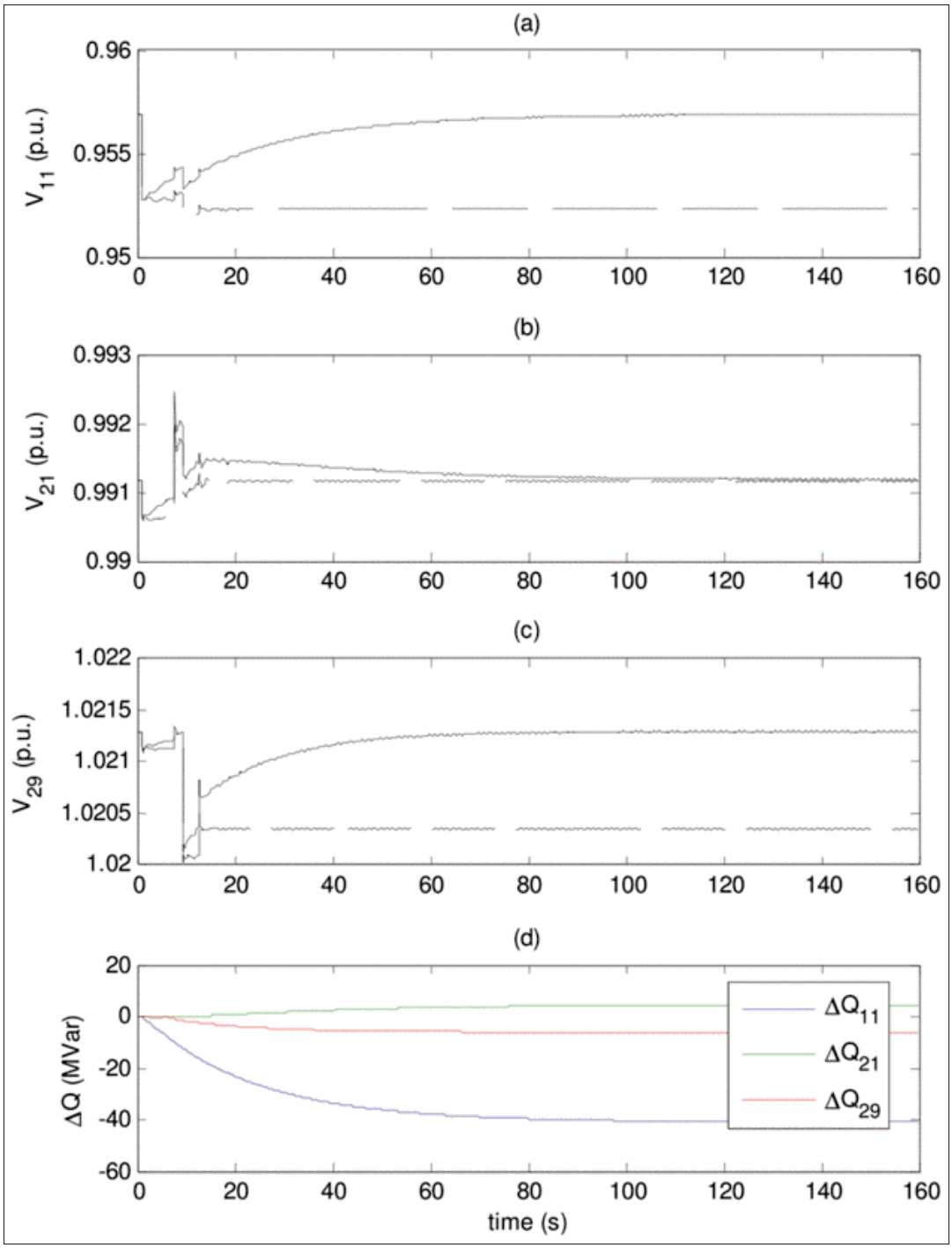

Figure-A I-8 Simulation Results for Scenario 2: (a,b,c) Voltage Profile at pilot nodes. Solid line: MPC CSVC, dashed line: No Control. (d) Reactive power changes on pilot nodes by static var compensators

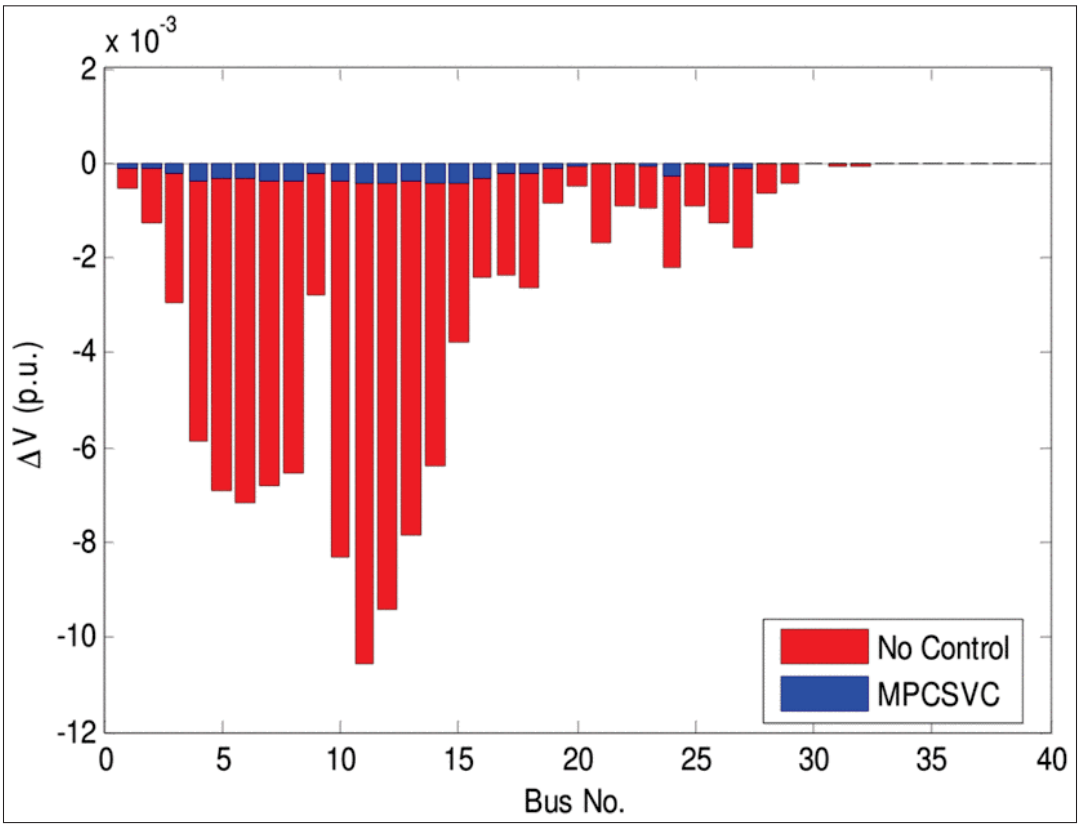

Figure-A I-9 Comparison of steady state voltage change before and after the disturbance for Scenario 1

APPENDIX II

DECENTRALIZED COORDINATED SECONDARY VOLTAGE CONTROL OF MULTI-AREA HIGHLY INTERCONNECTED POWER GRIDS

Arvin Morattab[1], Maarouf Saad[1], Ouassima Akhrif[1], Asber Dalal[2], Serge Lefebvre[2]

[1] Department of Electrical Engineering, École de Technologie Supérieure,
1100 Notre-Dame Ouest, Montréal, Québec, Canada, H3C 1K3
[2] Institut de Recherche en Électricité du Québec (IREQ),
1800 Boulevard Lionel-Boulet, Varennes, Quebec, Canada, J3X 1S1

[2013] IEEE. Reprinted, with permission, from [Morattab A., Saad M., Akhrif O., Dalal A., Lefebvre S., *Decentralized coordinated secondary voltage control of multi-area highly interconnected power grids*, 2013 IEEE PowerTech Conference, Pages: 1-5, June 2013, Grenoble, France]

Abstract

In this paper, a decentralized method based on SA approach is proposed in a decentralized way for coordinated secondary voltage control problem of highly interconnected multi-area power networks. The algorithm finds the best possible pilot buses and corresponding control simultaneously, in each area, to compensate for voltage contingencies. The tie-line active and reactive powers transferred between two areas are measured at the borders of each area and the effect of neighbor areas will be considered as variable loads at mutual buses of tie-line. Comparison of the proposed decentralized method with the centralized case shows the effectiveness of the proposed algorithm.

Introduction

In a large scale power system, the voltage control problem is usually divided spatially and temporally into three hierarchical levels which are primary, secondary and tertiary voltage control. While primary controllers are taking care of local voltage stability of generator buses, secondary controllers try to control voltage of sensitive buses of the network, called pilot nodes, by balancing of reactive power supply and demand over a control area. This reactive power

can be injected into the power system through generation level by means of generators or through transmission level by means of VAR compensation devices such as capacitor banks, tap-changers, static var compensators, etc. At the top level of this hierarchy there is a tertiary level controller which deals with the economic and security concerns of the overall power system. These levels work in different timescales so that their actions do not affect each other. Primary controllers take action in a few seconds, secondary level in few minutes and tertiary level in 15 minutes.

The idea of CSVC was first introduced by Électricité De France in 1985 Paul *et al.* (1987) and further discussed in Vu *et al.* (1996), Lefebvre *et al.* (2000). The amount of change in reference voltage of generators who take part in CSVC is calculated by solving a static optimization problem considering voltage deviation at pilot buses, generators voltage deviation and reactive power limits. Although usually for secondary voltage control, power network is split into distinct areas with minimum interconnections and controlled individually, highly interconnected areas are dealt with as one large area and controlled in a centralized way. Despite its improvements on voltage profile, the amount of time and computations done by this centralized controller grows exponentially as the size of large scale interconnected system increases and it is not suitable for decentralized structure of nowadays power networks.

In Ilic-Spong *et al.* (1988), Ilic et al. have proposed a method based on linear feedback control theory. The goal is to find the best possible pilot buses using SA algorithm which minimizes an objective function representing contingencies over the network. Once the pilot buses are chosen, calculating the control feedback becomes straightforward. The method has considered no interaction between two areas and the interaction effect was suggested as an open problem for further research.

This paper proposes to modify the idea of CSVC proposed in Ilic-Spong *et al.* (1988) and restructure it in a decentralized way to fit well with the needs of todays decentralized power grids. The algorithm finds the best possible pilot buses and corresponding control simultaneously, in each area, to compensate for voltage contingencies. The tie-line active and reactive

powers transferred between two areas are measured at the borders of each area and the effect of neighboring areas are considered as variable loads at mutual buses of tie-lines. Comparison of the proposed decentralized method with the centralized case shows the effectiveness of the proposed method.

The following of the paper is organized as follows. Section II presents the decentralized coordinated secondary voltage control. The simulation results for the decentralized case are given in section III. Finally, a conclusion is given in section IV.

3. Decentralized coordinated secondary voltage control

The structure of a multi-area power network is shown in Figure II-1. In this figure, represent measured values in each area while red lines represent control actions. As could be seen, besides measuring voltage at pilot buses, there are also measurement units on tie-line branches. The idea of decentralized controller design is to replace the tie-lines in network model for each area with loads equal to active and reactive powers imported or exported through them. These virtual loads are located on the mutual buses in regional models to which these tie-lines are connected.

After decentralization of multi-area power network model, the next step is control design based on SA method proposed in Ilic-Spong *et al.* (1988). For our decentralized case, a local controller is designed for each area considering corresponding active and reactive powers imported or exported through the tie-line as loads connected to the buses which these tie-lines are connected to.

Figure II-2 illustrates coordinated secondary voltage control algorithm for each area which has been done in two steps. In the first step, shown in Figure II-2.(a), tie-line active and reactive powers, P_{tie} and Q_{tie} respectively, are measured and in case of a significant change in comparison to previous values, their values are updated in the regional model. In the next step, sensitivity matrix is calculated using Equation A II-1 as follows:

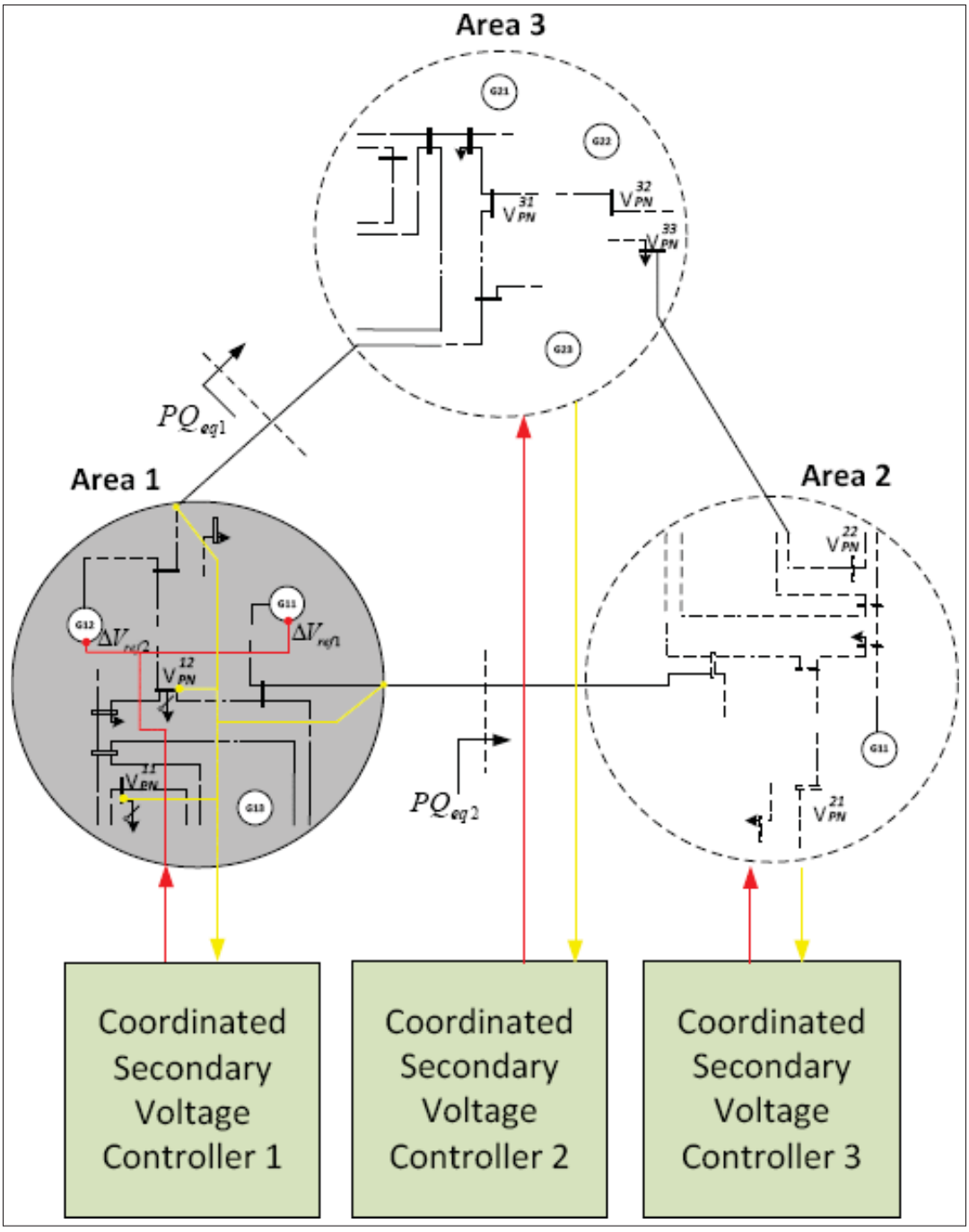

Figure-A II-1 decentralized control structure for multi area power network

$$\frac{dS}{dV_m} = diag(V) * conj\left(Y_{bus} * diag(V/|V|)\right) + conj\left(diag(I_{bus})\right) * diag(V/|V|) \qquad \text{(A II-1)}$$

In which $S = P + jQ$ is apparent power, V is complex bus voltage vector, Y_{bus} is admittance matrix and I_{bus} is complex bus injected current vector. More details about this formula can be found in Zimmerman (2011).

The imaginary part of Equation A II-2 represents sensitivity matrix which relates reactive power rate of change to voltage deviation at all PV and PQ buses of the network. Mathematically:

$$\begin{bmatrix} \Delta Q_1 \\ \Delta Q_2 \end{bmatrix} = \begin{bmatrix} B_{11} & B_{12} \\ B_{21} & B_{22} \end{bmatrix} \begin{bmatrix} \Delta V_1 \\ \Delta V_2 \end{bmatrix} \tag{A II-2}$$

In which ΔQ_1 and ΔV_1 represent respectively reactive power rate of change and voltage deviation at PV buses while ΔQ_2 and ΔV_2 represent the same values related to PQ buses.

Once the sensitivity matrix in Equation A II-2 is obtained, the next goal is to find pilot buses and corresponding control feedback gains. in this way, feedback control law matrix is defined as K and pilot bus location matrix as P in the following equation:

$$\Delta V_1^m = K \Delta V_2^{PN} = K(P B_{22}^{-1} \Delta Q_2) \tag{A II-3}$$

In this equation, ΔV_2^{PN} is voltage deviation vector at pilot nodes and ΔV_1^m is the corresponding change of voltage (as control signal) at PV buses which has been chosen to take part in CSVC to compensate for these deviations. P matrix is defined as follows:

$$P_{ij} = \begin{cases} 1 & if\ bus\ i\ is\ the\ j^{th}\ pilot\ node \\ 0 & otherwise \end{cases} \tag{A II-4}$$

P and K are obtained using the SA algorithm in Ilic-Spong *et al.* (1988).

Figure II-2.(b) shows the second step. As soon as the first step is completed, the controller checks the voltages at defined pilot buses to see if they are beyond the limits. If so, the feedback controller reacts and adjusts the voltage at PV buses to bring back the voltages within the limits.

4. Simulation results for decentralized case

The decentralized algorithm is tested on three area IEEE-39 bus system shown in Figure II-3, and compared with the centralized case discussed in Ilic-Spong *et al.* (1988). The three areas interact with each other by transferring active and reactive power through tie-lines. Table II-1 shows the transferred active and reactive power between neighbor areas in normal conditions without any disturbance in the system, measured at corresponding buses which represents the effect of neighbor areas. Considering the equivalent quantities at mutual buses of tielines, the SA algorithm is applied for each area independently. Notice that the amount of reactive and active power at sending and receiving nodes are different because of the losses over tie-lines.

Table-A II-1 Neighbor equivalent for each area of IEEE-39 bus system

	Area 1	
To Area	**from bus i → to bus j**	**P (MW) , Q (MVAR)**
Area 1	0	0
Area 2	4 → 3 8 → 9	-37.13 , -132.59 34.81 , -132.06
Area 3	15 → 14	-50.26 , 3.62
	Area 2	
	from bus i → to bus j	P (MW) , Q (MVAR)
Area 1	3 → 4 9 → 8	37.34 , 113.06 -34.48 , 97.72
Area 2	0	0
Area 3	16 → 17	224.02 , -42.54
	Area 3	
	from bus i → to bus j	P (MW) , Q (MVAR)
Area 1	17 → 16	-223.68 , 32.5
Area 2	14 → 15	50.31 , -40.68
Area 3	0	0

In each area two generators with maximum reactive power supply have been chosen to take part in CSVC which are Generator 9 and 10 in Area 1, Generator 2 and 3 in Area 2 and Generator 5 and 6 in Area 3.

To validate the proposed decentralized CSVC method, two scenarios are considered. In the first scenario, all the PQ buses over the network are perturbed with 35% of nominal reactive power which is 100 MVAR. Table II-2 shows the obtained pilot buses as well as feedback gains in both centralized and decentralized cases.

Table-A II-2 Obtained pilot bus and feedback gains in both centralized and decentralized cases

Controller type	**Pilot bus No.**	**Controller gain**
Centralized CSVC	2, 6, 16	$K=\begin{bmatrix} 0.25 & -1.47 & 0.05 \\ -0.13 & -0.65 & 0.40 \\ -9.81 & 0.26 & 8.54 \\ 6.88 & 0.56 & -9.49 \\ 0.10 & -1.0 & 0.17 \\ 0.28 & -2.18 & 0.54 \end{bmatrix}$
Decentralized CSVC	11, 16, 17	$K=\begin{bmatrix} -1.59 & 0 & 0 \\ -0.37 & 0 & 0 \\ 0 & -0.82 & 0 \\ 0 & -1.14 & 0 \\ 0 & 0 & -0.81 \\ 0 & 0 & -1.63 \end{bmatrix}$

Figure II-4 shows voltage deviation over the network comparing centralized CSVC, decentralized CSVC and the case with no SVC. As can be seen from Figure II-4, both centralized and decentralized controllers improved the voltage at pilot buses. Although the centralized CSVC works better than the decentralized one, the following comments describe the advantages of the decentralized controller:

- Since the centralized optimisation problem is divided into three parallel optimisation problems with smaller size, the simulation is done more quickly in decentralized case. For this

scenario, it takes 0.8s for centralized controller to do the calculation while the maximum time spent by decentralized controllers is 0.2s;

- Algorithm to find neighbor is done very faster since number of pilot buses is divided between areas;
- Since the algorithm is done for each Area, the existence of pilot point for each area is guaranteed. Buses 17, 11 and 16 are chosen by Areal, Area2 and Area3 respectively as pilot buses.

The second scenario to validate the controller is to apply 45% of nominal reactive power as disturbances on each area separately. Figures II-5, II-6 and II-7 show the simulation results applying disturbance on Areal, Area2 and Area 3 respectively. The buses at the left side of dashed line are PQ buses of which the controllers try to control the voltage and the buses at the right side are PV buses which have been used as controllers to control the voltage of the network by changing reference voltage of the generators.

Comparing centralized and decentralized CSVCs shows that in Figure II-5, the centralized one shows better results. In two other cases however, while disturbances area applied on Area2 and Area3, the decentralized CSVC shows a better control to compensate for voltage deviation. More importantly, it can be seen in Figure II-6 that in PV bus 32, the control action is deviated from 5% of IEEE standard while decentralized controller still remains in the limits.

5. Conclusions

In this paper a modified version of coordinated secondary voltage controller based on SA optimization was proposed in a decentralized way to fit well with the current multi-area highly interconnected power networks. The algorithm finds the best possible pilot buses and corresponding control simultaneously, in each area, to compensate for voltage contingencies. The tie-line active and reactive powers transferred between two areas were measured at the borders of each area and the effect of neighbor areas are considered as variable loads at mutual buses

of tie-line. Comparison of proposed decentralized method with centralized case for IEEE-39 bus power network shows the effectiveness of the proposed algorithm.

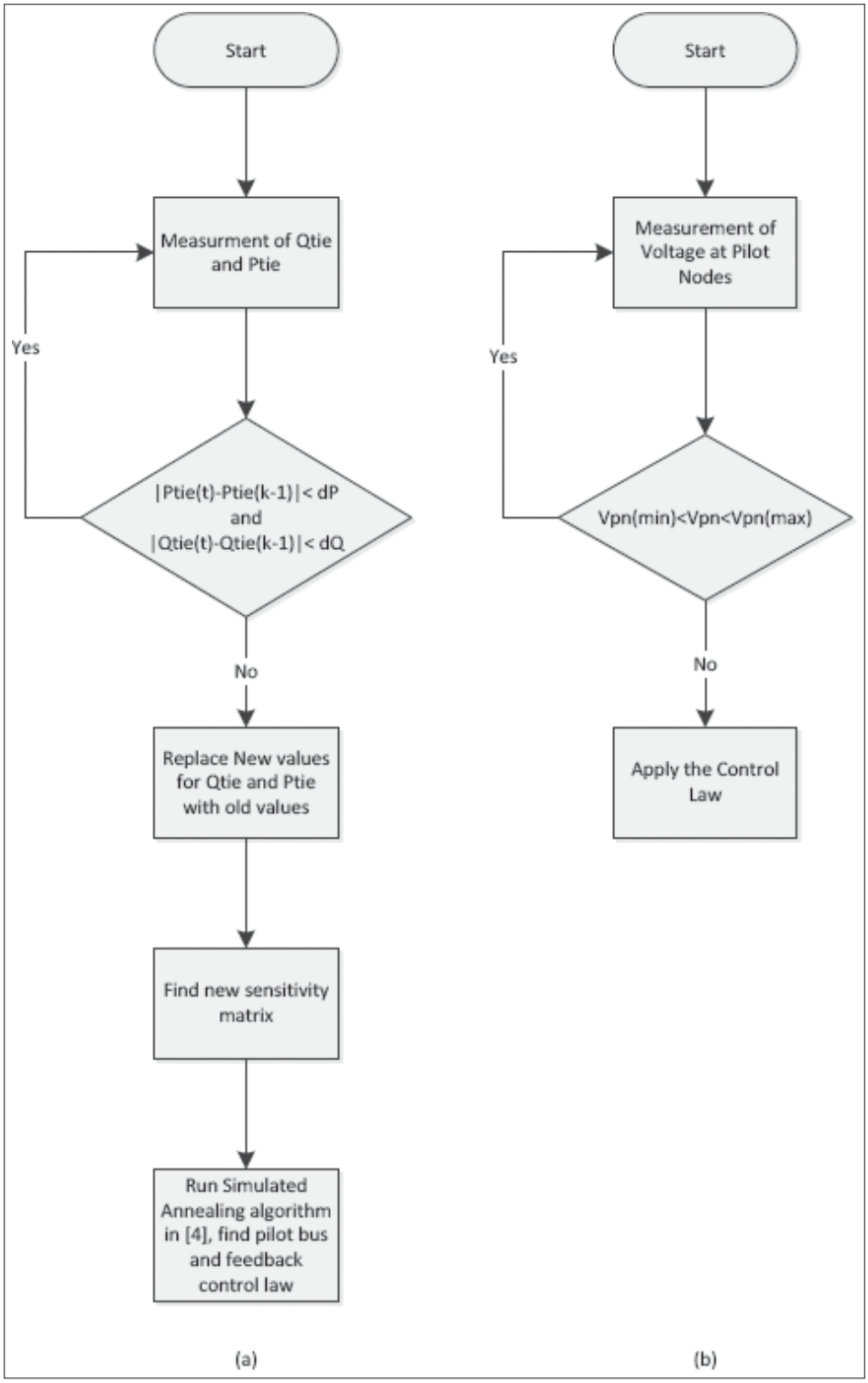

Figure-A II-2 Coordinated Secondary Voltage Control flowchart. (a) first loop (b) second loop

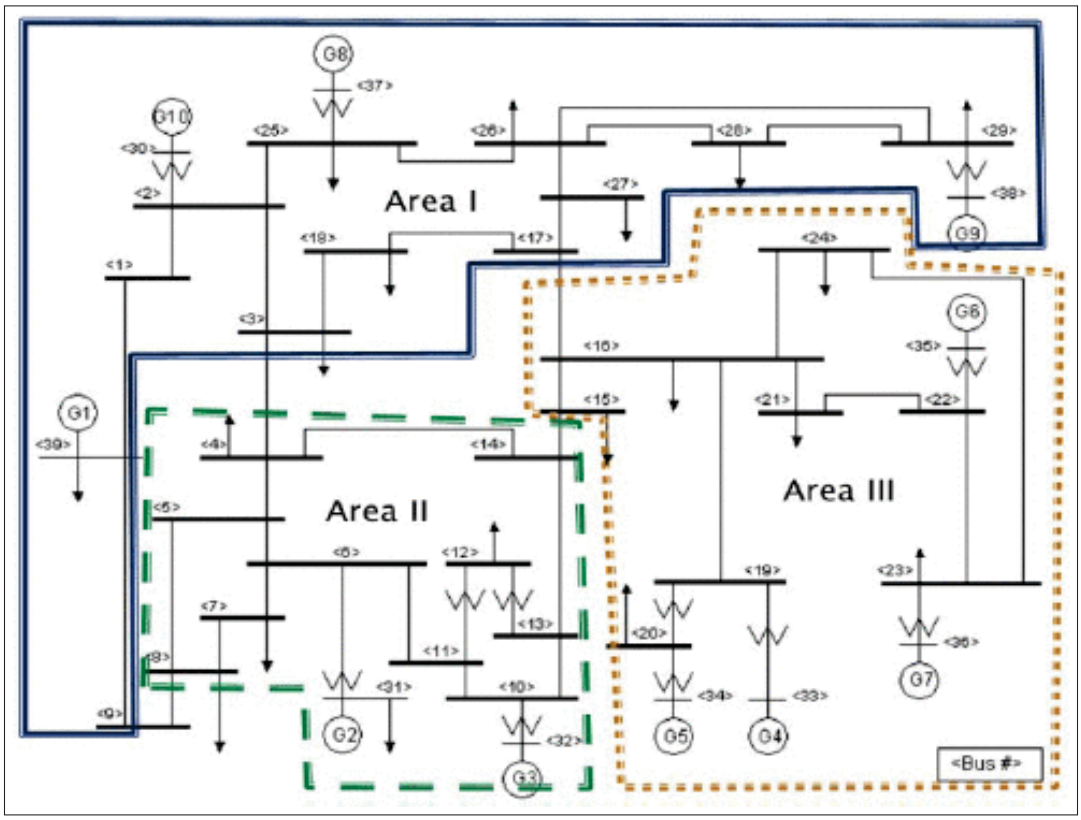

Figure-A II-3 Three area IEEE-39 bus power network

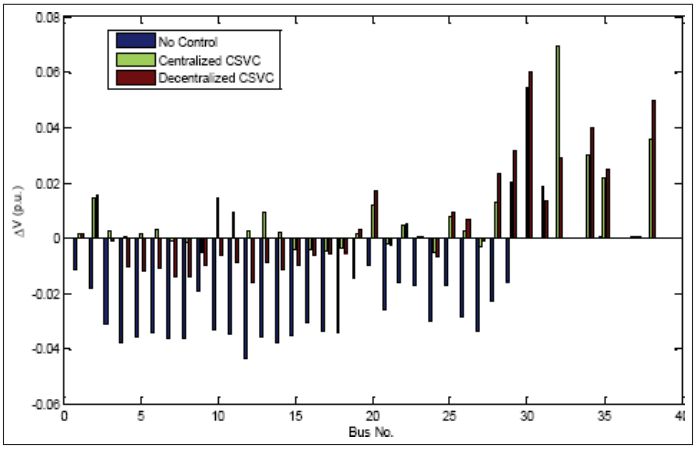

Figure-A II-4 Comparison of voltage deviations applying Centralized and Decentralized controllers with no control case, Scenario 1

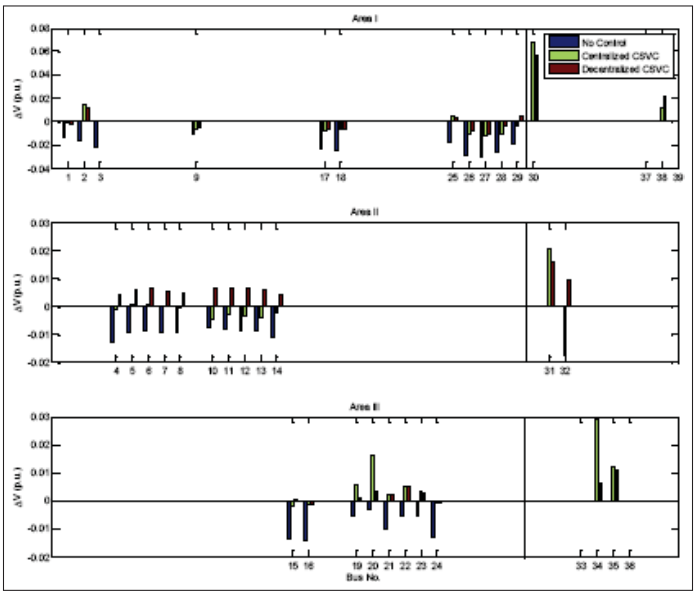

Figure-A II-5 Comparison of voltage deviations applying Centralized and Decentralized controllers with no control case, Scenario 2, Area 1 disturbed

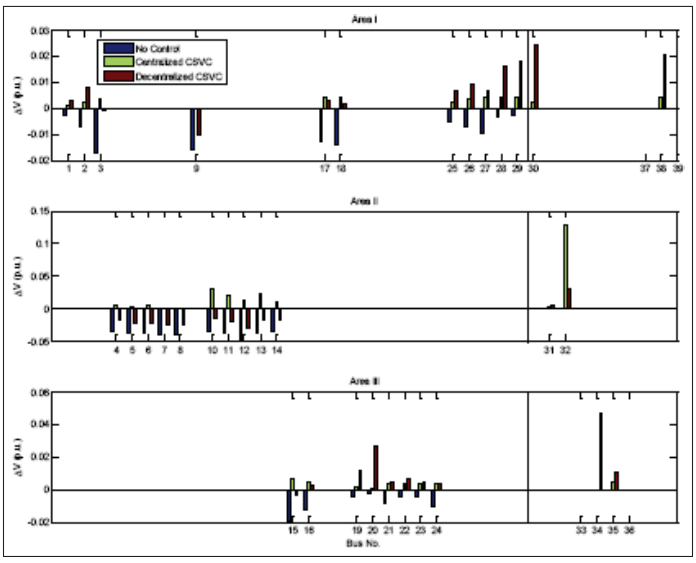

Figure-A II-6 Comparison of voltage deviations applying Centralized and Decentralized controllers with no control case, Scenario 2, Area2 disturbed

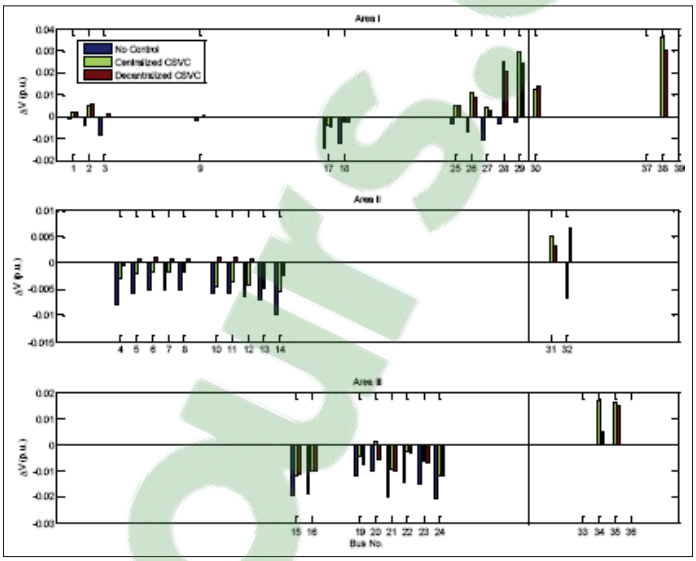

Figure-A II-7 Comparison of voltage deviations applying Centralized and Decentralized controllers with no control case, Scenario 2, Area3 disturbed

BIBLIOGRAPHY

Aggelogiannaki, E. & Sarimveis, H. (2007). A Simulated Annealing Algorithm for Prioritized Multiobjective Optimization mdash;Implementation in an Adaptive Model Predictive Control Configuration. *Systems, Man, and Cybernetics, Part B: Cybernetics, IEEE Transactions on*, 37(4), 902-915. doi: 10.1109/TSMCB.2007.896015.

Alimisis, V. & Taylor, P. C. (2015). Zoning evaluation for improved coordinated automatic voltage control. *IEEE Transactions on Power Systems*, 30(5), 2736–2746.

Amadou, M. D., Mehrjerdi, H., Lefebvre, S., Saad, M. & Asber, D. (2014). Area voltage control analysis in transmission systems based on clustering technique. *IET Generation, Transmission & Distribution*, 8(12), 2134-2143.

Amraee, T., Soroudi, A. & Ranjbar, A. M. (2012). Probabilistic determination of pilot points for zonal voltage control. *IET Generation, Transmission Distribution*, 6(1), 1-10. doi: 10.1049/iet-gtd.2011.0334.

Amraee, T., Ranjbar, A. & Feuillet, R. (2010). Immune-based selection of pilot nodes for secondary voltage control. *European Transactions on Electrical Power*, 20(7), 938–951.

Arcidiacono, V. (1983). Automatic voltage and reactive power control in transmission systems. *CIGRE-IFAC Survey Paper E, Florence*.

Arcidiacono, V., Corsi, S., Garzillo, A. & Mocenigo, M. (1977). Studies on area voltage and reactive power control at ENEL. *Proc. 1977 of CIGRE*, 32–77.

Bastian, M., Heymann, S. & Jacomy, M. (2009). Gephi: An Open Source Software for Exploring and Manipulating Networks. Consulted at http://www.aaai.org/ocs/index.php/ICWSM/09/paper/view/154.

Beccuti, A. G., Demiray, T. H., Andersson, G. & Morari, M. (2010). A Lagrangian Decomposition Algorithm for Optimal Emergency Voltage Control. *IEEE Transactions on Power Systems*, 25(4), 1769-1779. doi: 10.1109/TPWRS.2010.2043749.

Bernard, S., Trudel, G. & Scott, G. (1996). A 735 kV shunt reactors automatic switching system for Hydro-Quebec network. *Power Systems, IEEE Transactions on*, 11(4), 2024-2030. doi: 10.1109/59.544680.

Bhattacharya, K. & Zhong, J. (2001). Reactive power as an ancillary service. *IEEE Transactions on Power Systems*, 16(2), 294-300. doi: 10.1109/59.918301.

Borghetti, A., Bottura, R., Barbiroli, M. & Nucci, C. A. (2017). Synchrophasors-Based Distributed Secondary Voltage/VAR Control via Cellular Network. *IEEE Transactions on Smart Grid*, 8(1), 262-274. doi: 10.1109/TSG.2016.2606885.

Bottura, R. & Borghetti, A. (2014). Simulation of the Volt/Var Control in Distribution Feeders by Means of a Networked Multiagent System. *IEEE Transactions on Industrial Informatics*, 10(4), 2340-2353. doi: 10.1109/TII.2014.2331025.

Cai, H., Hu, G., Lewis, F. L. & Davoudi, A. (2016). A Distributed Feedforward Approach to Cooperative Control of AC Microgrids. *IEEE Transactions on Power Systems*, 31(5), 4057-4067. doi: 10.1109/TPWRS.2015.2507199.

Camacho, E. F. & Alba, C. B. (2013). *Model predictive control*. Springer Science & Business Media.

Chavali, P. & Nehorai, A. (2015). Distributed power system state estimation using factor graphs. *IEEE Transactions on Signal Processing*, 63(11), 2864–2876.

Chen, C. L. (2007). Simulated annealing-based optimal wind-thermal coordination scheduling. *IET Journal of Generation, Transmission & Distribution*, 1(3), 447-455.

Chen, F., Chen, M., Li, Q., Meng, K., Guerrero, J. M. & Abbott, D. (2016). Multiagent-Based Reactive Power Sharing and Control Model for Islanded Microgrids. *IEEE Transactions on Sustainable Energy*, 7(3), 1232-1244. doi: 10.1109/TSTE.2016.2539213.

Chen, Y. & Sun, X. (2014, Oct). Cyber security assessment of wide area controlled power system based on co-simulations. *2014 International Conference on Power System Technology*, pp. 1986-1991. doi: 10.1109/POWERCON.2014.6993908.

Chen, Z., Xie, Z. & Zhang, Q. (2015). Community detection based on local topological information and its application in power grid. *Neurocomputing*, 170, 384-392.

Conejo, A. & Aguilar, M. J. (1998). Secondary voltage control: nonlinear selection of pilot buses, design of an optimal control law, and simulation results. *IEE Proceedings - Generation, Transmission and Distribution*, 145(1), 77-81. doi: 10.1049/ip-gtd:19981535.

Conejo, A., de la Fuente, J. I. & Goransson, S. (1994, Apr). Comparison of alternative algorithms to select pilot buses for secondary voltage control in electric power networks. *Electrotechnical Conference, 1994. Proceedings., 7th Mediterranean*, pp. 940-943 vol.3. doi: 10.1109/MELCON.1994.380947.

Corsi, S. (2015). *Voltage Control and Protection in Electrical Power Systems: From System Components to Wide-Area Control*. Springer London. Consulted at https://books.google.ca/books?id=o8i8oQEACAAJ.

Cotilla-Sanchez, E., Hines, P. D. H., Barrows, C., Blumsack, S. & Patel, M. (2013). Multi-Attribute Partitioning of Power Networks Based on Electrical Distance. *IEEE Transactions on Power Systems*, 28(4), 4979-4987. doi: 10.1109/TPWRS.2013.2263886.

Da Silva, R. J. G. C., Zambroni de Souza, A. C., Leme, R. C. & Sonoda, D. (2013). Decentralized secondary voltage control using voltage drop compensator among power plants. *International Journal of Electrical Power & Energy Systems*, 47(0), 61-68.

Daher, N. A., Mougharbel, I., Saad, M., Kanaan, H. Y. & Asber, D. (2015, Aug). Pilot buses selection based on reduced Jacobian matrix. *Smart Energy Grid Engineering (SEGE), 2015 IEEE International Conference on*, pp. 1-7. doi: 10.1109/SEGE.2015.7324611.

Daher, N. A., Mougharbel, I., Saad, M. & Kanaan, H. Y. (2013). Comparative study of partitioning methods used for secondary voltage control in distributed power networks. *2013 IEEE International Conference on Smart Energy Grid Engineering (SEGE)*.

Dragosavac, J., Janda, Z. & Milanovic, J. V. (2012). Coordinated Reactive Power-Voltage Controller for Multimachine Power Plant. *IEEE Transactions on Power Systems*, 27(3), 1540-1549.

Dragosavac, J., Janda, Z., Milanovic, J. V. & Arnautovic, D. (2013). Robustness of Commissioned Coordinated q - V Controller for Multimachine Power Plant. *IEEE Transactions on Power Systems*, 28(2), 1415-1424.

El Moursi, M. S. & Mehrjerdi, H. (2014). A Coordinated Control Strategy of Voltage Regulation in Power System based on Multi-Agent System. *Industrial Engineering & Management*, 2014.

Ertem, S. & Tudor, J. R. (1987). Optimal Shunt Capacitor Allocation by Nonlinear Programming. *IEEE Transactions on Power Delivery*, 2(4), 1310-1316. doi: 10.1109/TPWRD.1987.4308258.

Fenichel, N. (1979). Geometric singular perturbation theory for ordinary differential equations. *Journal of Differential Equations*, 31(1), 53 - 98. doi: http://dx.doi.org/10.1016/0022-0396(79)90152-9.

Fleming, P. & Purshouse, R. (2002). Evolutionary algorithms in control systems engineering: a survey. *Control Engineering Practice*, 10(11), 1223 - 1241. doi: http://dx.doi.org/10.1016/S0967-0661(02)00081-3.

Flórez, J., Tapia, A., Criado, R. & Griajalba, J. M. (1994). Secondary voltage control based on a robust multivariable PI controller. *International Journal of Electrical Power & Energy Systems*, 16(3), 167-173.

Ghahremani, E. & Kamwa, I. (2013). Optimal placement of multiple-type FACTS devices to maximize power system loadability using a generic graphical user interface. *IEEE Transactions on Power Systems*, 28(2), 764-778. doi: 10.1109/TPWRS.2012.2210253.

Glavic, M., Hajian, M., Rosehart, W. & Cutsem, T. V. (2011). Receding-Horizon Multi-Step Optimization to Correct Nonviable or Unstable Transmission Voltages. *IEEE Transactions on Power Systems*, 26(3), 1641-1650. doi: 10.1109/TPWRS.2011.2105286.

Guo, Q., Wu, H., Lin, L., Bai, Z. & Ma, H. (2016). Secondary Voltage Control for Reactive Power Sharing in an Islanded Microgrid. *Journal of Power Electronics*, 16(1), 329–339.

Hamidi, R. J., Livani, H., Hosseinian, S. & Gharehpetian, G. (2016). Distributed cooperative control system for smart microgrids. *Electric Power Systems Research*, 130, 241 - 250. doi: http://dx.doi.org/10.1016/j.epsr.2015.09.012.

Hano, I., Tamura, Y., Narita, S. & Matsumoto, K. (1969). Real Time Control of System Voltage and Reactive Power. *Power Apparatus and Systems, IEEE Transactions on*, PAS-88(10), 1544-1559. doi: 10.1109/TPAS.1969.292283.

Happ, H. H. & Wirgau, K. A. (1978). Static and Dynamic Var Compensation in System Planning. *IEEE Transactions on Power Apparatus and Systems*, PAS-97(5), 1564-1578. doi: 10.1109/TPAS.1978.354648.

Hiskens, I. & Gong, B. (2006). Voltage stability enhancement via model predictive control of load. *Intelligent Automation & Soft Computing*, 12(1), 117-124.

Ilic-Spong, M., Christensen, J. & Eichorn, K. (1988). Secondary voltage control using pilot point information. *Power Systems, IEEE Transactions on*, 3(2), 660-668.

Jalili-Marandi, V., Ayres, F. J., Ghahremani, E., Bélanger, J. & Lapointe, V. (2013, July). A real-time dynamic simulation tool for transmission and distribution power systems. *2013 IEEE Power Energy Society General Meeting*, pp. 1-5. doi: 10.1109/PESMG.2013.6672734.

Jang, G., Vittal, V. & Kliemann, W. (1998). Effect of nonlinear modal interaction on control performance: use of normal forms technique in control design. I. General theory and procedure. *IEEE Transactions on Power Systems*, 13(2), 401-407. doi: 10.1109/59.667359.

Jin, L., Kumar, R. & Elia, N. (2010). Model Predictive Control-Based Real-Time Power System Protection Schemes. *IEEE Transactions on Power Systems*, 25(2), 988-998. doi: 10.1109/TPWRS.2009.2034748.

Juang, J.-N. & Pappa, R. S. (1985). An eigensystem realization algorithm for modal parameter identification and model reduction. *Journal of guidance, control, and dynamics*, 8(5), 620–627.

Juang, J.-N. (1994). *Applied System Identification*. Upper Saddle River, NJ, USA: Prentice-Hall, Inc.

Kamwa, I. & Gerin-Lajoie, L. (2000). State-space system identification-toward MIMO models for modal analysis and optimization of bulk power systems. *IEEE Transactions on Power Systems*, 15(1), 326-335. doi: 10.1109/59.852140.

Kamwa, I., Pradhan, A. K., Joos, G. & Samantaray, S. R. (2009). Fuzzy Partitioning of a Real Power System for Dynamic Vulnerability Assessment. *IEEE Transactions on Power Systems*, 24(3), 1356-1365. doi: 10.1109/TPWRS.2009.2021225.

Karakatsanis, T. S. & Hatziargyriou, N. D. (1994). Probabilistic constrained load flow based on sensitivity analysis. *IEEE Transactions on Power Systems*, 9(4), 1853-1860. doi: 10.1109/59.331441.

Katsigiannis, Y. A., Georgilakis, P. S. & Karapidakis, E. S. (2012). Hybrid Simulated Annealing & Tabu Search Method for Optimal Sizing of Autonomous Power Systems With Renewables. *IEEE Transactions on Sustainable Energy*, 3(3), 330-338.

Krantz, S. & Parks, H. (2012). *The Implicit Function Theorem: History, Theory, and Applications*. Springer. Consulted at http://books.google.co.uk/books?id=7QqickY0yh8C.

La Gatta, P. O., Passos Filho, J. A. & Pereira, J. L. (2014). Comparison among methodologies for identification of pilot buses and its impact on the steady state secondary voltage control. *Industry Applications (INDUSCON), 2014 11th IEEE/IAS International Conference on*, pp. 1-6.

Lagonotte, P., Sabonnadiere, J.-C., Leost, J. & Paul, J. P. (1989). Structural analysis of the electrical system: application to secondary voltage control in France. *Power Systems, IEEE Transactions on*, 4(2), 479-486. doi: 10.1109/59.193819.

Lai, J., Zhou, H., Lu, X., Yu, X. & Hu, W. (2016). Droop-Based Distributed Cooperative Control for Microgrids With Time-Varying Delays. *IEEE Transactions on Smart Grid*, 7(4), 1775-1789. doi: 10.1109/TSG.2016.2557813.

Larsson, M. & Karlsson, D. (2003). Coordinated system protection scheme against voltage collapse using heuristic search and predictive control. *IEEE Transactions on Power Systems*, 18(3), 1001-1006. doi: 10.1109/TPWRS.2003.814852.

Larsson, M. (1999). Coordination of cascaded tap changers using a fuzzy-rule-based controller. *Fuzzy Sets and Systems*, 102(1), 113 - 123. doi: http://dx.doi.org/10.1016/S0165-0114(98)00208-5. Applications of Fuzzy Theory in Electronic Power Systems.

Larsson, M. (2000). *Coordinated voltage control in electric power systems*. (Ph.D. thesis).

Larsson, M., Hill, D. J. & Olsson, G. (2002). Emergency voltage control using search and predictive control. *International Journal of Electrical Power and Energy Systems*, 24(2), 121 - 130. doi: http://dx.doi.org/10.1016/S0142-0615(01)00017-5.

Lefebvre, H., Fragnier, D., Boussion, J. Y., Mallet, P. & Bulot, M. (2000). Secondary coordinated voltage control system: feedback of EDF. *Power Engineering Society Summer Meeting, 2000. IEEE*, 1, 290-295 vol. 1. doi: 10.1109/PESS.2000.867598.

Lerm, A. A. P. (2006, Oct). Using the bifurcation theory to select pilot busbars in a secondary voltage regulation shceme. *2006 IEEE PES Power Systems Conference and Exposition*, pp. 2096-2100. doi: 10.1109/PSCE.2006.296268.

Li, Q., Chen, F., Chen, M., Guerrero, J. M. & Abbott, D. (2016). Agent-Based Decentralized Control Method for Islanded Microgrids. *IEEE Transactions on Smart Grid*, 7(2), 637-649. doi: 10.1109/TSG.2015.2422732.

Ljung, L. (1998). System identification. In *Signal Analysis and Prediction* (pp. 163–173). Springer.

Loia, V., Vaccaro, A. & Vaisakh, K. (2013). A Self-Organizing Architecture Based on Cooperative Fuzzy Agents for Smart Grid Voltage Control. *IEEE Transactions on Industrial Informatics*, 9(3), 1415-1422. doi: 10.1109/TII.2013.2249074.

Lu, X., Yu, X., Lai, J., Wang, Y. & Guerrero, J. M. (2016). A Novel Distributed Secondary Coordination Control Approach for Islanded Microgrids. *IEEE Transactions on Smart Grid*, PP(99), 1-1. doi: 10.1109/TSG.2016.2618120.

Ma, H. & Hill, D. J. (2014a). Adaptive Coordinated Voltage Control. Part I: Basic Scheme. *IEEE Transactions on Power Systems*, 29(4), 1546-1553. doi: 10.1109/TPWRS.2013.2293577.

Ma, H. & Hill, D. J. (2014b). Adaptive Coordinated Voltage Control, Part II: Use of Learning for Rapid Response. *IEEE Transactions on Power Systems*, 29(4), 1554-1561. doi: 10.1109/TPWRS.2013.2293572.

Ma, H. & Hill, D. J. (2017). Sensitivity Studies for Adaptive Coordinated Voltage Control: Scale and Similarity of Contingencies. *IEEE Transactions on Power Systems*, PP(99), 1-1. doi: 10.1109/TPWRS.2017.2653226.

Ma, H., Chan, K. W. & Liu, M. (2013). An Intelligent Control Scheme to Support Voltage of Smart Power Systems. *IEEE Transactions on Industrial Informatics*, 9(3), 1405-1414. doi: 10.1109/TII.2013.2243741.

Marinescu, B. & Bourles, H. (1999). Robust predictive control for the flexible coordinated secondary voltage control of large-scale power systems. *IEEE Transactions on Power Systems*, 14(4), 1262-1268. doi: 10.1109/59.801882.

Martins, N. & Corsi, S. (2007). *Coordinated Voltage Control In Transmission Networks*.

Mehrjerdi, H., Ghahremani, E., Lefebvre, S., Saad, M. & Asber, D. (2013a). Authenticated voltage control of partitioned power networks with optimal allocation of STATCOM using heuristic algorithm. *IET Generation, Transmission Distribution*, 7(9), 1037-1045. doi: 10.1049/iet-gtd.2013.0042.

Mehrjerdi, H., Lefebvre, S., Saad, M. & Asber, D. (2013b). A Decentralized Control of Partitioned Power Networks for Voltage Regulation and Prevention Against Disturbance Propagation. *IEEE Transactions on Power Systems*, 28(2), 1461-1469. doi: 10.1109/TPWRS.2012.2225154.

Mehrjerdi, H., Lefebvre, S., Asber, D. & Saad, M. (2013c). Eliminating voltage violations in power systems using secondary voltage control and decentralized neural network. *2013 IEEE Power & Energy Society General Meeting*, pp. 1–5.

Mehrjerdi, H., Lefebvre, S., Saad, M. & Asber, D. (2013d). Coordinated control strategy considering effect of neighborhood compensation for voltage improvement in transmission systems. *IEEE Transactions on Power Systems*, 28(4), 4507-4515.

Mendoza, J. E., Morales, D. A., Lopez, R. A., Lopez, E. A., Vannier, J. C. & Coello, C. A. C. (2007). Multiobjective Location of Automatic Voltage Regulators in a Radial Distribution Network Using a Micro Genetic Algorithm. *IEEE Transactions on Power Systems*, 22(1), 404-412. doi: 10.1109/TPWRS.2006.887963.

Mezquita, J., Asber, D., Lefebvre, S., Saad, M. & Lagacé, P. J. (2011). Power network partitioning with a fuzzy C-means. *Proc. IASTED Int. Conf. Power and Energy Systems and Applications (PESA 2011)*, pp. 7–9.

Mezquita, J., Mehrjerdi, H., Lefebvre, S., Saad, M., Lagacé, P. J. & Asber, D. (2015). A secondary voltage regulation approach for Hydro-Québec in transmission level. *Electric Power Systems Research*, 121, 183-191.

Mitra, D., Romeo, F. & Sangiovanni-Vincentelli, A. (1985, Dec). Convergence and finite-time behavior of simulated annealing. *Decision and Control, 1985 24th IEEE Conference on*, pp. 761-767. doi: 10.1109/CDC.1985.268600.

Moore, B. (1981). Principal component analysis in linear systems: Controllability, observability, and model reduction. *IEEE Transactions on Automatic Control*, 26(1), 17-32. doi: 10.1109/TAC.1981.1102568.

Moradzadeh, M., Boel, R. & Vandevelde, L. (2013). Voltage Coordination in Multi-Area Power Systems via Distributed Model Predictive Control. *IEEE Transactions on Power Systems*, 28(1), 513-521. doi: 10.1109/TPWRS.2012.2197028.

Morattab, A., Akhrif, O. & Saad, M. (2017a). Decentralized Coordinated Secondary Voltage Control of Multi-Area Power Grids using Model Predictive Control. *IET Generation, Transmission and Distribution*. Consulted at http://digital-library.theiet.org/content/journals/10.1049/iet-gtd.2016.2054.

Morattab, A., Saad, M., Akhrif, O., Dalal, A. & Lefebvre, S. (2017b). Nonlinear Sensitivity-based Coordinated Control of Reactive Resources in Power Grids Under Large Disturbances. *IEEE Transactions on Power Systems*.

Mozafari, B., Amraee, T., Ranjbar, A. & Mirjafari, M. (2007). Particle swarm optimization method for optimal reactive power procurement considering voltage stability. *Scientia Iranica*, 14(6), 534–545.

Nakamura, Y. & Okada, T. (1969). Voltage and Reactive Power Controls by Dividing a System into Several Blocks. *Electrical Engineering in Japan*, 89(12), 75.

Narita, S. & Hammam, M. (1971a). A Computational Algorithm for Real-Time Control of System Voltage and Reactive Power Part I - Problem Formulation. *Power Apparatus and Systems, IEEE Transactions on*, PAS-90(6), 2495-2501. doi: 10.1109/TPAS.1971.292861.

Narita, S. & Hammam, M. (1971b). A Computational Algorithm for Real-Time Control of System Voltage and Reactive Power Part II - Algorithm of Optimization. *Power Apparatus and Systems, IEEE Transactions on*, PAS-90(6), 2502-2508. doi: 10.1109/TPAS.1971.292862.

Negenborn, R. R. (2007). *Multi-agent model predictive control with applications to power networks*. (Ph.D. thesis).

Opal-RT. (2018). ePHASORsim Real-Time Transient Stability Simulator. Consulted at http://www.opal-rt.com/new-product/ephasorsim-real-time-transient-stability-simulator.

Paul, J. P., Leost, J. Y. & Tesseron, J. M. (1987). Survey of the Secondary Voltage Control in France : Present Realization and Investigations. *IEEE Transactions on Power Systems*, 2(2), 505-511. doi: 10.1109/TPWRS.1987.4335155.

Piacentini, C., Alimisis, V., Fox, M. & Long, D. (2015). An extension of metric temporal planning with application to AC voltage control. *Artificial Intelligence*, 229, 210-245.

Pretelt, A. M. (1971). Automatic Allocation of Network Capacitors. *IEEE Transactions on Power Apparatus and Systems*, PAS-90(1), 54-61. doi: 10.1109/TPAS.1971.292898.

Rajasekaran, S. (2000). On simulated annealing and nested annealing. *Journal of Global Optimization*, 16(1), 43–56.

Richardot, O., Viciu, A., Besanger, Y., Hadjsaid, N. & Kieny, C. (2006, May). Coordinated Voltage Control in Distribution Networks Using Distributed Generation. *2005/2006 IEEE/PES Transmission and Distribution Conference and Exhibition*, pp. 1196-1201. doi: 10.1109/TDC.2006.1668675.

Ruey-Hsun, L. & Yung-Shuen, W. (2003). Fuzzy-based reactive power and voltage control in a distribution system. *Power Delivery, IEEE Transactions on*, 18(2), 610-618.

Sancha, J. L., Fernandez, J. L., Cortes, A. & Abarca, J. T. (1995, May). Secondary voltage control: analysis, solutions and simulation results for the Spanish transmission system. *Power Industry Computer Application Conference, 1995. Conference Proceedings., 1995 IEEE*, pp. 27-32. doi: 10.1109/PICA.1995.515161.

Sancha, J. L., Fernandez, J. L., Cortes, A. & Abarca, J. T. (1996). Secondary voltage control: analysis, solutions and simulation results for the Spanish transmission system. *Power Systems, IEEE Transactions on*, 11(2), 630-638.

Savard, A. G. (2013). *Méthode globale d'implantation d'un réglage secondaire coordonné de tension hybride*. (Master's thesis, Ecole de Technologie Superieure, Montreal, Quebec, Canada).

Schiffer, J., Seel, T., Raisch, J. & Sezi, T. (2016). Voltage Stability and Reactive Power Sharing in Inverter-Based Microgrids With Consensus-Based Distributed Voltage Control. *IEEE Transactions on Control Systems Technology*, 24(1), 96-109. doi: 10.1109/TCST.2015.2420622.

Schmid, C. & Biegler, L. T. (1994). Quadratic programming methods for reduced hessian SQP. *Computers & chemical engineering*, 18(9), 817–832.

Shafiee, Q., Dragičević, T., Vasquez, J. C. & Guerrero, J. M. (2014a). Hierarchical Control for Multiple DC-Microgrids Clusters. *IEEE Transactions on Energy Conversion*, 29(4), 922-933. doi: 10.1109/TEC.2014.2362191.

Shafiee, Q., Guerrero, J. M. & Vasquez, J. C. (2014b). Distributed Secondary Control for Islanded Microgrids, A Novel Approach. *IEEE Transactions on Power Electronics*, 29(2), 1018-1031. doi: 10.1109/TPEL.2013.2259506.

Shafiee, Q., Stefanovic, C., Dragicevic, T., Popovski, P., Vasquez, J. C. & Guerrero, J. M. (2014c). Robust Networked Control Scheme for Distributed Secondary Control of Islanded Microgrids. *IEEE Transactions on Industrial Electronics*, 61(10), 5363-5374. doi: 10.1109/TIE.2013.2293711.

Simpson-Porco, J. W., Shafiee, Q., Dörfler, F., Vasquez, J. C., Guerrero, J. M. & Bullo, F. (2015). Secondary Frequency and Voltage Control of Islanded Microgrids via Distributed Averaging. *IEEE Transactions on Industrial Electronics*, 62(11), 7025-7038. doi: 10.1109/TIE.2015.2436879.

Simpson-Porco, J. W. & Bullo, F. (2016). Distributed Monitoring of Voltage Collapse Sensitivity Indices. *IEEE Transactions on Smart Grids*, 7(4), 1979-1988.

Su, H. Y., Kang, F. M. & Liu, C. W. (2016). Transmission Grid Secondary Voltage Control Method Using PMU Data. *IEEE Transactions on Smart Grid*, PP(99), 1-1. doi: 10.1109/TSG.2016.2623302.

Sun, H., Guo, Q., Zhang, B., Wu, W. & Wang, B. (2013). An Adaptive Zone-Division-Based Automatic Voltage Control System With Applications in China. *IEEE Transactions on Power Systems*, 28(2), 1816-1828. doi: 10.1109/TPWRS.2012.2228013.

Sybille, G. (2013). Initializing a 29-Bus, 7-Power Plant Network With the Load Flow Tool of Powergui. Consulted at https://www.mathworks.com/help/physmod/sps/examples/initializing-a-29-bus-7-power-plant-network-with-the-load-flow-tool-of-powergui.html.

Taylor, C., Balu, N. & Maratukulam, D. (1994). *Power system voltage stability*. McGraw-Hill Ryerson, Limited. Consulted at https://books.google.ca/books?id=CPtSAAAAMAAJ.

Trakas, D., Voumvoulakis, E. & Hatziargyriou, N. (2014). Decentralized control of power system zones based on probabilistic constrained load flow. *Probabilistic Methods Applied to Power Systems (PMAPS), 2014 International Conference on*, pp. 1-6.

Trovao, J. P. F., Santos, V. D. N., Pereirinha, P. G., Jorge, H. M. & Antunes, C. H. (2013). A Simulated Annealing Approach for Optimal Power Source Management in a Small EV. *Sustainable Energy, IEEE Transactions on*, 4(4), 867-876.

Tsuji, T., Magoules, F., Uchida, K. & Oyama, T. (2015). A partitioning technique for a waveform relaxation method using eigenvectors in the transient stability analysis of power systems. *IEEE Transactions on Power Systems*, 30(6), 2867-2879.

Tuglie, E. D., Iannone, S. M. & Torelli, F. (2008). A Coherency Recognition Based on Structural Decomposition Procedure. *IEEE Transactions on Power Systems*, 23(2), 555-563. doi: 10.1109/TPWRS.2008.919313.

Černý, V. (1985). Thermodynamical approach to the traveling salesman problem: An efficient simulation algorithm. *Journal of Optimization Theory and Applications*, 45(1), 41-51. doi: 10.1007/BF00940812.

Vaccaro, A., Velotto, G. & Zobaa, A. F. (2011). A Decentralized and Cooperative Architecture for Optimal Voltage Regulation in Smart Grids. *IEEE Transactions on Industrial Electronics*, 58(10), 4593-4602. doi: 10.1109/TIE.2011.2143374.

Van Cutsem, T. & Vournas, C. (1998). *Voltage Stability of Electric Power Systems*. Boston, MA: Springer US. doi: $10.1007/978-0-387-75536-6_6$.

Vu, H., Pruvot, P., Launay, C. & Harmand, Y. (1996). An improved voltage control on large-scale power system. *IEEE Transactions on Power Systems*, 11(3), 1295-1303. doi: 10.1109/59.535670.

Wang, H. F. (2001). Multi-agent co-ordination for the secondary voltage control in power-system contingencies. *IEE Proceedings - Generation, Transmission and Distribution*, 148(1), 61-66. doi: 10.1049/ip-gtd:20010025.

Wang, H. F., Li, H. & Chen, H. (2003). Coordinated secondary voltage control to eliminate voltage violations in power system contingencies. *IEEE Transactions on Power Systems*, 18(2), 588-595. doi: 10.1109/TPWRS.2003.810896.

Wen, J. Y., Wu, Q. H., Turner, D. R., Cheng, S. J. & Fitch, J. (2004). Optimal coordinated voltage control for power system voltage stability. *IEEE Transactions on Power Systems*, 19(2), 1115-1122. doi: 10.1109/TPWRS.2004.825897.

Yang, X., Du, Y., Su, J., Chang, L., Shi, Y. & Lai, J. (2016). An Optimal Secondary Voltage Control Strategy for an Islanded Multibus Microgrid. *IEEE Journal of Emerging and Selected Topics in Power Electronics*, 4(4), 1236-1246. doi: 10.1109/JESTPE.2016.2602367.

Yu, Z., Ai, Q., Gong, J. & Piao, L. (2016). A Novel Secondary Control for Microgrid Based on Synergetic Control of Multi-Agent System. *Energies*, 9(4). doi: 10.3390/en9040243.

Yurong, W., Fangxing, L., Qiulan, W. & Hao, C. (2011). Reactive Power Planning Based on Fuzzy Clustering, Gray Code, and Simulated Annealing. *Power Systems, IEEE Transactions on*, 26(4), 2246-2255.

Zhong, J., Nobile, E., Bose, A. & Bhattacharya, K. (2004). Localized reactive power markets using the concept of voltage control areas. *IEEE Transactions on Power Systems*, 19(3), 1555-1561. doi: 10.1109/TPWRS.2004.831656.

Zima, M. & Andersson, G. (2003, June). Stability assessment and emergency control method using trajectory sensitivities. *Power Tech Conference Proceedings, 2003 IEEE Bologna*, 2, 7 pp. Vol.2-. doi: 10.1109/PTC.2003.1304313.

Zimmerman, R. D. (2011). *AC Power Flows, Generalized OPF Costs and their Derivatives using Complex Matrix Notation*.